Lessons from Vaccinia Virus Post-Exposure Prophylaxis: Insights into Control of Diseases and Epidemics

by

Susan A. Holechek

A Dissertation Presented in Partial Fulfillment
of the Requirements for the Degree
Doctor of Philosophy

Approved November 2011 by the
Graduate Supervisory Committee:

Bertram Jacobs, Chair
Carlos Castillo-Chavez
Wayne Frasch
Brenda Hogue
Valerie Stout

ARIZONA STATE UNIVERSITY

December 2011

ABSTRACT

The concept of vaccination dates back further than Edward Jenner's first vaccine using cowpox pustules to confer immunity against smallpox in 1796. Nevertheless, it was Jenner's success that gave vaccines their name and made vaccinia virus (VACV) of particular interest. More than 200 years later there is still the need to understand vaccination from vaccine design to prediction of vaccine efficacy using mathematical models. Post-exposure vaccination with VACV has been suggested to be effective if administered within four days of smallpox exposure although this has not been definitively studied in humans. The first and second chapters analyze post-exposure prophylaxis of VACV in an animal model using v50ΔB13RMγ, a recombinant VACV expressing murine interferon gamma (IFN-γ) also known as type II IFN. While untreated animals infected with wild type VACV die by 10 days post-infection (dpi), animals treated with v50ΔB13RMγ 1 dpi had decreased morbidity and 100% survival. Despite these differences, the viral load was similar in both groups suggesting that v50ΔB13RMγ acts as an immunoregulator rather than as an antiviral. One of the main characteristics of VACV is its resistance to type I IFN, an effect primarily mediated by the E3L protein, which has a Z-DNA binding domain and a double-stranded RNA (dsRNA) binding domain. In the third chapter a VACV that independently expresses both domains of E3L was engineered and compared to wild type in cells in culture. The dual expression virus was unable to replicate in the JC murine cell line where both domains are needed together for replication. Moreover, phosphorylation of the dsRNA dependent protein kinase (PKR) was

observed at late times post-infection which indicates that both domains need to be linked together in order to block the IFN response. Because smallpox has already been eradicated, the utility of mathematical modeling as a tool for predicting disease spread and vaccine efficacy was explored in the last chapter using dengue as a disease model. Current modeling approaches were reviewed and the 2000-2001 dengue outbreak in a Peruvian region was analyzed. This last section highlights the importance of interdisciplinary collaboration and how it benefits research on infectious diseases.

DEDICATION

To my Dad, Angel, who always believed in me no matter what, I know you are watching over me.

To my Mom, Yola, my best friend, even when we do not agree on everything.

To my beloved husband Jason, my soul mate, whose patience and love surrounds me every day. I love you. Forever.

ACKNOWLEDGMENTS

I would like to acknowledge all my mentors throughout these years, because of you this is possible. Dad and Mom this is thanks to you. A special thanks to my husband, you changed my life and supported my love for science. Thanks for providing your patience and your scientific mind, for that and for just being you, thank you.

I would like to thank my family in Peru, thank you for your unconditional love and support, my heart aches to see you all again soon. A special note of gratitude to my aunt Tere and my aunt Juan, the best godparents I could ever had, you gave me everything and more and for that I will always be in debt. To my family here in the U.S. especially my new parents Michelle and Jim, I cherish every precious moment together, thank you for your love and for always being there for me.

I would like to thank Dr. Bertram Jacobs for welcoming and nurturing my scientific path in his lab, thank you for your patience and for your support along these years. To all my committee members Dr. Carlos Castillo-Chavez, Dr. Brenda Hogue, Dr. Wayne Frasch and Dr. Valerie Stout, for all the valuable discussions and for helping me think outside the box. Thank you.

To past and present members of the Jacobs' lab especially Dr. Karen Denzler, for sharing her knowledge and always finding time to work with me. Thank you. To my friends in the lab, for sharing moments of wisdom, patience, failures and successes, because science is all that and more. A special thanks to

Mrs. Cruz Lotz, for the unconditional support throughout these years, you were always like a Mom to me. I miss you.

A special thanks to my undergraduates and interns at the Biodesign Institute, Troy Trevino, Hansa Done, Josh Darland, Mari Funabashi and Lynda Idouraine, you make life at the lab fun, thank you for your hard work, you are the best. To all my undergraduates throughout the years as a Teaching Assistant at ASU, with you I discovered how passionate I am about teaching.

To all my friends in the Graduate College, specially Dr. Joan Brett, for being such a great role model during the Preparing Future Faculty Program and beyond.

To my new friends at the Applied Mathematics for the Life and Social Sciences program at ASU, especially David Murillo, Anarina Murillo and Dr. Fabio Sanchez for making interdisciplinary collaborations possible. Thank you.

I also would like to thank the More Graduate Education at Mountain States Alliance (MGE@MSA)-Alliance for Graduate Education and the Professoriate (AGEP) program funded by the National Science Foundation (NSF), for all the opportunities and funding throughout all these years, you played a pivotal role in my career. Thank you for believing in me. A special note of gratitude to Laura Serrano and Elisabeth Luquez for all their help and kindness.

To the Graduate Professional Student Association at ASU, the ASU Faculty Emeriti Association and the ASU Graduate College for providing funding support to continue working on my projects. Thank you.

TABLE OF CONTENTS

LIST OF TABLES

LIST OF FIGURES

Figure Page

Figure Page

Figure Page

OVERALL INTRODUCTION

The importance of vaccines and the concept of vaccination dates back to 1796 and Edward Jenner's most important health intervention in history when he used cowpox pustules to confer immunity against smallpox (108, 197). Jenner's contributions led to eradication of smallpox and made him founder of the new science of vaccinology (46). Of special interest is vaccinia virus (VACV), which is believed to have evolved from variola virus (VARV), cowpox virus or a hybrid of both (218). VACV have been routinely used as a vaccine for smallpox as it provides cross-protection to VARV, the causative agent for smallpox (108). Now, more than 200 years later and following the eradication of smallpox in the late 1970s (4, 237), there is still the need to understand vaccination from vaccine design to prediction of vaccine efficacy using mathematical models.

Following smallpox eradication, routine smallpox vaccination was discontinued in the U.S. in 1972 (4). This left the majority of the world population susceptible to severe diseases from certain orthopoxvirus infections. After September 11, 2001, there was heightened concern for the use of VARV or monkeypox virus (MPXV) as a bioterrorism agent and the low, but real, risk of an accidental VARV release (134, 169, 227). Moreover, inoculation in humans with VACV can lead from mild to life-threatening reactions and these complications vary according to each VACV strain (58, 127, 206). All these reasons make the need of a post-exposure prophylaxis vaccine for smallpox one of the ultimate worldwide goals. Post-exposure vaccination using VACV has been suggested to

be effective against smallpox if administered within four days of initial exposure (157). While there is anecdotal evidence for efficacy of post-exposure vaccination, this has not been definitively studied in humans.

There are diverse antiviral agents that have been used for post-exposure treatment of smallpox. Of these it is worth to mention (S)-1-(3-hydroxy-2-phosphonylmethoxypropyl)-cytosine also known as HPMPC, Vistide, and cidofovir (45, 222), although its use is limited due to nephrotoxicity and the lack of oral availability (222). Another antiviral agent is vaccine immune globulin (VIG), which has been suggested to be used by patients for whom smallpox vaccine is contraindicated (240). The most promising anti-poxviral drug and post-exposure agent is ST-246 (167, 185, 186, 219, 246), which have been used to protect ground squirrels that have been infected with MPXV (209) and in combination therapy with other compounds to treat humans exposed to VACV (29-31, 231).

Post-exposure has been recently studied using modified VACV Ankara (MVA) and the VACV-Lister strain for post-exposure treatment in the murine model (173, 221). While immunization with MVA and the Lister strain proved to be effective against an ECTV infection when post-exposure was performed up to 3 days post-infection (dpi) (173), post-exposure vaccination with MVA was effective at 1 dpi after challenge with the Western Reserve (WR) strain of VACV (221). Moreover, post-exposure treatment with the Lister strain failed to provide any protection (221).

The approach for post-exposure prophylaxis that was used in the first chapter of this dissertation relies in the fact that VACV allows the insertion of foreign DNA using double-homologous recombination and that certain cytokines have shown to decrease virulence during VACV infection (70, 163, 191, 212). In this context a recombinant VACV expressing murine IFN-γ (v50ΔB13RMγ), which has previously been described (136), was found to be the best candidate in an animal model for post-exposure treatment following a challenge with wild type VACV (WR strain). Post-exposure protection with v50ΔB13RMγ was dose and time dependent with 100% survival in animals treated 1 dpi. The mechanism of action for post-exposure treatment using v50ΔB13RMγ is explored in Chapter 2. The effects of this virus at the site of infection can be observed by 2 dpi with the recruitment of specialized myeloid derived suppressor cells whose role in post-exposure protection is yet to be determined. Moreover, activation of the inducible nitric oxide synthase by IFN-γ could be playing a role in the survival of the animals.

While the first two chapters describe the use of a recombinant VACV that expresses IFN-γ for post-exposure treatment, one of the innate characteristics of VACV is that it is IFN-resistant. This characteristic is primarily due to the E3L gene (106) which has also been associated to neurovirulence in mice (19, 122). E3L encodes a 25-kDa protein that has two essential domains, an N-terminal domain with sequence similarity to the vertebrate Zα family of Z-DNA binding domains (110, 121, 122, 129), and a C-terminal domain that has a typical double-

stranded RNA (dsRNA) binding domain (34, 43, 133). Furthermore, the E3L gene is a common feature of orthopox viruses. In fact, when comparing VACV and VARV, the N-terminal and C-terminal E3L domains are both nearly identical (187).

Deletion of E3L leads to a virus that is completely non-pathogenic (19, 35). Unfortunately, expression of foreign genes from this virus is also greatly reduced (109). The E3L gene is involved in inhibiting the host antiviral response. The C-terminal domain of E3L has been previously characterized and its function is to bind and mask dsRNA synthesized during VACV infection (34, 102, 103). In the absence of E3L, the dsRNA dependent protein kinase (PKR) binds to dsRNA, dimerizes and becomes autophosphorylated. This activation of PKR leads to phosphorylation of the eukaryotic initiation factor 2 alpha subunit (eIF2α) which becomes inactivated and halts translation of viral and host proteins (36, 119). Moreover, analysis of several VACV with mutations in the dsRNA binding domain demonstrated that E3L can bind to PKR suggesting that this interaction can enhance the inhibition of PKR activation by sequestering the dsRNA activator (177).

Although the C-terminus has been associated with IFN resistance and PKR inhibition, recent data showed that the N-terminus is also necessary for both mechanisms providing a new insight into the function of the Z-DNA binding domain *in vivo* (235). This N-terminus domain has also been associated with neurovirulence and neuroinvasion following VACV infection in C57/BL6 mice

(18, 122). Furthermore, it is necessary to inhibit PKR activation at late times post-infection as well as eIF2α phosphorylation in HeLa cells and in nasal turbinates of C57/BL6 mice (132).

The third chapter explores the role of the Z-DNA binding domain and its independent expression from the dsRNA binding domain. A dual expression virus was engineered and compared to wild type VACV in cells in culture and for its ability to inactivate the IFN response. The dual expression virus was unable to replicate in the murine JC cell line, a previously described cell line where E3L mutants lacking either the Z-DNA binding domain or the dsRNA binding domain are unable to replicate (228). Moreover, PKR phosphorylation was observed at late times post-infection indicating that both domains of E3L need to be linked together in order to block the IFN response.

Because smallpox has already been eradicated, the utility of mathematical modeling as a tool for predicting vaccine efficacy was explored in the fourth chapter using dengue as a disease model. Dengue virus, is a single-stranded, positive-sense RNA virus that belongs to family *Flaviviridae* (49). Dengue has four antigenically different serotypes also known as DENV-1, DENV-2, DENV-3 and DENV-4. The pathogenicity of the disease ranges from asymptomatic or mild dengue fever (DF) to the more severe dengue hemorrhagic fever (DHF) and dengue shock syndrome (DSS), which affect mostly children under 15 (49, 93).

The World Health Organization has declared that two fifths of the world population are at risk of being infected with dengue and although dengue has been

commonly presented as a tropical disease, it has spread to U.S. (32, 236). It is clear that dengue has expanded to a vast amount of territories, in part due to the adaptation of one of mosquito vectors, *Aedes albopictus,* to colder climates (101, 156) and the evidence of vertical transmission from the infected female to her eggs in both *Aedes aegypti*, the primary vector, and *Aedes albopictus* (9, 17, 33, 89, 126, 203).

One of the main issues with dengue is that there is not yet a commercial available vaccine although many efforts are being made by diverse research groups in academic and industrial settings (53). These vaccine candidates include live vaccines, attenuated vaccines, vaccines created using recombinant DNA technology, as well as subunit vaccines like the ones developed by Merck/Hawaii Biotech (90). Of these vaccines, the tetravalent dengue vaccine from Sanofi Pasteur was the first one to go into Phase III of clinical trials and results are expected by the end of 2012 (91).

Dengue is considered one of the most important emerging and re-emerging infectious diseases worldwide (93, 98, 178, 236). It will require a multidisciplinary effort to fully understand the complex dynamic of dengue and the efficacy of the introduction of a vaccine candidate. This is in part due to the complexity of the immunology, epidemiology, pathology and the interactions between the vector and the host. In 2010 the World Health Organization organized a workshop designed to bring together mathematical modelers, clinicians, vaccinologists, virologists, immunologists, entomologists and

epidemiologists to explore what is currently being done and what needs to be done with respect to dengue vaccine modeling (238).

The fourth chapter provides an overview of current dengue transmission models and their diverse challenges, as they cannot predict for example an early rainy season and how this will affect the outcome of the model. Understanding the current dengue models will lead to a better evaluation of the efficacy of future vaccination strategies. Thus, it is of great importance that scientists across disciplines come together and evaluate the use of mathematical models as tools to understand the risks and potential successes or pitfalls of vaccination strategies worldwide.

CHAPTER 1

POST-EXPOSURE ADMINISTRATION OF A RECOMBINANT VACCINIA VIRUS EXPRESSING INTERFERON GAMMA PROTECTS MICE FROM LETHAL INTRANASAL INFECTIONS WITH VACCINIA VIRUS

ABSTRACT

Post-exposure vaccination with vaccinia virus (VACV) has been suggested to be effective in minimizing death if administered within four days of smallpox exposure. While there is anecdotal evidence for efficacy of post-exposure vaccination this has not been definitively studied in humans. The experiments analyze post-exposure prophylaxis of VACV in an animal model using VACV E3L mutants as well as recombinant VACV expressing murine interferon-γ (IFN-γ) or murine interleukin-18 (IL-18). A recombinant VACV expressing murine IFN-γ was most effective at post-exposure protection of mice infected with VACV. While all untreated animals infected with VACV exhibited severe weight loss and morbidity leading to 100% mortality by 8 to 10 days post-infection, animals treated one day post-infection had milder symptoms, decreased weight loss and morbidity, and 100% survival. Treatment on days 2 or 3 post-infection resulted in 40% and 20% survival, respectively. Despite the differences in survival rates when animals were treated at 1 day post-infection, the viral load was similar in both treated and untreated mice. These results suggest that

protection provided by IFN-γ expressed by VACV is mediated by its immunoregulatory activities rather than its antiviral effects.

INTRODUCTION

Vaccinia virus (VACV) is a member of the genus *Orthopoxvirus* of the family *Poxviridae*. Other members of this family include variola virus (VARV), the causative agent of smallpox; monkeypox virus (MPXV), ectromelia virus (ECTV), camelpox virus (CMLV) and cowpox virus (CPXV) (66, 159). After an intensive vaccination strategy using VACV, which was initiated in 1967, smallpox was declared eradicated from the world in 1980 and routine smallpox vaccination was discontinued in the U.S. in 1972 (4, 237). This left the majority of the world population susceptible to severe disease from certain orthopoxvirus infections. After September 11, 2001, there was heightened concern for the use of VARV or MPXV as a bioterrorism agent and the low, but real, risk of an accidental VARV release (134, 169, 227). For these reasons it was important to develop a post-exposure prophylaxis strategy.

There are diverse antiviral agents that have been considered as alternative strategies for post-exposure treatment of smallpox. One of the antiviral drugs that has been shown to be effective against different poxviruses is (S)-1-(3-hydroxy-2-phosphonylmethoxypropyl)-cytosine also known as HPMPC, Vistide, and more commonly as cidofovir (45, 222). While cidofovir has been shown to protect monkeypox-infected macaques when administered 24 hours post-infection (hpi),

its potential is limited by nephrotoxicity and the lack of oral availability (222). Likewise, vaccine immune globulin (VIG), has also been suggested to be used as prophylaxis in patients for whom smallpox vaccine is contraindicated (240).

Another antiviral, ST-246, has shown promise as an antipoxviral drug (167, 185, 186, 219, 246). ST-246 protects ground squirrels against monkeypox challenge when administered up to 3 days post-exposure (209). Treatment with VIGIV (VIG Intravenous) and cidofovir along with ST-246 (multiple doses) has proven to be successful in the treatment of a 28-month-old child with severe eczema vaccinatum (29, 231). Similarly, a combination therapy using VIGIV, ST-246, Imiquimod and CMX001, a lipid conjugate of cidofovir, were used to treat progressive vaccinia in a military vaccinee (31). Moreover, VIGIV and ST-246 have recently been used to treat human vaccinia infection in a 35 year-old woman after contact with raccoon rabies bait (30). Although it is difficult to assess the contribution of each agent because of the close timing of administration, these cases are an example of the utility of new treatments.

Post-exposure vaccination with VACV has also been suggested to be an effective treatment if administered within four days of smallpox exposure (157). While there is anecdotal evidence for efficacy of post-exposure vaccination this has not been definitively studied in humans.

A recent model of post-exposure immunization with modified VACV Ankara (MVA) and the VACV-Lister strain proved to be effective in an ECTV infection model when post-exposure vaccination was performed at 1, 2 and 3 days

post-infection (dpi). Protection was shown to be dependant on the vaccine dose as well as the day of vaccination (173). A second model employs the Western Reserve (WR) strain of VACV as a challenge virus in mice. Therapeutic vaccination with MVA was minimally protective only at 1 dpi while the Elstree strain failed to provide any detectable protection (221).

Because cytokines are highly regulated during VACV infection, they have been thoroughly studied in this context (70, 163, 191, 212). While IL-2, TNF-α and IFN-γ decrease virulence during a VACV infection, others such as IL-4 have been shown to increase virulence and pathogenicity (70, 163, 191, 212). Another cytokine, IL-18, which can induce endogenous synthesis of IFN-γ, has been shown to promote clearance of VACV infection when expressed together with IL-12, indicating the synergistic action of both cytokines (78).

The present work employed recombinant VACV for post-exposure prophylaxis in an animal model. Several recombinant VACVs as therapeutic vaccines were evaluated including 1) viruses containing mutations in the VACV E3L gene, an IFN resistance gene (19, 213) and 2) viruses expressing murine IFN-γ (muIFN-γ) (136) or murine IL-18 (muIL-18) from the VACV B13R locus.

This chapter outlines the use of different VACV E3L mutants and VACV recombinant viruses for post-exposure prophylaxis treatment. The results show that post-exposure prophylaxis with a recombinant VACV expressing IFN-γ is 100% effective in protecting mice infected with 100 LD_{50s} of wt VACV when administered 1 dpi.

MATERIALS AND METHODS

Recombinant viruses. The WR strain of VACV was used as the parental virus for these studies. The E3L VACV mutants were generated by standard methods routinely employed in Dr. Bertram Jacobs' laboratory. Construction of VACV mutants expressing E3LΔ7C and E3LΔ26C has previously been described (119). VACVΔE3L::ATVeIF2α has a replacement of the E3L gene with the eukaryotic initiation factor 2 alpha (eIF2α) homologue from the *Ambystoma tigrinum* virus, genus *Ranavirus*, family *Iridoviridae* (131).

The recombinant VACV expressing IFN-γ (v50ΔB13RMγ) virus was constructed as previously described (136). This virus expresses the vesicular stomatitis virus glycoprotein (VSV-G) at the TK locus and *lacZ*, gpt, and muIFN-γ at the B13R site. The recombinant VACV expressing IL-18 (v50ΔB13RMIL-18) is essentially the same as v50ΔB13RMγ, but expresses the muIL-18 gene instead of muIFN-γ. The muIL-18 gene was cloned from mouse spleen cDNA (Verardi *et al.*, manuscript in preparation). Construction of the parental virus (v50ΔB13R) has already been described (137).

Cell culture. Viruses were amplified in Baby Hamster Kidney 21 (BHK) cells and partially purified by pelleting through a 36% sucrose pad, as previously described (15, 54). BHK and Rabbit Kidney 13 (RK13) cells were cultured in Eagle's Minimal Essential Medium (MEM, Gibco, BRL) containing 5% fetal bovine serum (FBS, Hyclone), 50 μg/ml of gentamycin, and 0.1 mM nonessential

amino acid solution (Gibco, BRL) and vitamin supplements. Both BHK and RK-13 cells were incubated at 37˚C with 5% CO_2.

Mice. Four-week old female C57BL/6 mice were obtained from Charles River Laboratories. Mice were housed at the Arizona State University Department of Animal Care and Technologies according to the university IACUC regulations. Each cage contained a maximum of 5 mice and a separate cage was used for each experimental condition. Treatment groups consisted of 5 to 15 mice.

***In vivo* infections.** An anesthetic cocktail containing xylazine (7.5 mg/ml), acepromazine maleate (2.5 mg/ml), and ketamine (37.5 mg/ml) was prepared. Approximately 1-µl of cocktail was injected intramuscularly per gram of body weight (19). Following anesthesia, one naris was infected with a 5-µl dose of 10^6 pfu (~100 LD_{50s}) of wt VACV. Mice were treated 1, 2 or 3 dpi with 10^2 – 10^7 pfu of treatment virus administered intranasally (IN) into the same naris as the challenge virus. Scarification was done as previously described (109). Disease symptoms and animals' health were monitored every other day for the length of the experiment. The IACUC protocol number 08-970R was followed.

Weight loss. Weight loss was determined by weighing each mouse on alternate days. The percent weight gain or loss was determined and animals that lost more than 30% of their original body weight were euthanized and considered dead from the challenge.

Sickness index. A relative sickness index that takes into consideration typical symptoms of a wt VACV infection was created. Each animal from each

group was assigned an arbitrary score (1-4) based on the severity of the following symptoms: ruffled fur, lack of activity, breathing difficulty, eye infection, hunching and weight loss. This index also takes into consideration the number of animals euthanized within each group (each death accounts for a value of 0.8 in the death/life score, if all animals in the group die, the line stops).

Tissue distribution. Animals were infected IN with 10^6 pfu of wt VACV (Day 0) and treated with 10^7 pfu of v50ΔB13RMγ. On alternate days beginning with 2 dpi, three animals were euthanized and then immediately dissected. The organs removed (nasal cavity, brain, lungs, heart, liver, spleen, kidney and ovaries) were immediately frozen in liquid nitrogen and then stored at -80˚C. A 10% homogenate was prepared for each organ by adding 1 mM Tris pH 8.8 with gentamycin. All tissues with the exception of the nasal cavity were then homogenized using a PCR tissue homogenizing kit (Fisher). The nasal cavity was homogenized using a Mixer Miller 301 device (Retsch). All homogenates were subjected to three rounds of freezing (-80°C)-thawing for 30 minutes on ice and then quick thawing (37°C). After three rounds of freezing-thawing, samples were subjected to a 7-minute spin using a tabletop centrifuge at 700 x *g* at 4˚C to remove all cell debris. After centrifugation, supernatants were retained and dilutions were performed for plaque assays on RK13 cells.

Viral loads for tissue distribution were conducted in triplicate by infecting monolayers of RK13 cells. Twenty-four hours post-infection, two replicas were stained with crystal violet to determine the viral load within the tissue (pfu per

gram of tissue). Differentiation of wt VACV and the treatment v50ΔB13RMγ virus was done by overlaying the third replica with 1% agarose, MEM 5% FBS and 400 μg/ml X-Gal (5-bromo-4-chloro-3-indolyl-β-D-galactopyranoside). The v50ΔB13RMγ could be identified due to the fact that this virus expresses *lacZ* at the B13R site.

Immunohistochemistry. Tissues were perfused with phosphate-buffered saline (PBS) via cardiac perfusion followed by fixation with 10% formalin. After the soft tissue was removed the skull was decalcified using EGTA. The skull was embedded in paraffin and sliced at 3-μm thickness using a microtome. Deparaffinized tissue sections of the nose were incubated with 2% H_2O_2 in methanol for 10 minutes to quench endogenous peroxidases and then rinsed in PBS. Detection of VACV antigen was done using rabbit anti-VACV and the VECTASTAIN Elite ABC kit (Rabbit IgG) from VECTOR Laboratories following the manufacturer's protocol.

Data analysis. Errors band indicate standard error of the mean. Survival analysis was done using Kaplan-Meier curves and the log-rank test analyses were performed using the statistical software program GraphPad Prism (version 5.0c for Macintosh).

RESULTS

v50ΔB13RMγ causes weight recovery and protects mice from death. The WR strain of VACV was originally derived from serial passages in mouse

brain and thus is a neurotropic, highly virulent strain of VACV (111). Several VACV WR mutants of E3L (an IFN antagonist protein) as well as VACV WR recombinants expressing either muIL-18 or muIFN-γ were tested for their ability to confer post-exposure prophylaxis in mice upon challenge with a lethal dose of VACV WR. The VACV E3L mutants chosen for this study have previously been shown to have reduced pathogenesis and neurovirulence phenotypes in mice (19). Similarly, IL-18 was selected due to its pro-inflammatory properties, ability to induce synthesis of IFN-γ, activation of NK cells and its main role in the T-lymphocyte helper type 1 response (242). IFN-γ was chosen due to its multiple immune stimulatory effects on macrophage activities, NK cell cytolysis, and T and B cell responses (140, 163, 166, 190, 210).

IN infections of C57BL/6 mice were performed with ~100 LD_{50s} wt VACV as described in the materials and methods section. Animals were then treated 1 dpi with 10^7 pfu of the mutant or recombinant virus (Fig. 1). As shown in Fig. 2, all animals lost weight to day 6 post infection, but only mice treated with v50ΔB13RMγ recovered. Fig. 3 shows the survival rate for each of the mutants tested. Treatment with v50ΔB13RMIL-18 resulted in 60% survival (P<0.005, log-rank test) while 30% survival was observed when animals were treated with either VACVΔE3L, VACVE3LΔ7C or VACVE3L::ATVeIF2α (P>0.05, log-rank test) and 20% survival when treated with VACVE3LΔ26C (P<0.05, log-rank test). Only treatment with v50ΔB13RMγ was able to confer 100% survival (P<0.0001, log-rank test). Partial protection was seen with doses

as low as 10^5 pfu, while full protection in the animals required treatment with 10^7 pfu (Fig. 5).

The parental virus of v50ΔB13RMγ, v50ΔB13R, was also evaluated in order to determine if the deletion of the serpin gene B13R was responsible for the protection. B13R is nonessential for VACV replication, and deletion from the virus results in reduced replication and pathogenesis in mice (137). Treatment of mice infected with wt VACV as described above with the parental virus (v50ΔB13R) was analyzed. This virus did not provide protection against infection with VACV with only 17% surviving (Fig. 6, $P>0.5$, log-rank test), suggesting that expression of IFN-γ and not the deletion of B13R, is responsible for the survival of the mice.

Post-exposure prophylaxis with v50ΔB13RMγ is more effective when administered one day post-infection. In order to determine the temporal requirements of protection, animals were infected with 10^6 pfu (~100 LD_{50s}) of wt VACV and then treated with 10^7 pfu of v50ΔB13RMγ at 1, 2, or 3 dpi. Animals showed 100% survival when treated 1 dpi, while all mock-treated animals died by day 8 ($P<0.005$, log-rank test). Protection was reduced to 40% ($P<0.05$, log-rank test) when treatment virus was administered at 2 dpi, and to 20% ($P>0.05$, log-rank test) when animals were treated at 3 dpi (Fig. 7A). Additionally, when animals were initially infected with ten-fold more wt VACV (10^7 pfu or 1000 LD_{50s}) followed by treatment 1 dpi with v50ΔB13RMγ a slight decrease to 80% survival was observed ($P<0.005$, log-rank test).

A relative sickness index with values from 0 to 4 was created as indicated in the materials and methods section. Animals that were untreated reached a relative sickness index of 2.7 by 6 dpi and succumbed to the infection by 8 dpi. However, mice that were treated with 10^7 pfu v50ΔB13RMγ at 1 dpi reached a maximum relative sickness of 0.86 by 6 dpi. By day 18, these mice attained weights that were comparable to the mock-infected mice and had a relative sickness index of 0. Interestingly, animals that were treated either 2 or 3 dpi showed similar morbidity and had a sickness index similar to that of the untreated animals at 8 dpi, (2.5 versus 2.66). When animals were infected with 10^7 pfu of wt VACV and treated 1 dpi, they reached a maximum score of 1.14 by 8 dpi and the animals that survived showed a slightly delayed recovery as compared to mice infected with 10^6 pfu wt VACV and treated 1 dpi (Fig. 7B).

The intranasal route of administration of post-exposure prophylaxis with v50ΔB13RMγ is most effective. In the previous experiments, all viral infections were administered into the same naris of the animal. Since the current smallpox vaccine is given by scarification and several vaccines are administered by intramuscular (IM) injection, animals were challenged IN as described above and treated with v50ΔB13RMγ into the opposite naris (INON), by scarification (SC) and by IM injection. The results show that 100% protection occurred only when the treatment was given into the same naris as the challenge virus (Fig. 8A). On the other hand, mice that remain untreated had marked weight loss, morbidity and died 8 dpi. INON treatment resulted in 40% survival ($P<0.005$, log-rank test),

and IM or SC treatment resulted in 20% and 15% survival, respectively (P>0.5, log-rank test) (Fig. 8A). As in previous experiments, a relative sickness index was generated. Animals that were treated within the same naris had the lowest relative sickness index, 0.6 at 8 dpi, while treatment in the opposite naris had an index of 1.74 and treatment via SCA or IM injection had the highest sickness index of 2.0 by 8 dpi, similar to untreated animals (Fig. 8B).

Viral spread of wt VACV was similar in untreated and treated animals. IFN-γ is both an effective antiviral as well as a modulator of the innate immune response by leading to the activation of macrophages, neutrophils and to increased expression of MHC class I and II proteins (140, 163), which could limit the spread of VACV, and lead to protection against mortality. To determine the kinetics of replication and viral spread, various mouse tissues (nasal cavity, brain, lungs, heart, liver, spleen, kidney and ovaries) were examined. At 2 dpi wt VACV was observed in the nose, brain, lungs and spleen of mock-treated animals (Fig. 9). Animals that were treated with v50ΔB13RMγ showed similar viral loads in the nose, brain and spleen as in untreated animals, but no virus was detected in the lungs (Fig 9). By 4 dpi wt VACV was detected in all of the organs examined with similar titers in most tissues in both untreated and treated animals (Fig. 9 and data not shown). However, at 4 dpi titers in the brain of treated animals were two logs lower than titers in the brain of untreated mice (Fig. 9), while titers in the ovaries of treated mice were two logs higher than in untreated mice (data not shown). By 6 dpi, viral loads in treated animals peaked within the nose, brain, heart, and lungs

and reached titers close to those observed in untreated animals at 4 dpi (Fig. 9 and data not shown). By 10 dpi VACV could only be detected in the nose, brain, and lungs indicating that the treated animals were effectively clearing the viral load (Fig. 9). X-gal staining was done in order to differentiate v50ΔB13RMγ from wild-type virus. Examination of the different tissues revealed low level replication of this virus in the nose (4-8 dpi) and brain (2 and 6 dpi), as well as detection in the heart and lungs of one animal at 6 and 8 dpi respectively. These results are similar to viral loads in tissues from mice infected with 10^7 pfu of v50ΔB13RMγ alone (Fig. 10 and data not shown).

Animals treated with v50DB13RMγ show decreased tissue necrosis, edema, and epithelial sloughing into the nasal cavity. Histological analyses of nasal tissues (Fig. 11) were performed in order to determine differences in pathology following treatment with v50ΔB13RMγ (Fig. 12). Staining for VACV antigen showed that in a wt VACV infection followed by mock treatment, virus replicated in the epithelial cell layer early during infection at day 3. As infection progressed, VACV replication moved into the underlying lamina propria and epithelial sloughing, tissue necrosis, and edema were evident (Fig. 13). By 8 dpi in an untreated animal, it could be observed that the nasal cavity was unilaterally blocked and replication had progressed in both dorsal and lateral directions (Fig. 14). In animals treated with v50ΔB13RMγ, VACV staining was observed at day 3 in the epithelial cell layer, however at days 5 and 8, a reduced progression of VACV staining into the lamina propria was observed as well as reduced levels of

tissue necrosis and edema (Fig. 13). At 8 dpi in treated animals VACV replication was evident along the airway epithelium but did not progress laterally (Fig. 14).

DISCUSSION

In this chapter a recombinant VACV that expresses IFNγ, v50ΔB13RMγ, was found to be the best post-exposure prophylaxis candidate in a VACV-WR animal model and results indicate that this recombinant virus may be eliciting an immunoregulatory rather than an antiviral effect when used as a treatment.

There are currently anecdotal studies regarding the efficacy of post-exposure vaccination protection of individuals when administered up to 4 days post-exposure (157). The present work was intended to evaluate potential vaccine candidates for prophylaxis after post-exposure to a pathogenic orthopoxvirus. While other post-exposure prophylaxis studies have been done using replication-deficient and replication-competent VACV vaccine strains in order to protect against a lethal infection with VACV-WR or ECTV (168, 173, 221), to current knowledge this study is the only one that successfully uses a recombinant VACV expressing IFN-γ, v50ΔB13RMγ, for post-exposure protection.

The present results demonstrate that IFN-γ is not acting as an antiviral as it was observed that viral replication in different organs analyzed is similar between animals infected with wt VACV and animals infected with wt VACV but treated 1 dpi. Moreover, several parameters were studied in order to optimize post-exposure protection in our animal model. Intranasal infection was chosen as the

route of challenge as this is considered to be the natural route of transmission for smallpox (174). In this VACV-WR post-exposure model, the route of treatment was important being IN treatment the most effective as survival rate of animals infected IN with wt VACV and treated with v50ΔB13RMγ, especially into the same naris as challenge, provided complete protection. The use of other routes of treatment reduced the survival rate to 40% (INON) and 20% (IM and SCA) (Fig. 8A). Similarly, in a study by Staib *et al*. (221), mice infected IN with 5 x 10^4 pfu (1 LD_{50}) VACV-WR strain and then treated IM at 1, 2, 3 or 4 dpi with 10^8 infectious units of the modified VACV Ankara (MVA) died by day 9 and had no effect compared with mock-vaccinated animals. Mice infected IN with 10^6 pfu VACV-WR and treated by scarification with 10^6 pfu VACV Elstree strain presented similar results (221). The fact that in the model treatment is more effective when administered in the same site of the infection could be explained in part by the low replication levels of v50ΔB13RMγ in the tissues examined (Fig. 10). Despite its low levels of replication in animal models, v50ΔB13RMγ is known to elicit potent humoral, T helper and cytotoxic T cell immune responses suggesting that the efficacy of this recombinant VACV is not compromised (136).

Another parameter that was examined was time of post-exposure treatment. Results have shown that post-exposure immunization with v50ΔB13RMγ is more effective in protecting mice against a lethal infection with VACV-WR when administered one day post-infection (Fig. 7). Other studies have proven that post-exposure protection against a challenge dose of 1 to 3 LD_{50s} is

possible when treatment with MVA is applied the same day of infection (221). The action of IFN-γ by itself has been proven to be effective against a challenge dose of 8 LD_{50s} when treatment was administered one day before or the same day of infection and using a total of five consecutive doses of IFN-γ with treatments that were started at 1, 2, and 3 dpi, resulting in 90, 70, and 50% survival rates respectively (140). In contrast, the present results show the efficacy of v50ΔB13RMγ for post-exposure vaccination prophylaxis following higher challenge doses of 100 LD_{50s} of VACV-WR with 100, 40 and 20% survival when treatment was administered at 1, 2 or 3 dpi respectively and 80% when mice were challenge with 1000 LD_{50s} and treated 1 dpi (Fig. 7). Moreover, the effectiveness of IN vaccination was dependent on both the dose of v50ΔB13RMγ and on expression of IFN-γ as treatment with the parental virus v50ΔB13R, only provided 17% efficacy in this model (Fig. 6).

Although v50ΔB13RMγ does not spread well in tissues, it replicates to low levels in the nose of treated animals (Fig. 10), which could contribute to an increase in the effectiveness of the prophylactic treatment. Additionally, murine IFN-γ has a low affinity for the VACV-expressed IFN-γ binding protein (IFN-γ BP) (3), making its availability higher when used for treatment of a VACV-WR infection.

Despite seeing less morbidity and no mortality in the treated animals with v50ΔB13RMγ, viral replication was observed in the organs that were examined. One of the morbidity symptoms that was evaluated was weight loss which has

been correlated with fever and is a reliable method of determining relative pathogenesis (16). This study shows a continual weight loss in animals infected with wt VACV. However, animals treated with v50ΔB13RMγ lose a maximum of 25% weight and recover rapidly (Fig. 7B) reaching a weight comparable to uninfected animals by day 18 (data not shown). While data show that viral load and tissue distribution were similar for both untreated and treated groups up to 6 dpi, most mice infected with wt VACV did not survive to day 8 (Fig. 9 and data not shown). In this study, viral titers in all the affected organs from treated animals diminished after day 6 and by day 10 wt VACV is only found in nose, brain and lungs (Fig. 9). Viral replication of wt VACV in the nose, brain, lungs, ovary, spleen and liver has been previously observed in other studies (19, 87, 173). Immunohistochemistry results in this post-exposure VACV model showed less necrosis and edema blocking the air passage in all of the animals that were treated with v50ΔB13RMγ as compared to the mock-treated animals (Figs. 12 and 13).

Treatment with a similar recombinant virus, v50ΔB13RMIL-18, which expresses IL-18 (an IFN-γ inducing factor), was partially successful in protecting mice from death and the viral spread to tissues was similar to wt VACV (data not shown). This partial protection could be due to the fact that VACV expresses an IL-18 binding protein, which binds IL-18 tightly (192, 224).

Altogether these results suggest that post-exposure treatment in the VACV-WR model has more efficacy when administered in the same site of

infection and that the expression of IFN-γ is more effective than treatment with conventional vaccine strains.

Because IN vaccination with v50ΔB13RMγ was shown to prevent death in mice infected with wt VACV in this VACV-WR model, a parallel study was performed by Dr. R. Mark Buller's group in order to determine the efficacy of post-exposure protection in a mousepox model which has been useful for testing both antivirals and vaccines (24). In this study A/Ncr and C57BL/6 mice were challenged IN with a lethal dose of ECTV. Opposite to what was observed in the VACV-WR model, IN treatment with v50ΔB13RMγ was unable to prevent mortality in A/Ncr and C57BL/6 mice and all animals died by day 10. The footpad route was then chosen as the route of treatment as this mimics natural ECTV infection in an experimental setting (59). Interestingly in this ECTV model, survival was 83.3% when animals were treated 1 dpi with v50ΔB13RMγ, and a 50% survival was observed when vaccinating with the parental v50ΔB13R. Previous results have demonstrated that post-exposure protection against ECTV was dose and time dependent with a similar 83% of mice protected at 1 dpi following ID vaccination with VACV Lister (173).

Differences between the VACV and the ECTV model may be due to the events following infection using different routes of inoculation as well as disease progression. Such differences have been previously reported in an ECTV infection model (59, 65, 173). Moreover, failure to protect infected mice could be attributed to the fact that the IFN-γ BP expressed by ECTV has been shown to

inhibit the biological activity of murine IFN-γ while the IFN-γ BP expressed by VACV has low binding affinity for murine IFN-γ (161, 207, 220).

Overall the results presented in this chapter indicate that v50ΔB13RMγ is likely not working as an antiviral but as a stimulator and modulator of the immune responses. IFN-γ is known to mediate several immune responses including activation of macrophages and neutrophils, enhancement of the NK cell activity, regulation of B cell functions, stimulation of specific cytotoxic T cell immunity, chemokine gene expression, increase in expression of MHC class I and II proteins, leukocyte attraction to the site of infection as well as contributing to the growth, maturation and differentiation of many cell types (140, 163, 166, 190, 210). While v50ΔB13RMγ is a highly attenuated virus, it is still able to induce humoral and cell-mediated immune responses (136). A possible mechanism of action will be that following infection with VACV, v50ΔB13RMγ infects cells and initiates a rapid Th1 response at the site of infection, which includes macrophage activation, complement binding and opsonizing antibodies and neutrophil activation for enhanced microbial killing. This rapid response would have a "delay" effect on the infection giving the animal time to mount a more robust immune response against VACV. Further studies are necessary in order to determine the immunological mechanisms involved in this process and which cells are the key players.

This work suggests that expression of murine IFN-γ by a recombinant VACV is able to confer reduction in pathogenesis and prevent mortality in mice

infected with a lethal dose of wt VACV. These results highlight the importance of IFN-γ as a modulator of the immune response for post-exposure prophylaxis. Immunization with a recombinant virus expressing IFN-γ is known to prevent viremia and death (140, 190) as well as promote a potent immune response (136). Thus, the use of v50ΔB13RMγ could be an effective way to optimize post-exposure prophylaxis against smallpox and other orthopoxviruses infections. Moreover, together with ST-246, cidofovir and VIGIV, a recombinant VACV expressing IFN-γ could be utilized as another tool for post-exposure prophylaxis treatment.

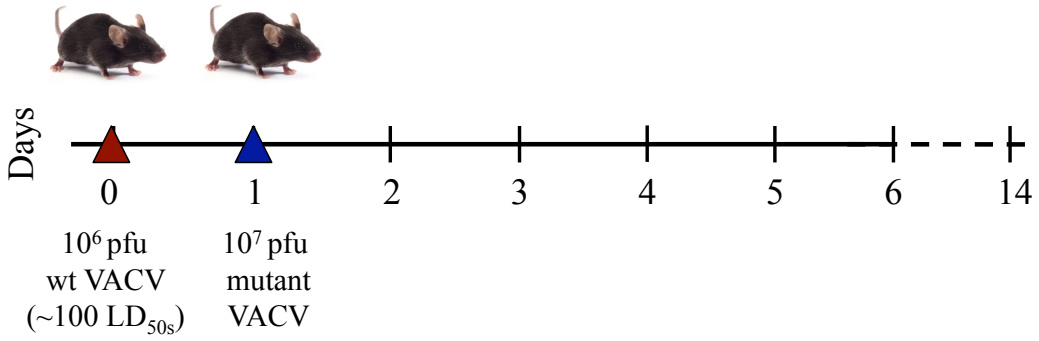

FIG. 1. Study design. Groups of 5 to 10 four-week-old C57BL/6 mice were infected intranasally with 10^6 pfu (~100 LD_{50s}) of wt VACV and treated one day post-infection with 10^7 pfu of VACVE3LΔ7C, VACVE3LΔ26C, VACVΔE3L, VACVΔE3L::ATVeIF2α, v50ΔB13RMγ and v50ΔB13RMIL-18. There were two groups of control animals, one group was infected with wt VACV and was mock-treated, and the second group of animals was mock-infected and mock-treated.

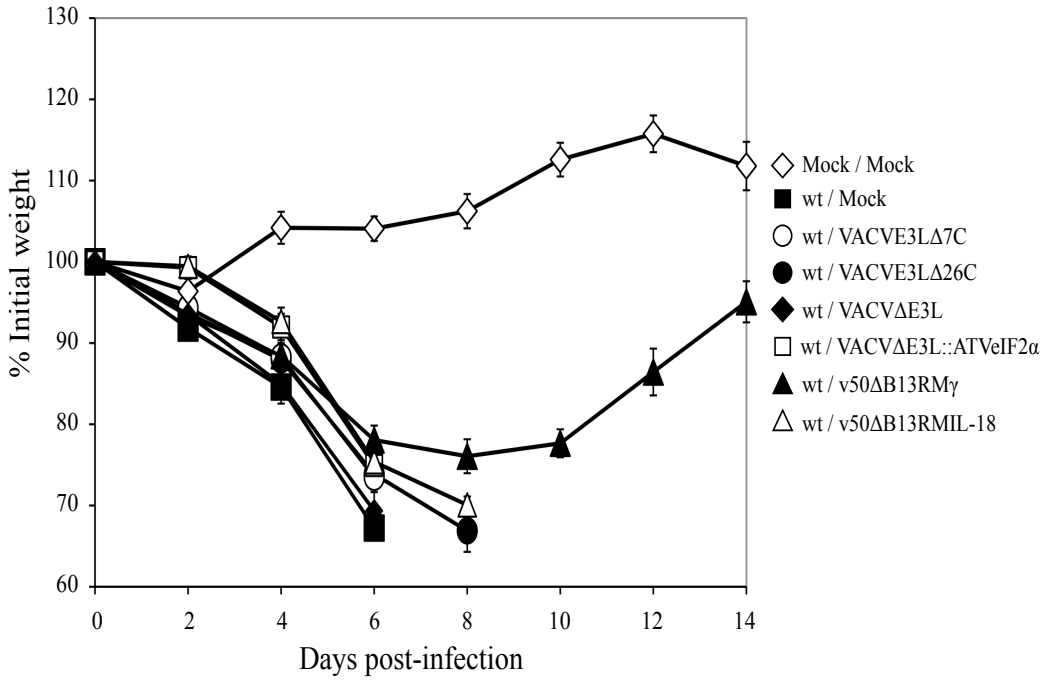

FIG. 2. Weight change after intranasal infection with a lethal dose of wt VACV and subsequent treatment with different VACV mutants. Groups of 5 to 10 four-week-old C57BL/6 mice were infected intranasally with 10^6 pfu (~100 LD_{50s}) of wt VACV and treated one day post-infection with 10^7 pfu of VACVE3LΔ7C (○), VACVE3LΔ26C (●), VACVΔE3L (♦), VACVΔE3L::ATVeIF2α (□), v50ΔB13RMγ (▲) and v50ΔB13RMIL-18 (Δ). There were two groups of control animals, one group was infected with wt VACV alone and was mock-treated (■), the second group of animals was mock-infected and mock-treated (◊). Each mouse was weighed at the indicated times. Average percentage of initial weight of the animals infected with each virus is plotted versus time (days post-infection). Lines ending prematurely indicate mortality. Error bars indicate the standard error of the mean.

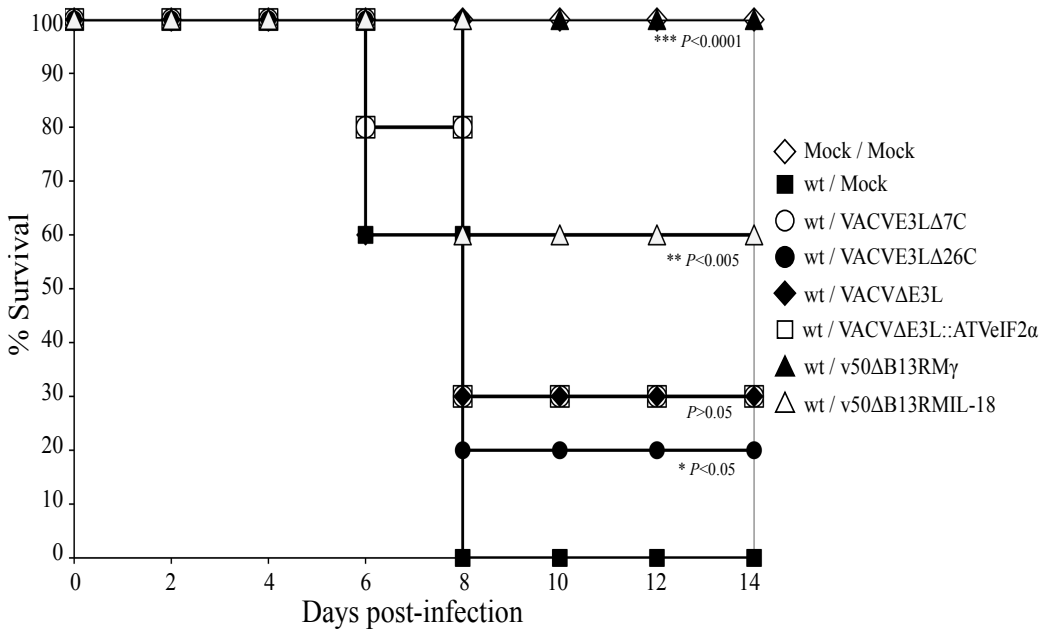

FIG. 3. Survival curve after intranasal infection with a lethal dose of wt VACV and subsequent treatment with different VACV mutants. The data represent a pool of two independent experiments using group sizes of 5 mice. Groups of 5 to 10 four-week-old C57BL/6 mice were infected intranasally with 10^6 pfu (~100 LD_{50s}) of wt VACV and treated one day post-infection with 10^7 pfu of VACVE3LΔ7C (○), VACVE3LΔ26C (●), VACVΔE3L (♦), VACVΔE3L::ATVeIF2α (□), v50ΔB13RMγ (▲) and v50ΔB13RMIL-18 (Δ). There were two groups of control animals, one group was infected with wt VACV and was mock-treated (■), the second group of animals was mock-infected and mock-treated (◊).

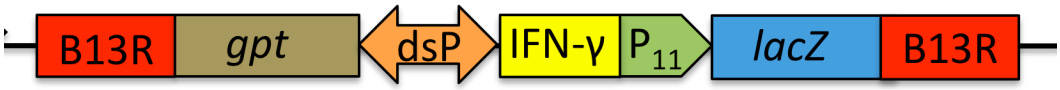

FIG. 4. Schematic representation of v50ΔB13RMγ B13R locus. The xanthine-guanine phosphorybosyltransferase (*gpt*) gene and the murine IFN-γ gene are under of the two back-to-back synthetic VACV promoters (dsP). The *lacZ* marker gene is under the P_{11} promoter. Position of the genes was obtained through DNA sequencing.

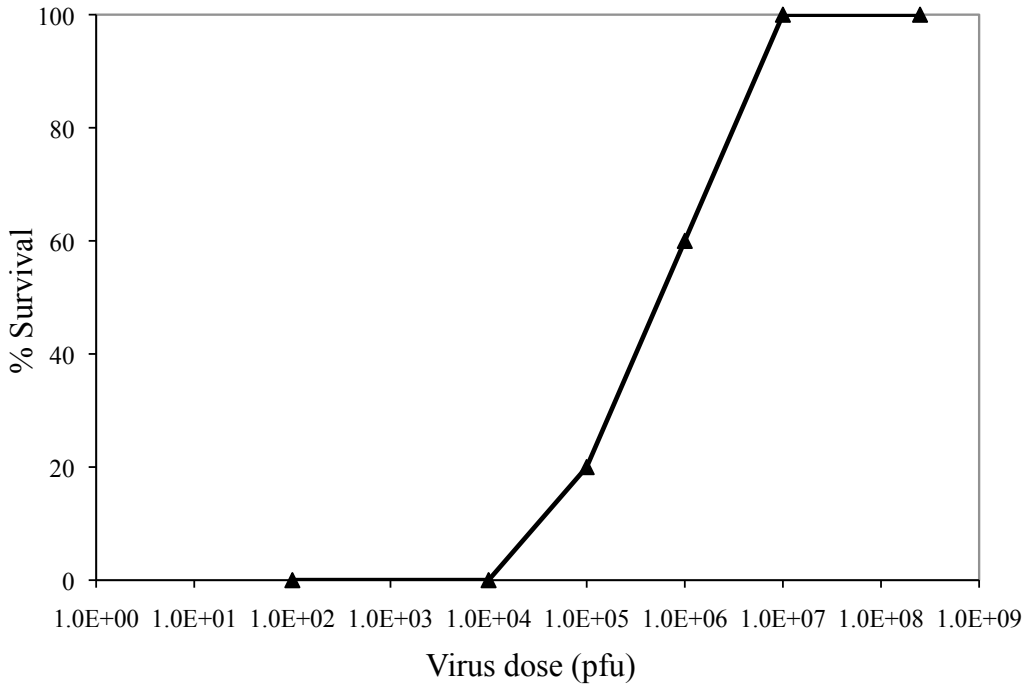

FIG. 5. v50ΔB13RMγ dose response. Groups of 10 four-week-old C57BL/6 mice were infected intranasally with 10^6 pfu (~100 LD_{50s}) and treated one day post-infection with doses of 10^2, 10^3, 10^4, 10^5, 10^6, 10^7 and 5 x 10^8 pfu of v50ΔB13RMγ (▲).

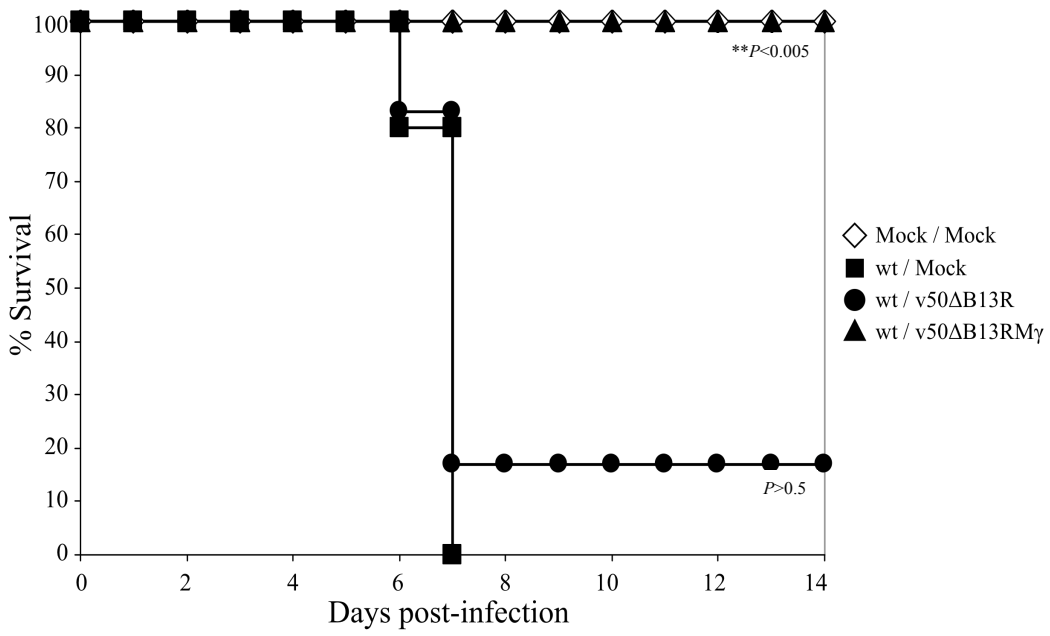

FIG. 6. Survival curve after intranasal infection with a lethal dose of wt VACV and subsequent treatment with the parental virus v50ΔB13R. Groups of 5 four-week-old C57BL/6 mice were infected intranasally with 10^6 pfu (~100 LD_{50s}) of wt VACV and treated one day post-infection with 10^7 pfu of v50ΔB13R (●), and v50ΔB13RMγ (▲). There were two groups of control animals, one group was infected with wt VACV alone and was mock-treated (■), the second group of animals was mock-infected and mock-treated (◊).

FIG. 7. Protection of wt VACV infected animals by post-exposure vaccination with v50ΔB13RMγ at one, two or three days post-infection. Groups of 5 to 10 C57BL/6 mice were infected intranasally with 10^6 pfu (~100 LD_{50s}) wt VACV. Animals were treated with 10^7 pfu of v50ΔB13RMγ at one (▲), two (●) or three (♦) days post-infection. One group was infected with 10^7 pfu (~1000 LD_{50s}) wt VACV and treated with 10^7 pfu of v50ΔB13RMγ 1 dpi (Δ). As controls, animals were mock-treated (■), or mock-infected and mock-treated (◊). (A) Comparison of survival curves was done using the log-rank test. (B) The graph indicates the relative sickness of each group during the course of the infection. Lines ending prematurely indicate death of all the animals from the group. A value of 0 indicates that all the animals from that group were healthy.

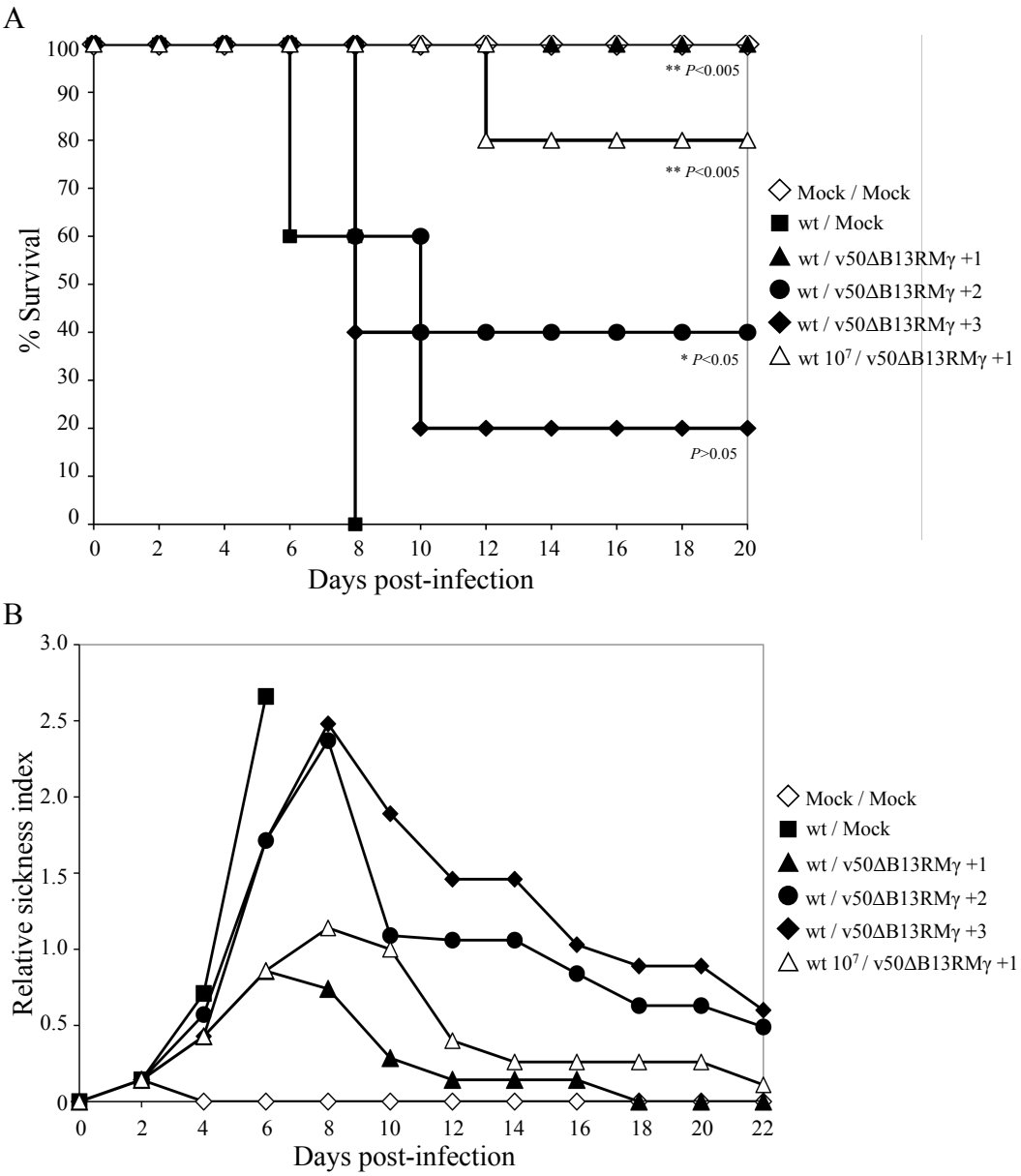
A
100
90
80
70
60
50
40
30
20
10
0
% Survival
0
2
4
6
8
10
12
14
16
18
20
Days post-infection
** P<0.005
** P<0.005
* P<0.05
P>0.05
Mock / Mock
wt / Mock
wt / v50ΔB13RMγ +1
wt / v50ΔB13RMγ +2
wt / v50ΔB13RMγ +3
wt 10^7 / v50ΔB13RMγ +1
B
3.0
2.5
2.0
1.5
1.0
0.5
0
Relative sickness index
0
2
4
6
8
10
12
14
16
18
20
22
Days post-infection
Mock / Mock
wt / Mock
wt / v50ΔB13RMγ +1
wt / v50ΔB13RMγ +2
wt / v50ΔB13RMγ +3
wt 10^7 / v50ΔB13RMγ +1

FIG. 8. Post-exposure protection of wt VACV infected animals treated with v50ΔB13RMγ using different routes of treatment. Groups of 12 to 15 C57BL/6 mice were infected intranasally with 10^6 pfu of wt VACV. Animals were treated one day post-infection with 10^7 pfu of v50ΔB13RMγ intranasally, IN (▲), intranasally using the other nostril, INON (Δ), intramuscularly, IM (○) or via scarification, SCA (●). One group of animals was infected with wt VACV and then mock-treated (■), another group was mock-infected and mock-treated (◊). (A) Comparison of survival curves was done using the log-rank test. (B) The graph indicates the relative sickness of each group of animals during the course of the infection. Lines ending prematurely indicate death of all the animals from the group. A value of 0 indicates that all the animals from that group were healthy.

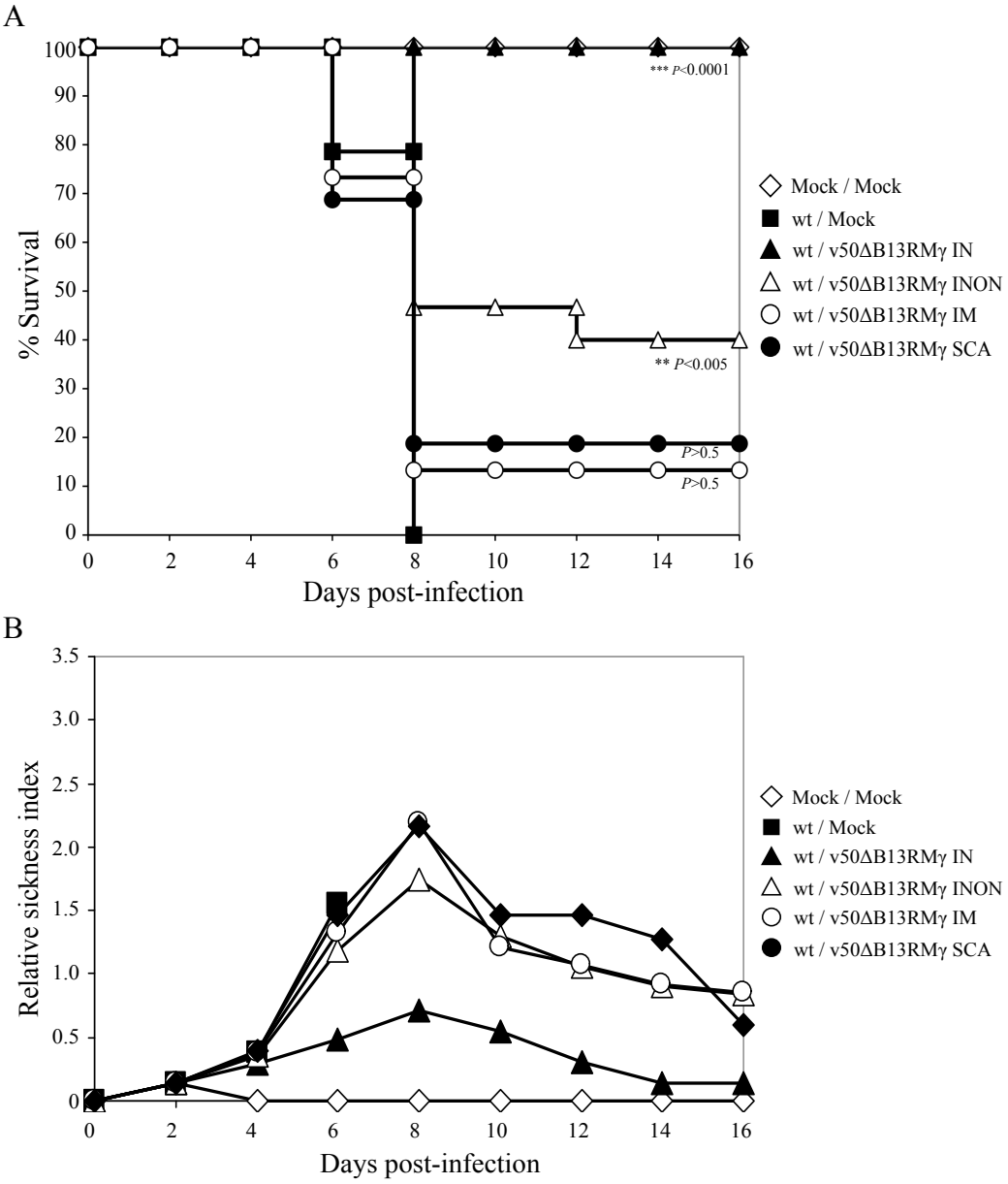
A
100
90
80
70
60
50
40
30
20
10
0
% Survival
*** P<0.0001
** P<0.005
P>0.5
P>0.5
0
2
4
6
8
10
12
14
16
Days post-infection
Mock / Mock
wt / Mock
wt / v50ΔB13RMγ IN
wt / v50ΔB13RMγ INON
wt / v50ΔB13RMγ IM
wt / v50ΔB13RMγ SCA
B
3.5
3.0
2.5
2.0
1.5
1.0
0.5
0
Relative sickness index
0
2
4
6
8
10
12
14
16
Days post-infection
Mock / Mock
wt / Mock
wt / v50ΔB13RMγ IN
wt / v50ΔB13RMγ INON
wt / v50ΔB13RMγ IM
wt / v50ΔB13RMγ SCA

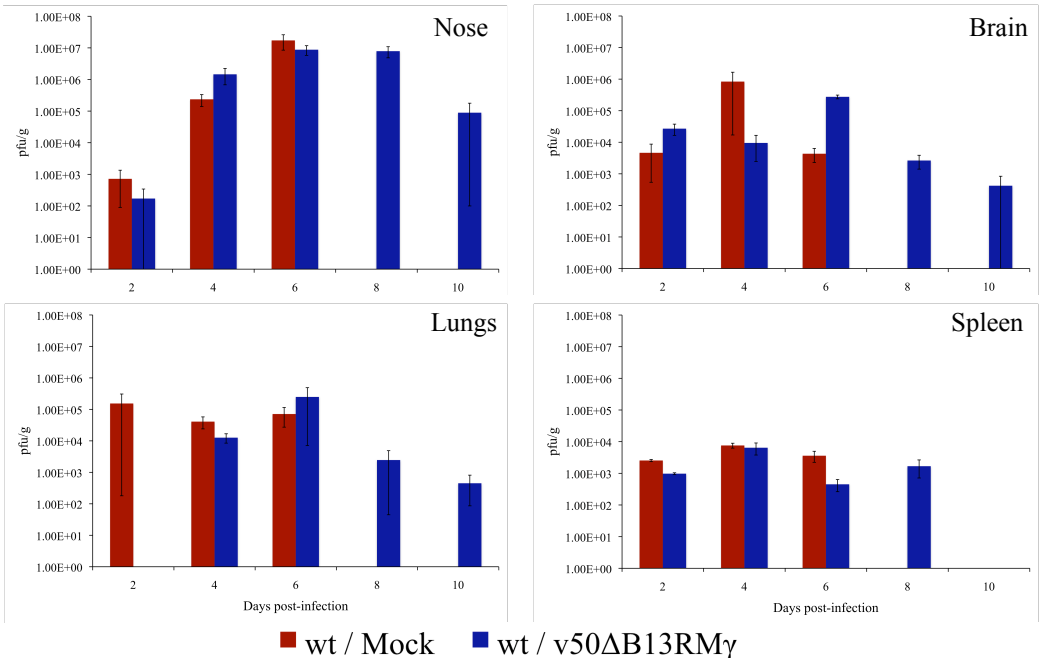

FIG. 9. Viral spread of wt VACV in infected animals. Groups of 3 C57BL/6 mice were infected intranasally with 10^6 pfu of wt VACV. Animals remained untreated or were treated one day post-infection with 10^7 pfu of v50ΔB13RMγ. Error bars indicate the standard error of the mean. Data represent two independent experiments.

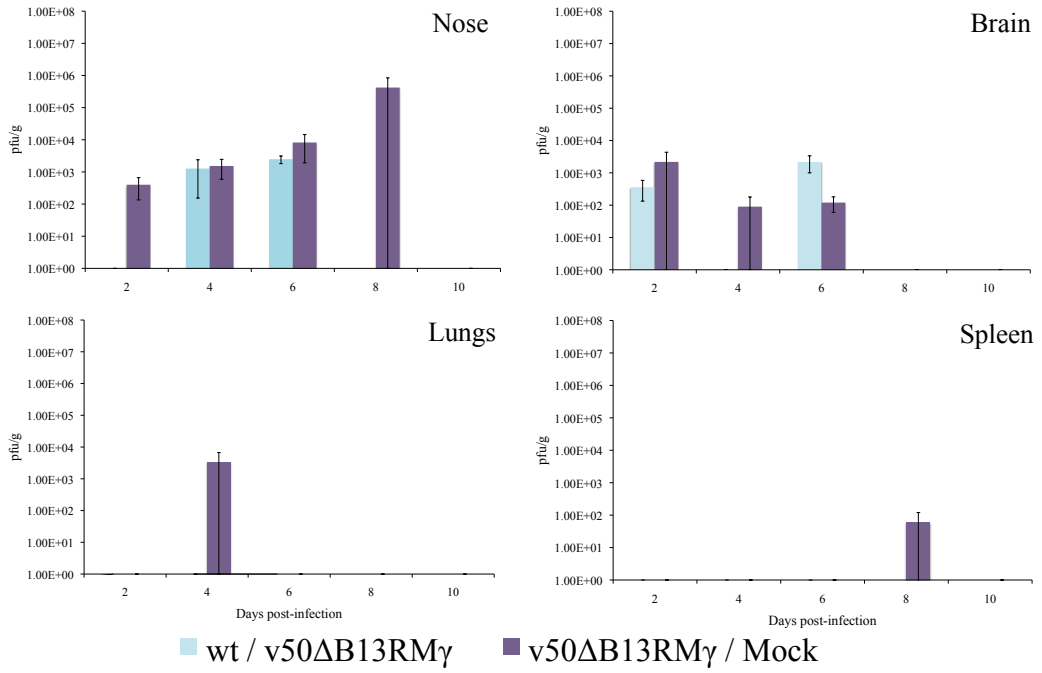

FIG. 10. Viral spread of v50ΔB13RMγ in infected animals. Groups of 3 C57BL/6 mice were infected intranasally with 10^6 pfu of wt VACV. Animals were treated one day post-infection with 10^7 pfu of v50ΔB13RMγ. Replication of v50ΔB13RMγ in the tissues from the treated group was examined by X-gal staining. Animals infected with 10^7 pfu of v50ΔB13RMγ. Error bars indicate the standard error of the mean. Data represent two independent experiments.

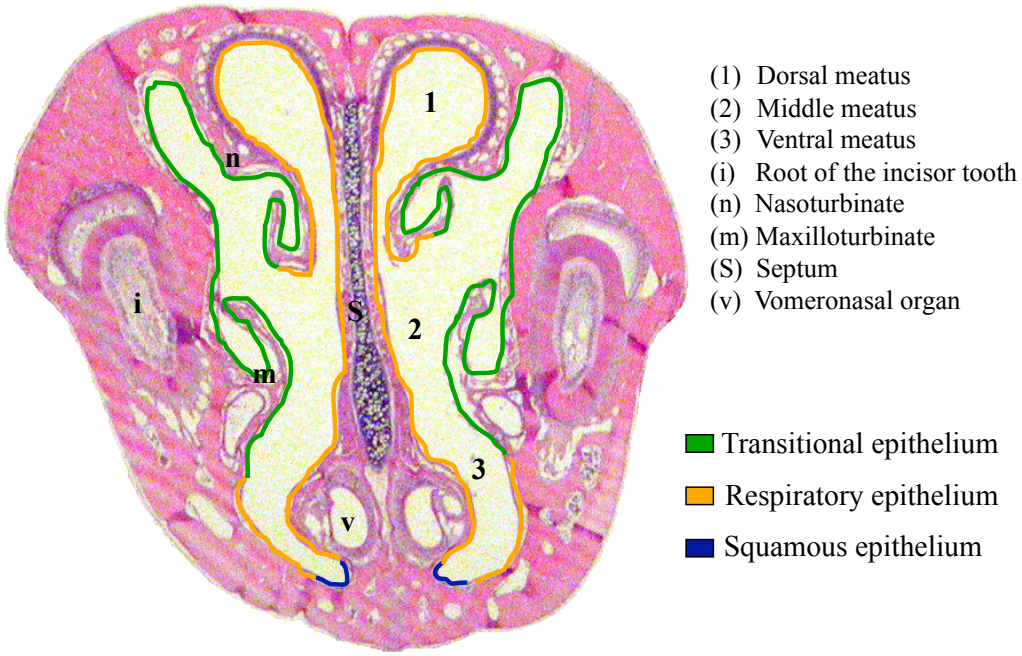

FIG. 11. Cross-section of the nose of an uninfected mouse at 2mm depth. Structures and type of epithelium found at this depth are indicated as a reference. (H&E staining).

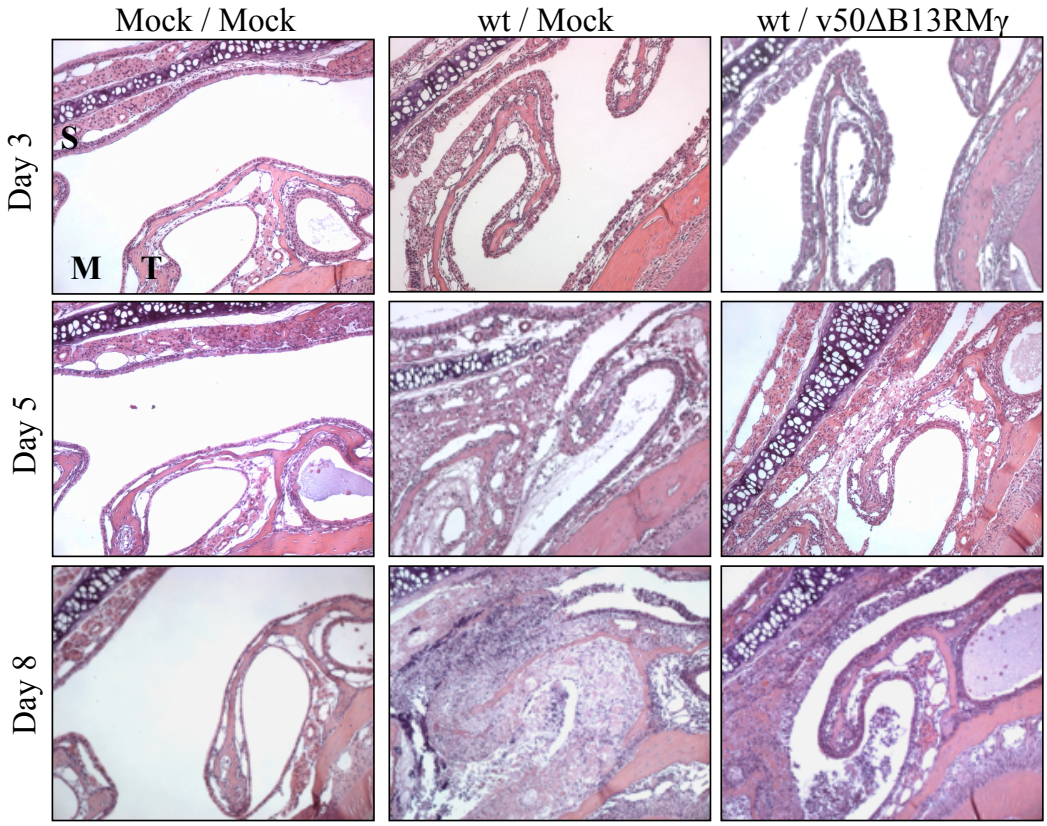

FIG. 12. Histopathologic comparison and infection progression in the nose section. Hematoxylin and eosin staining (H&E). All sections were obtained at 2 mm depth. S= septum, M=meatus (air passage) and T=Turbinate. 100X magnification.

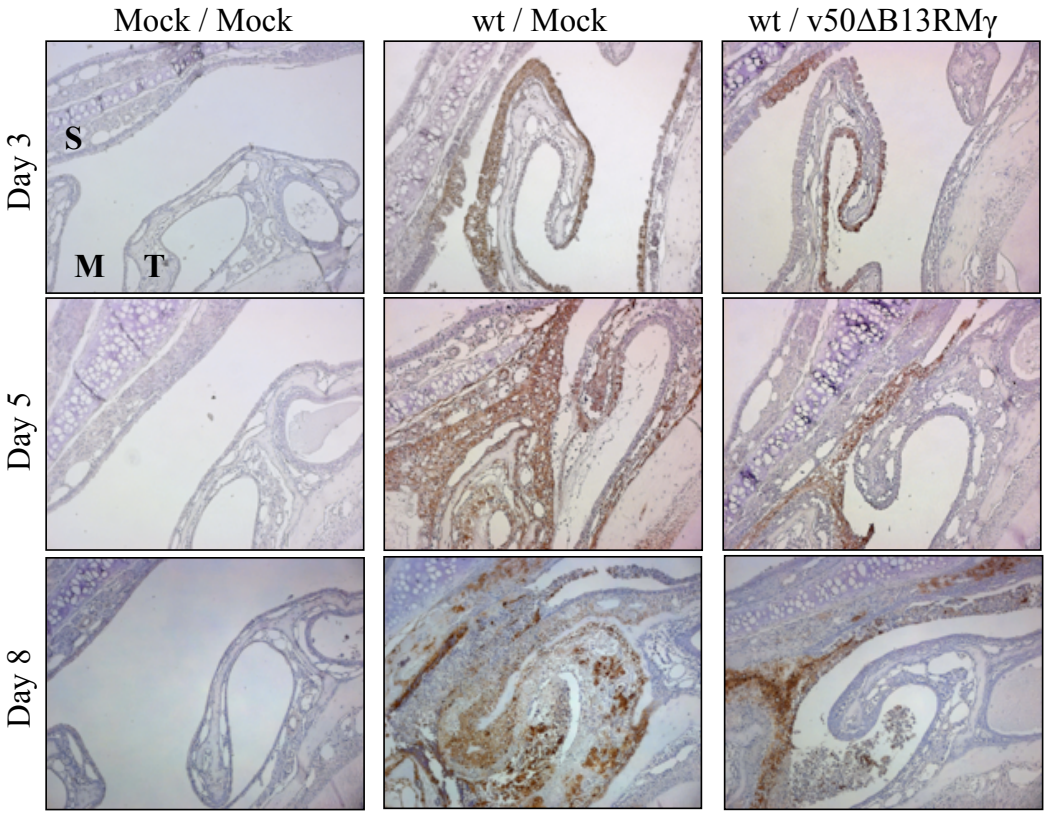

FIG. 13. Histopathologic comparison and infection progression of VACV in the maxilloturbinate section. Mice were infected IN with 10^6 pfu (~100 LD_{50s}) of wt VACV and treated one day post-infection with 10^7 pfu of v50ΔB13RMγ. All representative sections were obtained at 2 mm depth and were stained with polyclonal antibodies against VACV. S= septum, T=maxilloturbinate, M=meatus (air passage). 100X magnification.

FIG. 14. VACV replication in the whole nasal cavity section. Mice were infected IN with 10^6 pfu (~100 LD_{50s}) of wt VACV and treated one day post-infection with 10^7 pfu of v50ΔB13RMγ. Mice were sacrificed at 8 days post-infection. Sections were obtained at 2 mm depth and were stained with polyclonal antibodies against VACV. S= septum, T=maxilloturbinate, M=meatus (air passage), V=vomeronasal organ, i=incisor. 10X magnification. Bar=1mm.

A

wt / Mock
Anti-VACV

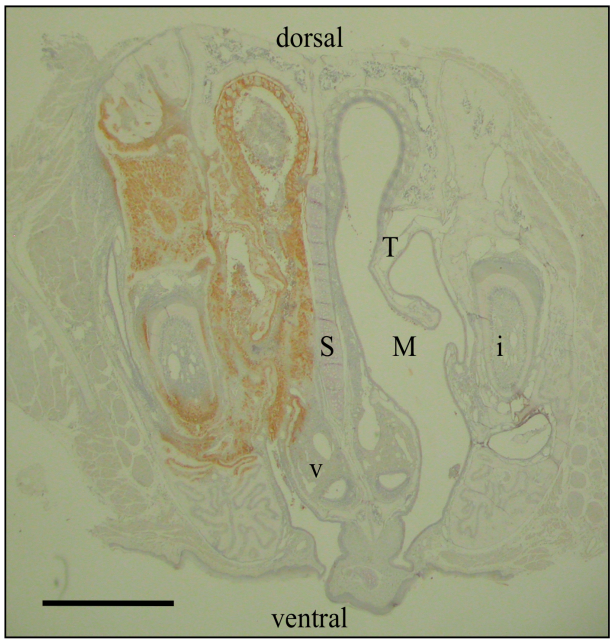

B

wt / v50ΔB13RMγ
Anti-VACV

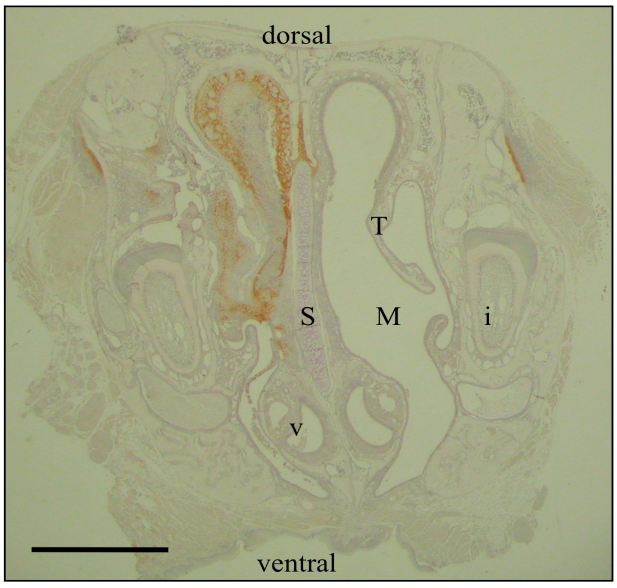

CHAPTER 2

MECHANISM OF ACTION OF A VACCINIA VIRUS EXPRESSING INTERFERON GAMMA DURING POST-EXPOSURE PROPHYLAXIS

ABSTRACT

While there is anecdotal evidence for efficacy of post-exposure vaccination against smallpox, this has not been definitively studied in humans. In this study the post-exposure prophylaxis phenomenon was analyzed using a recombinant vaccinia virus (VACV) that expresses interferon gamma (IFN-γ), which we have previously shown to prevent both morbidity and mortality in an animal model. Animals were infected intranasally with 100 LD_{50s} of wild-type VACV and then treated one day post-infection with a VACV expressing IFN-γ (v50ΔB13RMγ) or its parental (v50ΔB13R). Treatment with v50ΔB13RMγ but not the parental reduces the viral load in the olfactory bulb by day 6 post-infection although the same phenomenon was not observed in the rest of the brain. Nasal lavages were collected at different days post-infection and the immune cell populations recruited at the site of infection were analyzed using flow cytometry analysis. Results showed that at early times post-treatment the percentages of $CD8^+$ cells and $CD11b^+Gr1^+$, also known as myeloid derived suppressor cells, were increased in the group treated with v50ΔB13RMγ. Preliminary analyses of the T_H1 and T_H2 cytokine levels, showed higher levels of IL-12 and IL-5 in the treated group at early time post-infection. Moreover, the induction of the enzyme

nitric oxide synthase may be also playing a role during post-exposure prophylaxis. Overall, these results indicate that v50ΔB13RMγ may be acting as a regulator of the immune response and that this effect is most probably local affecting bystander cells at the site of infection.

INTRODUCTION

Vaccinia virus (VACV) has been used for the worldwide eradication of smallpox, a successful campaign led by the World Health Organization (WHO) in the 1970s (237). Although the effectiveness of smallpox vaccination as a preventive measure has been well documented there is not a lot of information regarding its efficacy for post-exposure treatment (157). Several antiviral drugs have been developed as alternative post-exposure treatment such as (S)-1-(3-hydroxy-2-phosphonylmethoxypropyl)-cytosine, more commonly known as cidofovir (45, 222). Other alternatives for treatment include vaccine immune globulin (VIG) (240) and ST-246, which has shown protection against monkeypox (MPXV) in animals models (209) and is regarded as one of the best choices as an antipoxviral drug (167, 185, 186, 219, 246).

While the search for antiviral treatments against, accidental or not, exposure to VACV, Variola virus (VARV) or MPXV still continues (222), the use of VACV as a recombinant vector for protein expression, vaccine development and even cancer treatment has also been explored (108, 158, 229). Currently, there are two effective recombinant vaccines, one for rabies (175) and

the one for rinderpest, a highly contagious disease with 80% fatality (80, 229, 248).

Because some complications with VACV have been observed specially in immunocompromised and immunosupressed people (74), there is a need to understand the immune responses upon exposure to the virus. While some cytokines such as interleukin 2 (IL-2), tumor necrosis factor alpha (TNF-α) and interferon gamma (IFN-γ) have shown to decrease virulence, others including interleukin 4 (IL-4) increase virulence and morbidity (70, 163, 191, 212).

Previous studies have demonstrated that VACV expressing IFN-γ can be used as an adjuvant as well as an attenuating agent for the production of live vaccines that are both safe and have high efficacy (80, 125). Moreover, expression of IFN-γ has also been used to influence the course of bacterial infection, were VACV as a vector was more effective than fowlpox (37). Other viruses such as bovine herpesvirus-1 (BHV-1) have also been used to express IFN-γ and the stability of the BHV-1/IFN-γ virus as well as its immunomodulating effects studied upon primary infection and following reactivation of a latent infection (188). Moreover, expression of human IFN-γ by a simian immunodeficiency virus (SIV_{HyIFN}) has shown reduced viral loads in the blood of rhesus macaque monkeys that were infected with virus, even in the presence of a progressive deletion of the IFN-γ gene. These results suggest that the early immune system activation by SIV_{HyIFN} was able to protect against new emerging SIV viruses lacking full expression of the lymphokine (79).

Expression of IFN-γ in bacteria has also been studied. Administration of a recombinant IFN-γ produced in *E. coli* at the time of a primary immunization with vesicular stomatitis virus glycoprotein (VSV-G) for example, has shown to enhance a secondary antibody response even a low doses (5).

The use of recombinant murine IFN-γ to prevent lethal respiratory VACV infection has also been successful (140) although the challenge dose of VACV was significantly lower as the ones used in this study.

The previous chapter described the use of v50ΔB13RMγ, a recombinant VACV expressing IFN-γ (v50ΔB13RMγ), for post-exposure treatment in a VACV animal model. This recombinant virus was100% effective in protecting mice infected with 100 LD_{50s} of wt VACV when administered 1 dpi reducing the morbidity symptoms in the treated animals. Moreover, while deletion of the B13R serpin homolog gene attenuates VACV (136, 137), it is not responsible for protecting mice against a lethal dose with VACV as it was noted in Chapter 1.

While v50ΔB13RMγ replicates to high titers in tissue culture, it is a highly attenuated virus and replicates at low levels in tissues of infected animals ((136) and data from Chapter 1). IFN-γ is known to regulate the immune system (Fig. 15) by activating macrophages and neutrophils, enhancing NK cells activity, regulating the B and T cell responses to antigens, stimulating specific cytotoxic T cells, promoting chemokine expression, as well as contributing to the protection against viral pathogenesis (140, 163, 166, 190, 210). Mice bearing a disrupted IFN-γ gene have impaired production of macrophage antimicrobial products,

reduced major histocompatibility complex (MHC) class II expression and are more vulnerable to infections against pathogens such as *Mycobacterium bovis* (42) and *Plasmodium falciparum* (6). It has also been observed that during a VACV infection IFN-γ inhibits VACV replication through the induction of nitric oxide synthase (iNOS) in murine macrophages which leads to the production of nitric oxide (NO) from the guanidine nitrogen of L-arginine (99). IFN-γ is the only known cytokine to induce NOS in macrophages, production of NO in turn affects DNA replication of VACV preventing virus particle formation (99, 113).

The purpose of this chapter is to determine v50ΔB13RMγ mechanism of action and the characterization of the immune response following post-exposure prophylaxis in a VACV-WR animal model. As noted in Chapter 1, although all animals infected with wt VACV survived upon treatment with v50ΔB13RMγ, VACV was found present in all the organs examined suggesting that this virus is acting more as an immunoregulator than as an antiviral. Thus, v50ΔB13RMγ could be indeed orchestrating some immune responses that could lead to less morbidity and 100% mortality in this animal VACV model.

MATERIALS AND METHODS

Recombinant viruses. The Western Reserve (WR) strain of VACV was used as the parental virus for these studies. The recombinant VACV expressing IFN-γ (v50ΔB13RMγ) virus was constructed as previously described (136). This virus expresses VSV-G at the TK locus and *lacZ*, *gpt*, and murine IFN-γ at the

B13R site. Construction of the parental virus (v50ΔB13R) has already been described (137).

Cell culture. Viruses were amplified in Baby Hamster Kidney 21 (BHK) cells and partially purified by pelleting through a 36% sucrose pad, as previously described in the literature (15, 54). BHK and Rabbit Kidney 13 (RK13) cells were cultured in Eagle's Minimal Essential Medium (MEM, Gibco, BRL) containing 5% fetal bovine serum (FBS, Hyclone), 50 μg/ml of gentamycin, and 0.1 mM nonessential amino acid solution (Gibco, BRL) and vitamin supplements. Both BHK and RK13 cells were incubated at 37˚C with 5% CO_2.

Mice. Four-week old female C57BL/6 from Charles River Laboratories and NOS2-/- mice (B6.129P2-*Nos2*^{tm1Lau}/J) from The Jackson Laboratory were housed at the Arizona State University Department of Animal Care and Technologies according to IACUC regulations. Each cage contained a maximum of 5 mice and a separate cage was used for each experimental condition.

***In vivo* infections.** An anesthetic cocktail containing xylazine (7.5 mg/ml), acepromazine maleate (2.5 mg/ml), and ketamine (37.5 mg/ml) was prepared. Approximately 1-μl of cocktail was injected intramuscularly per gram of body weight (19). Following anesthesia, one naris was infected with a 5-μl dose of 10^6 pfu (~100 LD_{50s}) of wt VACV. Mice were treated 1 dpi with 10^7 pfu of treatment virus administered intranasally (IN) into the same naris as the challenge virus. Disease symptoms and animals' health were monitored every other day for the length of the experiment. The IACUC protocol number 08-970R was followed.

Weight loss. Weight loss was determined by weighing each mouse on alternate days. The percent weight gain or loss was determined and animals that lost more than 30% of their original body weight were euthanized and considered dead from the challenge.

Recovery of virus from tissues. Animals were infected IN with 10^6 pfu of wt VACV (Day 0) and treated with 10^7 pfu of v50ΔB13RMγ or 10^7 pfu of v50ΔB13R at 1 dpi. On days 2 and 6 post-infection, five animals from each group were euthanized and then immediately dissected. The olfactory bulb was separated from the cerebrum/cerebellum and samples were immediately frozen in liquid nitrogen and then stored at -80°C. A 10% homogenate was prepared by adding 1 mM Tris pH 8.8 with gentamycin. The tissues were then homogenized using a PCR tissue homogenizing kit (Fisher). All homogenates were subjected to three rounds of freezing (-80°C)-thawing for 30 minutes on ice and then quick thawing (37°C). After three rounds of freezing-thawing, samples were subjected to a 7 minute spin using a tabletop centrifuge at 700 x *g* at 4°C to remove all cell debris. After centrifugation, supernatants were retained and dilutions were performed for duplicate plaque assays on RK13 cells. Thirty hours post-infection, the replicas were stained with crystal violet to determine the viral load within the tissue (pfu per gram of tissue).

Immunohistochemistry. Tissues were perfused with phosphate-buffered saline (PBS) via cardiac perfusion followed by fixation with 10% formalin. After the soft tissue was removed the skull was decalcified using ethylene glycol

tetraacetic acid (EGTA). The skull was embedded in paraffin and sliced at 3 μm thickness using a microtome. Deparaffinized tissue sections of the nose were incubated with 2% H_2O_2 in methanol for 10 minutes to quench endogenous peroxidases and then rinsed in PBS. Detection of VACV antigen was done using rabbit anti-VACV, VECTASTAIN Elite ABC kit (Rabbit IgG) and the 3,3'-diaminobenzidine (DAB) Substrate Kit from VECTOR Laboratories following the manufacturer's protocol. Detection of neutrophils was done using the rat anti-mouse neutrophils (MCA771GA, clone 7/4) monoclonal antibody by AbD Serotec. Biotinylated anti-rat IgG (mouse absorbed) made in rabbit and the VECTOR NovaRED Substrate Kit were used for the detection of neutrophils following manufacturer's protocol.

Harvesting and processing of sinus lavages. Mice were euthanized by intraperitoneal injection and held in the nose-down position. Following decapitation, the nasal lavages were done by introducing a single lumen catheter connected to the trachea and a lavage of 1 ml of sterile phosphate-buffered saline (PBS) with 1% fetal bovine serum (FBS) and collected below the nose.

Flow cytometry. Samples from the nasal lavages were centrifuged, the pellet resuspended, pooled (n=5) and filtered using a 70μm strainer. Following the addition of red blood cell lysis buffer, the samples were centrifuges and the pellet resuspended in FACS buffer. Cell counts were performed using a haemocytometer. Cells were then stained with FITC-conjugated anti-CD49b/Pan-NK cells (clone DX5), PE-Texas Red conjugated anti-CD45R (clone RA3-6B2),

APC conjugated anti-CD3e (clone 145-2C11), PB-conjugated anti-CD4 (clone RM4-5), APC-Cy7 conjugated anti-CD8a (clone 53-6.7), PerCP-Cy5.5 conjugated anti-Cd11b (clone M1/70), PE-Cy7 conjugated anti-Ly6G/Ly6C (clone RB6-8C5), PE conjugated anti-Ly6C (clone AL-21, PE-Cy7 anti-Ly6G (clone 1A8) or isotype controls using standard techniques. All antibodies and isotype controls were purchased from BD Biosciences. Stained cells were subsequently analyzed using the FACS Diva software (BD Biosciences).

Multiplexed microsphere cytokine immunoassay (Bio-Plex assay). Samples from the nasal lavages were collected and treated as above. The supernatants were assayed for the presence of cytokines using a multiplexed coupled magnetic beads immunoassay customized kit containing the Bio-Plex Pro Mouse cytokine T_H1/T_H2 assay (Bio-Rad, catalog number M60-00003J7) as well as detection antibodies for IL-6, IL-12(p40), KC, MIP-1 alpha, MIP-1 beta, RANTES and MIP-2, all from Bio-Rad. The assay was done following manufacturer's protocol.

Data analysis. Errors band indicate the standard error of the mean. Survival analyses were done using Kaplan-Meier curves and log-rank test analyses. The differences between experimental groups were analyzed using the one way ANOVA test. All analyses were performed using the statistical software program GraphPad Prism (version 5.0c for Macintosh).

RESULTS

Neutrophil recruitment following intranasal VACV infection. IFN-γ is known to activate neutrophils depending on the stimuli and environmental conditions (57). Previous studies have shown that recombinant IFN-γ does not have a chemotactic effect on neutrophils or macrophages both *in vitro* or *in vivo* (27) but rather it may act as a signal to allow adherence of neutrophils at the site of infection (57). Neutrophils can be observed as early as 3 dpi in both mice infected with 100 LD_{50s} of wt VACV and mice that were infected with 100 LD_{50s} of wt VACV and treated 1 dpi with 10^7 pfu of v50ΔB13RMγ (Fig. 16A). By day 8 post-infection, neutrophils can be clearly observed in areas where VACV is present. This is accompanied by tissue destruction, edema and blockage of the air passage in mice that were infected but not treated with v50ΔB13RMγ (Fig. 16B).

Treatment with v50ΔB13RMγ reduces viral replication in the olfactory bulb of animals infected with wt VACV. VACV virus replication has previously been detected in the brain from both untreated and treated animals (Chapter 1). Because of the importance of the olfactory bulb (Fig. 17) in VACV pathogenesis during an intranasal infection, it was required to assess if there was any difference in VACV replication between untreated animals and animals treated with v50ΔB13RMγ. A histopathologic comparison at 8 dpi showed VACV in the olfactory epithelium and the glomerular and outer plexiform layer of the olfactory bulb in untreated animals while VACV antigen was only present in the olfactory epithelium of treated animals (Figs. 18, 19A and 19B). To further

investigate a difference in viral load between animals infected with wt VACV and animals treated with either the parental virus v50ΔB13R or v50ΔB13RMγ, both the olfactory bulb and the cerebrum/cerebellum regions were harvested at 2 and 6 dpi. Following homogenization of the samples and three rounds of freeze/thaws, viral titers were obtained for each of the samples from each group. A statistical significant difference was observed between the viral load in the olfactory bulb of the treated group with v50ΔB13RMγ and the untreated group at 6 dpi (Fig. 20A). Viral replication of VACV was observed in both untreated and treated groups in the olfactory bulb at 2 dpi and in the cerebrum/cerebellum region of the brain at 2 and 6 dpi (Fig. 20B).

Production of nitric oxide (NO) by NOS2 might play a role in post-exposure prophylaxis. While previous work has provided insight about the importance of NO production for the inhibition of VACV replication, all these studies required induction by IFN-γ or expression of an iNOS gene in a recombinant VACV (99, 113, 152, 200, 201). In Chapter 1 of this dissertation it was shown that mice infected 10^6 pfu of wt VACV and then treated with 10^7 pfu of v50ΔB13RMγ 1 dpi had less morbidity as well as 100% survival. In an attempt to determine the importance of NO in the post-exposure prophylaxis model, NOS2-/- mice were infected with 10^2, 10^4 and 10^6 pfu of wt VACV and then treated 1 dpi with 10^7 pfu of v50ΔB13RMγ. Infection with 10^2 pfu of wt VACV and treatment with v50ΔB13RMγ did not cause any morbidity and all the animals survived (Fig. 21) similar to what is observed in the parental C57/BL6 mice (data

not shown). On the other hand, infection with 10^4 or 10^6 pfu of wt VACV and treatment with 10^7 pfu of v50ΔB13RMγ 1 dpi lead to only 60% of survival as compared to 100% survival in the parental mice (data not shown and Chapter 1).

Proliferation of $CD8^+$ but not $CD4^+$ T cells at 2 dpi in response to treatment with v50ΔB13RMγ. It has previously been observed that infection with VACV induces a strong $CD8^+$ T cell response in both C57BL/6 and Balb/c mice (243) and this response is thought to be the most important response in controlling a poxvirus infection (218). In order to evaluate if treatment with a recombinant virus that expresses IFNγ promotes the expansion of either $CD4^+$ or $CD8^+$ T cells, C57BL/6 mice infected with 10^6 pfu of VACV were mock-treated or treated with 10^7 pfu of v50ΔB13RMγ 1 dpi. Control animals were either mock-infected with or infected with 10^6 pfu of wt VACV and mock-treated or treated with v50ΔB13RMγ or v50ΔB13R 1 dpi. Nasal lavages were collected at days 2 and 6 post-infection and analyzed by FACS. $CD3^+$ cells were further analyzed by grouping them into $CD4^+$ or $CD8^+$ T cells. At 2 dpi the population of $CD8^+$ T cells was higher in the group infected with wt VACV and treated with v50ΔB13RMγ compared to the untreated and control groups (Fig. 22).

Infection of animals with wt VACV reduces the $Gr1^+$ $B220^+$ cell population at the site of infection. While examining the distinct populations of immune cells, it was noted a population of $Gr1^+$ $B220^+$ cells in the nasal lavages of animals that were mock-infected and then mock-treated 1 dpi as well as in the animals that were mock-infected and then treated with 10^7 pfu of v50ΔB13RMγ 1

dpi. This population of cells is not present in either the group that was infected with wt VACV and then mock-treated or the group that was infected with wt-VACV and then treated with 10^7 pfu of v50ΔB13RMγ 1 dpi (Fig. 23).

Increased amount of the myeloid derived suppressor cells population ($Gr1^+CD11b^+$) at early time post-infection in animals treated with v50ΔB13RMγ. While no significant differences were found in the nasal lavages from untreated or treated animals in the population of $CD49^+$ (NK) cells (Fig. 24), a greater number of $GR1^+CD11b^+$ cells was observed at 2 dpi in the group of animals that were infected with 10^6 pfu wt VACV and then treated with v50ΔB13RMγ (Fig. 25). By day 6 post-infection the percentages of $Gr1^+Cd11b^+$ cells were similar in both untreated and treated groups. These $Gr1^+Cd11b^+$ cells, also known as myeloid derived suppressor cells (MDSCs), have been previously described in the literature as a heterogeneous population that includes myeloid progenitor cells and immature macrophages, granulocytes and dendritic cells (75).

Analysis of the T_H1 cytokines show an increase of IL-12 at early times post-infection in mice treated with v50ΔB13RMγ. T_H1 and T_H2 cytokines (Fig. 26) were examined using the supernatants of the nasal lavage samples from mice that were either mock-infected and mock-treated or infected with wt VACV and either mock-treated or treated with v50ΔB13RMγ as previously described. Analysis of the T_H1 cytokines revealed no major differences in the levels of IFN-γ and TNF-α while IL-2 levels were undetectable in all the groups examined. On the other hand, IL-12 levels were statistically significant ($P<0.01$) at 2 dpi when

compared with the mock-infected/mock-treated group. Levels of IL-12 were similar among all groups at 4 and 6 dpi (Fig. 27).

T_H2 cytokine, IL-5, increases at early times post-infection in mice treated with v50ΔB13RMγ while IL-10 is upregulated at late-times post-infection in both untreated and treated groups. While levels of IL-4 were undetected in all the samples analyzed, analysis of the other T_H2 cytokines in the post-exposure prophylaxis model revealed increased levels of IL-5 in the mice treated with v50ΔB13RMγ at 2 dpi. IL-5 levels were statistically significant ($P<0.01$) when compared with the mock-infected/mock-treated group and the group that was mock-infected and then treated with v50ΔB13RMγ at 1 dpi. At 6 dpi, high IL-10 levels were observed in both untreated and treated groups in comparison with the mock-infected/mock-treated group and the group that was mock-infected and then treated with v50ΔB13RMγ at 1 dpi ($P<0.001$) (Fig. 28).

Higher levels of chemoattractants are observed in both untreated and treated groups at 6 dpi. The supernatants of the nasal lavages were also analyzed for the expression of chemoattractants using the Bio-Plex assay. By 6 dpi, levels of the macrophage inflammatory protein (MIP) 1 and 2 as well as the regulated upon activation, normal T cell expressed (RANTES) protein were higher in both the wt VACV infected/untreated group and the group treated with v50ΔB13RMγ than the levels in the mock-infected/mock-treated group or the mock-infected/v50ΔB13RMγ treated group ($P<0.01$ to $P<0.0001$) (Fig. 29).

Higher levels of IL-6 at early times post-infection in mice infected with wt VACV and then treated 1 dpi with v50ΔB13RMγ. When analyzing the levels of IL-6 in the different groups, higher levels were noted at 2 dpi in the group that was infected with wt VACV and then treated with v50ΔB13RMγ at 1 dpi as compared with the mock-infected/mock-treated group ($P<0.05$). Levels of IL-6 were similar among all groups at days 4 and 6 post-infection (Fig. 29).

DISCUSSION

In this chapter the mechanism of action of v50ΔB13RMγ as a post-exposure prophylaxis agent was fruther evaluated regarding its role in the spread of VACV to the central nervous system, recruitment of immune cells to the site of infection and the secretion of signaling molecules.

The use of cytokines as tools for modulating the immune response in VACV has been widely study in different systems (136, 140, 191, 212). Of these cytokines, IFN-γ has been shown to be an effective adjuvant leading to both potent humoral and cell-mediated immunological response (5, 136). IFN-γ is an inducible cytokine that plays a very important role in inhibiting virus replication and possess a diverse array of physiological activities (214). This cytokine is synthesized by $CD4^+$ T_H1 cells, $CD8^+$ T cells and NK cells following a response to antigens or mitogens (125, 214) and plays and has a key role in both innate and adaptive immune responses (210, 214).

Following the discovery of v50ΔB13RMγ as the best candidate for post-exposure prophylaxis in a VACV-WR model, the next step was to elucidate how this recombinant VACV regulates the immune response. Previous studies by Kohonen-Corish *et al.*, have shown that expression of IFN-γ in VACV promotes recovery from infection in both normal and immunodeficient athymic nude mice with an accompanying reduced viral replication indicating that expression of IFN-γ causes attenuation and pathogenicity reduction in the animal model (125). While Kohonen-Corish *et al*. study was done by expressing IFN-γ in the TK locus, similar results were observed when expression of murine IFN-γ was done in the B13R locus (136). Moreover, expression of IFN-γ in other viruses such as the Simian immunodeficiency virus has also led to an increased attenuation (79).

While research on IFN-γ has focused primarily on its interaction with cells of the secondary immune response, the role of IFN-γ as a modulator of the innate immune response has been overseen (57). Because inflammation usually follows a VACV infection, immunohistochemistry of the nose section was used to compared if there were any differences in the amount of neutrophils, the major cell type mediating acute inflammatory responses (2), recruited to the site of infection. By 3 dpi neutrophils are present and associated with both VACV-infected respiratory epithelium covering the septum and the transitional epithelium surrounding the maxilloturbinate. By 8 dpi, less tissue destruction and edema can be clearly observed in the representative histological sample from the treated group as compared with the sample from the mouse that was infected with

wt VACV but remained untreated. These results indicate that neutrophils are recruited at the site of infection following wt VACV infection intranasally although the potential role of v50ΔB13RMγ in the infected tissue still remains to be elucidated as IFN-γ has been shown to alter neutrophil function by activation of signaling pathways that use Ca^{2+} and regulation of gene expression including MHC II, chemokines and surfaces markers (57). Moreover, IFN-γ can act as a priming agent preparing neutrophils for enhanced activity upon secondary stimulation as well as induce the production in neutrophils of nitric oxide (NO) via the inducible nitric oxide synthase (iNOS) enzyme (57, 150, 233, 245).

Because replication of VACV in the central nervous system can lead to the a severe form of encephalitis in humans (76) and neurovirulence in mice (18), the next step was to determine if treatment with v50ΔB13RMγ has an effect in the viral invasion of the central nervous system. Different studies have shown how some viruses enter the central nervous systems following intranasal inoculation. Among these viruses are the vesicular stomatitis virus, rabies virus, mouse hepatitis virus and herpes simplex virus type 1 as well as cowpox virus (146, 180). The mechanism how these viruses invade the central nervous system varies as they can enter via the olfactory nerve, which connects to the olfactory bulb, via the trigeminal system or both (180). In the case of VACV this mechanism has not been completely elucidated. Poxvirus replication in the olfactory bulb has previously been observed at 6 hours post-infection following intranasal inoculation of MVA in C57BL/6 mice (189), intranasal inoculation with cowpox

virus in BALB/c mice (146) as well as in *ex vivo* experiments using VACV vsC9, encoding the β-gal gene under control of the VACV TK early promoter (21). Recent data from our lab have shown blood brain barrier (BBB) permeability in mice infected intranasally with wt VACV (Dr. Karen Denzler, unpublished data) while others have shown that the integrity of the BBB plays a important role in post-vaccinal encephalitis (76). Infection of the glomerular layer and the outer plexiform layer of the olfactory bulb can be clearly observed in a representative sample from a group of mice that were infected with wt VACV but remained untreated in comparison with the v50ΔB13RMγ treated sample (Fig. 19). These results correlate with the viral load observed in the olfactory bulb of the treated group as compared with the untreated (Fig. 20). While there was a difference between the olfactory bulbs of both groups, the viral load of the cerebrum/ cerebellum was similar in both. These results suggest that v50ΔB13RMγ could be delaying infection of the olfactory bulb while there could be another mechanism by which VACV enters the cerebrum/cerebellum region possibly with the participation of nonneuronal cells. This was further supported by preliminary data following bilateral bulbectomy, in which depletion of the olfactory bulb delayed but did not prevent death of mice infected with wt VACV (data not shown).

To further characterize the role of IFN-γ in the post-exposure prophylaxis model, iNOS, one of the more characterized IFN-γ inducible genes, was analyzed using iNOS knock-out mice (NOS2-/-). The present results show a partial effect of v50ΔB13RMγ in the survival of the mice which would indicate that iNOS is

required but not necessary for survival in the post-exposure prophylaxis model. These results correlate with other studies that have shown that treatment of mice with N^G-methyl-L-arginine (NMA), an inhibitor of NO production, did not influence the course of VACV infection (201) suggesting that while NO production controls viral replication, other factors could be sufficient for a complete clearance of the virus (200).

Induction of iNOS by IFN-γ leads to NO production in a different array of cells such as resident macrophages, fibroblasts, epithelial cells, keratinocytes, hepatocytes, mesangial cells and tumor cells (112, 113). Moreover, although IFN-γ is not consider a traditional activator of neutrophils, it enhances the production of reactive oxygen species (ROS) in the presence of a secondary stimulus (57) and expression iNOS as well as NO production has been observed in neutrophils following induction with IFN-γ in a concentration dependent manner (245). This induction has also been observed in mouse RAW 264.7 macrophage-like cells where viral replication of VACV can be inhibited by the production of NO (113). Similarly, infection of sublethally irradiated CBA/H athymic nude mice with a recombinant VACV expressing iNOS under the control of the early-late P7.5 promoter indicated that this virus is highly attenuated even following intracerebral infection (200). Attenuation was also observed when using a recombinant VACV virus expressing iNOS under the control of *Escherichia coli LacI* (152).

In a post-exposure prophylaxis context, production of NO by iNOS following treatment with v50ΔB13RMγ could increase the levels of nitrite after

infection, which is known to correlate with inhibition of VACV DNA replication and late gene protein synthesis, while no effect has been observed in the expression of early genes (99, 152).

In order to further examine the mechanism of action of v50ΔB13RMγ in the treated groups, the population of immune cells in each of the treated and untreated groups was evaluated using FACS analysis. Results showed an increase in the $CD8^+$ T cell population in the treated group by 2 dpi in comparison to the untreated group and controls. Although it has previously been suggested that $CD8^+$ T cells are not essential for wt VACV (WR) clearance (97, 244), these cells seems to be playing a role in preventing morbidity and reducing mortality although the mechanisms are not clearly understood. Thus, $CD8^+$ T cells role in post-exposure prophylaxis could be similar as it has previously been observed in other studies although $CD8^+$ T cells specificity for VACV needs to be determined.

While examining the population of immune cells that were recruited at the site of infection, it was noticed the reduction in numbers of a $Gr1^+B220^+$ cell population in the groups that were infected with wt VACV (Fig. 23). While such a specific population has not previously been described, $Cd11c^+B220^+Gr1^+$ cells in mice are known as plasmacytoid dendritic cells, which are able to produce IFN-α as a response mechanism to viral infection (10). Future studies are required in order to determined if this $Gr1^+B220^+$ cell population is indeed composed of plasmacytoid dendritic cells and why their numbers are reduced upon infection with wt VACV.

The presence of a higher population of $Gr1^+Cd11b^+$ cells, also known as myeloid derived suppressor cells or MDSCs, in animals treated with v50ΔB13RMγ at 1 dpi suggest that these cells may be playing an important role during post-exposure prophylaxis (Fig. 25). $Gr1^+Cd11b^+$ cells are a heterogeneous population of cells that include myeloid progenitor cells and immature myeloid cells and are thought to regulate the immune system in both healthy and sick individuals (75, 230, 251). Expansion of $Gr1^+Cd11b^+$ has been observed during acute and chronic infections with different organisms including *Trypanosoma cruzi* which is accompanied by an increased production of IFN-γ (82). Studies using a recombinant VACV expressing IL-2, which is thought to enhance the lytic capabilities of the $CD8^+$ T cells, showed the apoptotic death of this population following immunization through a mechanism due to $Gr1^+Cd11b^+$ (22).

A possible role of $Gr1^+Cd11b^+$ during post-exposure prophylaxis could be the down-modulation of the immune response by for example inducing apoptosis of activated lymphocytes, which could potentially lead to tissue destruction. This hypothesis is supported by recent studies by Fischer *et al*. (69), in which depletion of cells positive for Ly6G, one of the two antigens that can be bound by Gr1, leads to more damaged tissue at the site of infection. It was also observed in the same study that the $Cd11b^+Ly6C^+Ly6G^+$ population produces type I IFN and protects the VACV-infected tissue from immune-mediated damage by producing ROS molecules (69).

In order to better understand how v50ΔB13RMγ may be modulating the T_H1 and T_H2 cytokine levels, the cytokines from each group were analyzed using a Bio-plex assay. Upon examination of the results, the cytokine/chemokine profiles were similar among wt VACV-infected and wt VACV-infected/ v50ΔB13RMγ treated groups suggesting that immunoregulatory effects were local. While differences among the untreated and treated groups were not observed, it was noted that levels of IL-12 at 2 dpi were higher in the treated group compared to the mock-infected, mock-treated group. IL-12 is a T_H1 cytokine secreted by activated dendritic cells and macrophages and is the principal mediator of the early innate immune response to intracellular microbes (2, 52, 184). In the case of T_H2 cytokines, IL-5 levels were higher in the treated group at 2 dpi while IL-10 levels were higher in both the untreated and treated group when compared to the mock-infected/mock-treated group and the mock-infected/v50ΔB13RMγ-treated group. While IL-5 is produced by activated mast cells and stimulates the growth and differentiation of eosinophils as well as the activation of the mature eosinophils, IL-10 is produced by activated macrophages and its major role is to maintain homeostasis between the innate and cell-mediated immune response by inhibiting activated macrophages (2). Further studies are necessary in order to determine the specific role of these cytokines during post-exposure prophylaxis of VACV in this animal model.

Analysis of the specific chemoattractants, MIP-1β, MIP-2 and RANTES show higher levels of these proteins at in both untreated and treated groups by 6

dpi. MIP-1β is a chemokine produced by macrophages, dendritic cells and lymphocytes and it is involved in the recruitment and activation of granulocytes (211). MIP-2, on the other hand, is produced by epithelial cells and peripheral neutrophils and its function is to attract neutrophils to the sites of inflammation following injury and/or infection (8). RANTES expression has been observed in delayed-type hypersensitivity reactions and has been shown to be mediated by TNF-α and IFN-γ. This chemokine is released by cytotoxic T lymphocytes (CTLs) and is a selective attractant for T cells and monocytes (211). Furthermore, activation of CTLs through RANTES is mediated through cell surface aggregation, which could be prevented by MIP-1β (7).

Overall, the results presented in this chapter indicate that v50ΔB13RMγ is modulating the immune response by mostly promoting the $Gr1^{+}Cd11b^{+}$ as well as the $CD8^{+}$ T cell populations at early time post-infection. It was also observed that treatment with v50ΔB13RMγ has an effect in wt VACV replication in the olfactory bulb. This is of particular importance as the olfactory bulb in the animal model currently studied appears to be one of the entry points of VACV to the central nervous system. A delay in viral replication in this part of the brain would therefore play a key role in the morbidity and ultimately mortality in this post-exposure prophylaxis model.

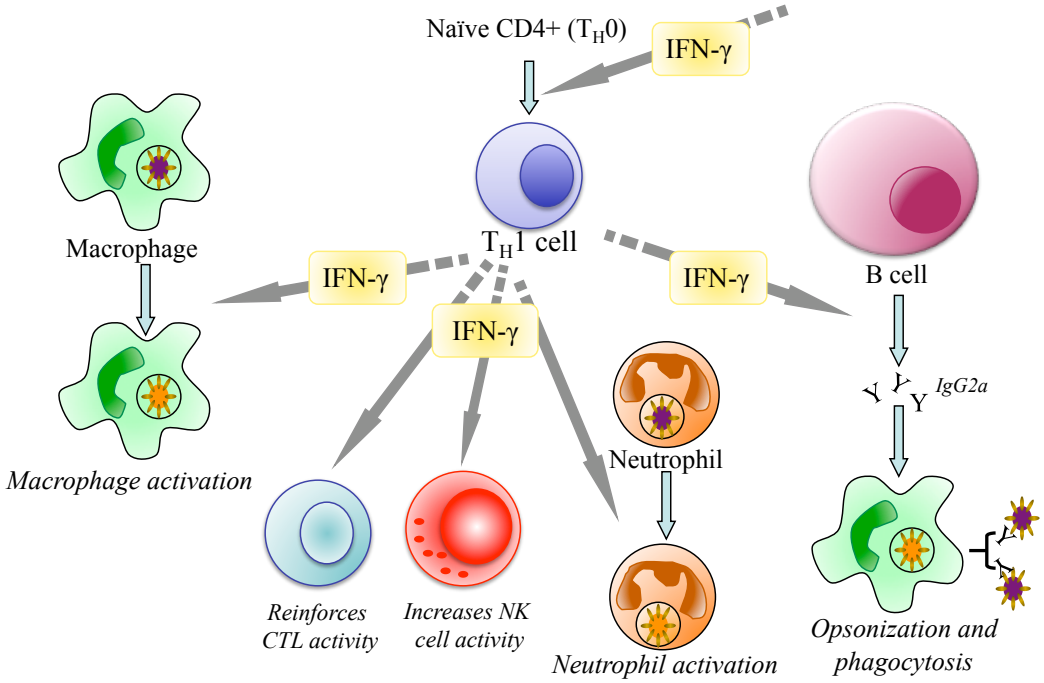

FIG. 15. Role of IFN-γ in the immune response. IFN-γ promotes the differentiation of naïve $CD4^+$ T cells (T_H0) to the T_H1 subset, which in turn secrete IFN-γ. Among the biological functions of IFN-γ are macrophage activation, reinforcement of cytotoxic T lymphocytes (CTL) activity, enhancement of natural killer (NK) cell activity, neutrophil activation and isotype switching (IgG2a in mice), which promotes opsonization and phagocytosis.

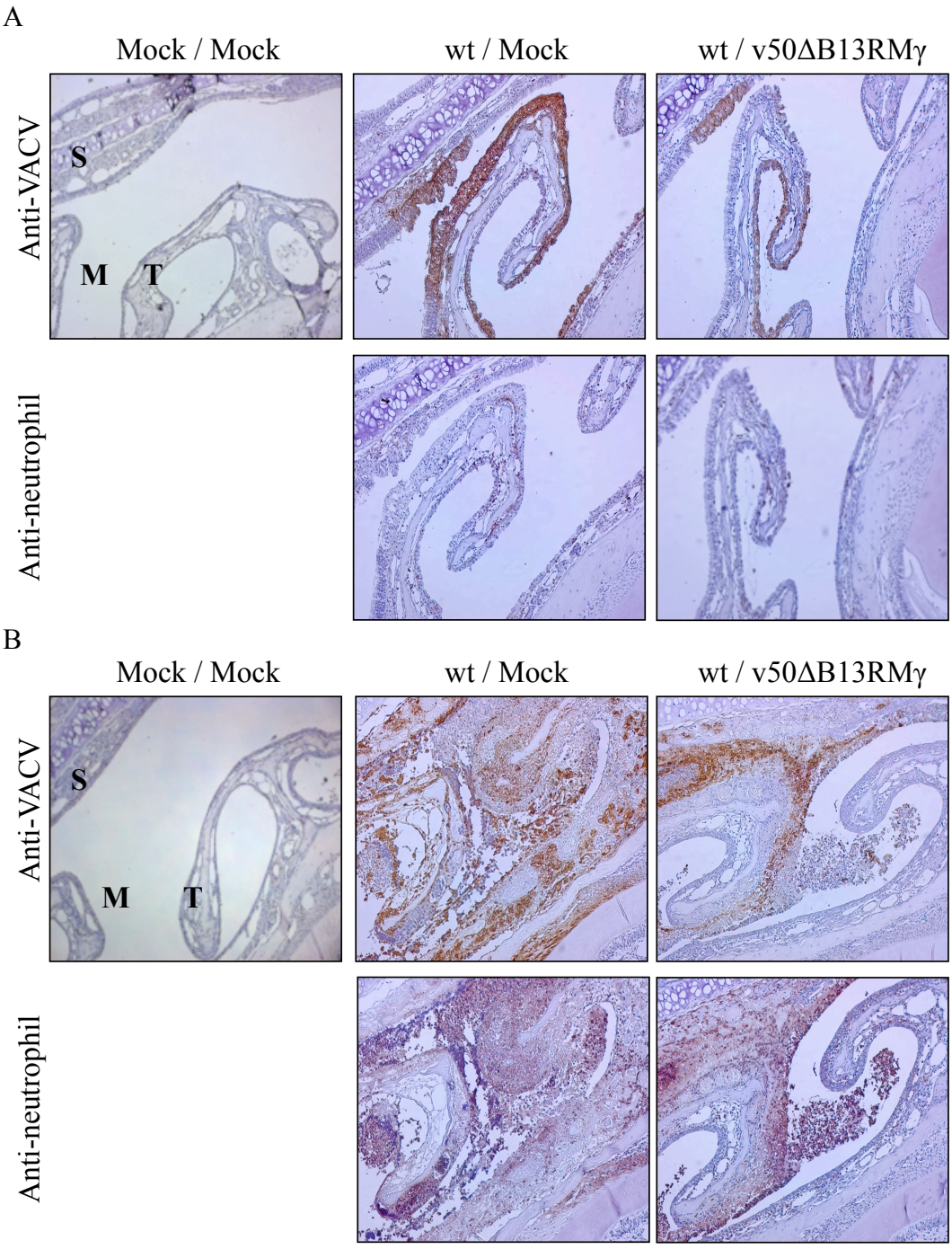

FIG. 16. Neutrophil spread in the maxilloturbinate section of wt VACV infected mice. Mice were infected intranasally with 10^6 pfu (~100 LD_{50s}) of wt VACV and treated 1 dpi with 10^7 pfu of v50ΔB13RMγ. (A) Samples at 3dpi and (B) samples at 8 dpi. All representative sections were obtained at 2 mm depth and were stained with polyclonal antibodies against VACV and 7/4 'anti neutrophil'. S= septum, T=maxilloturbinate, M=meatus (air passage). 100X magnification.

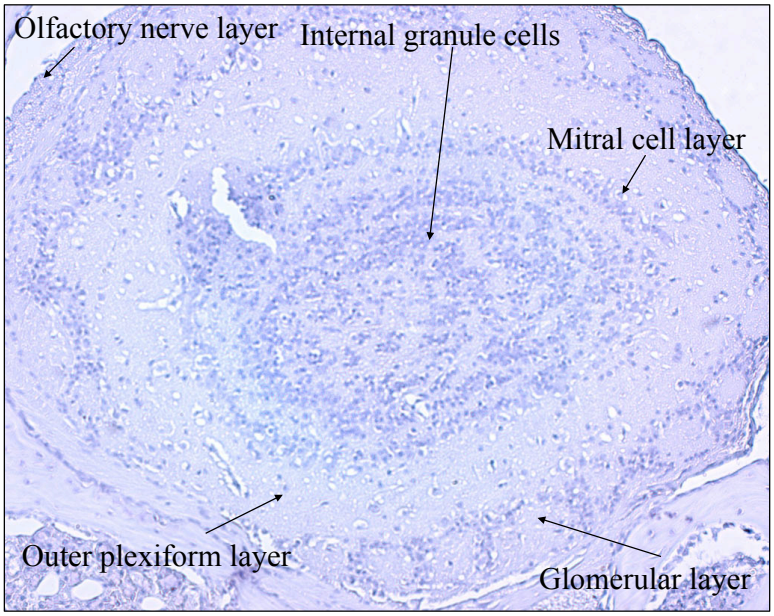

FIG. 17. Olfactory bulb section and its main components. A group of C57/BL6 mice were mock-infected and mock-treated intranasally at 1 dpi. The histology section depicts the olfactory bulb of one of these mice from this control group. 100X magnification.

FIG. 18. VACV replication in the olfactory bulb section. Mice were infected intranasally with 10^6 pfu (~100 LD_{50s}) of wt VACV and treated 1 dpi with 10^7 pfu of v50ΔB13RMγ. Mice were sacrificed at 8 days post-infection. Representative sections were obtained at 4 mm depth and were stained with polyclonal antibodies against VACV. OB= olfactory bulb, S=septum, NPM=nasopharyngeal meatus, HP=hard palate. (A) wt VACV infected / Mock treated (B) wt VACV infected / v50ΔB13RMγ treated. 10X magnification.

A

wt / Mock

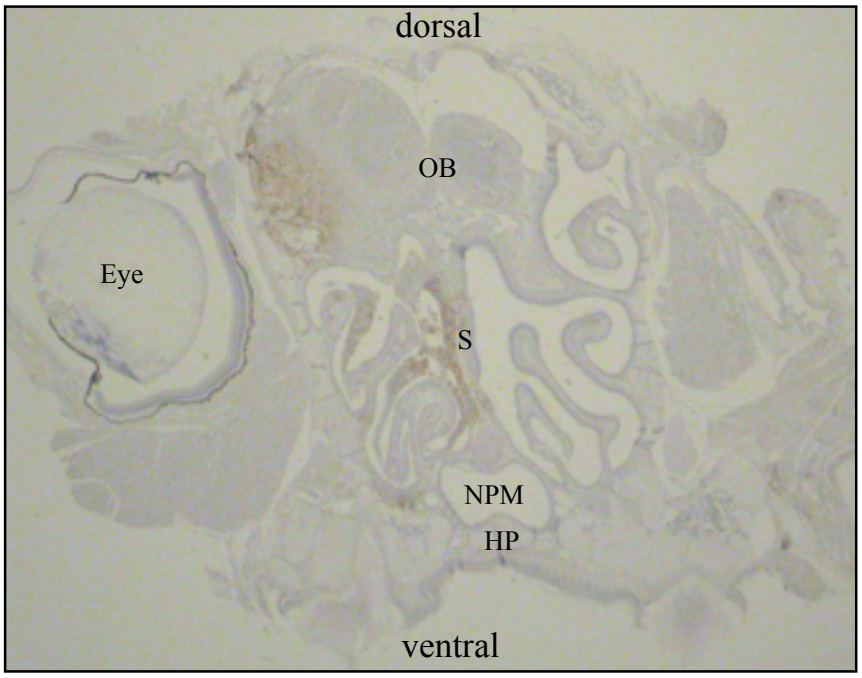

B

wt / v50ΔB13RMγ

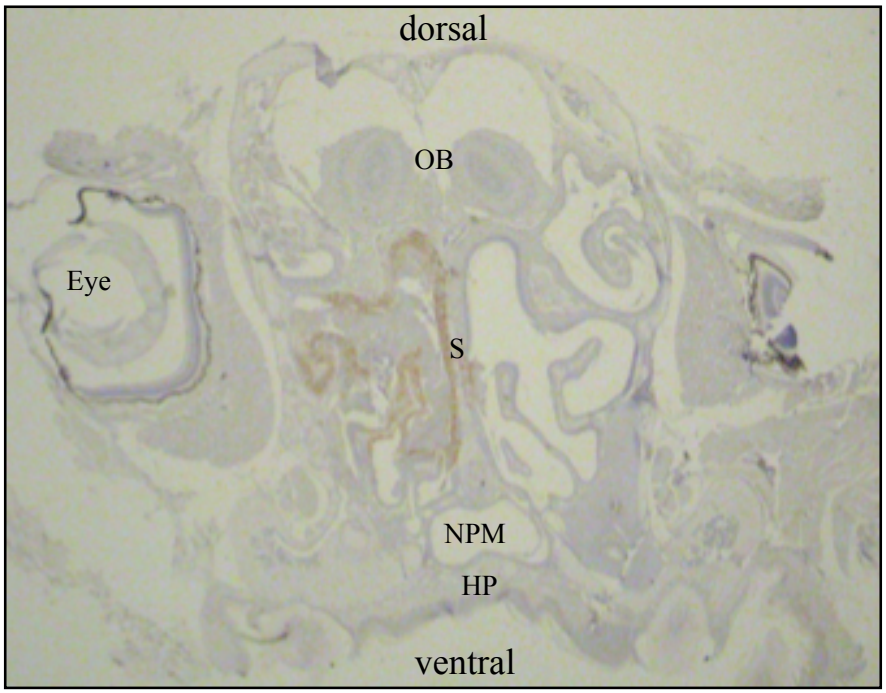

A

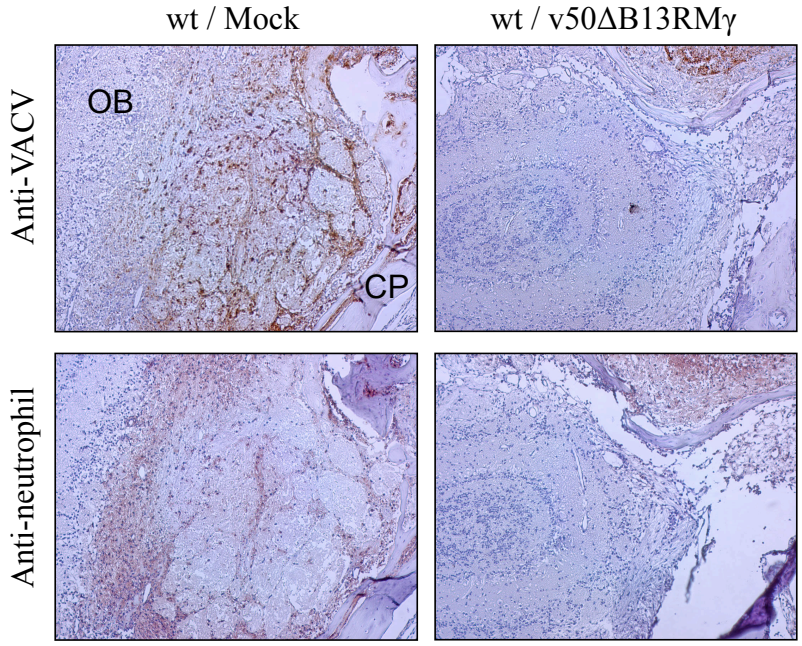

B

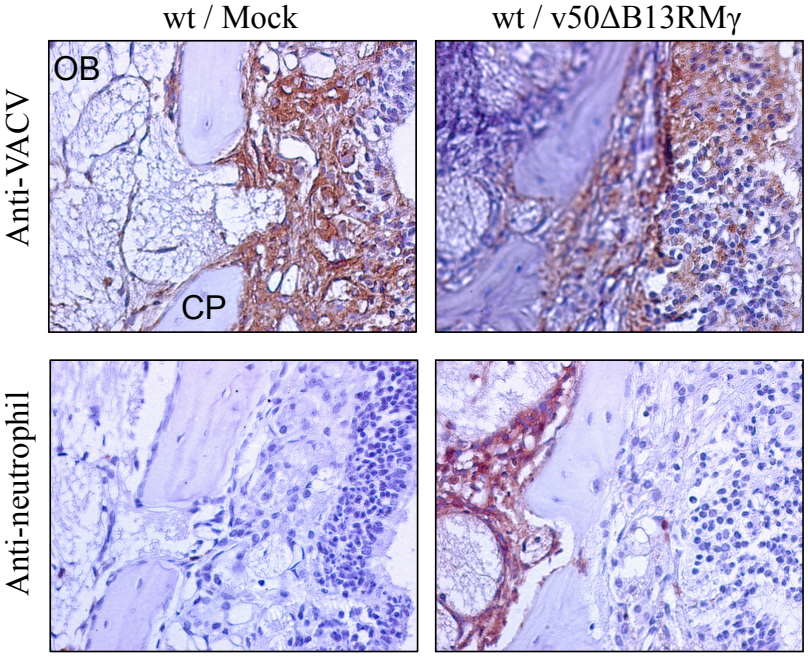

FIG. 19. Histopathologic comparison and infection progression in the olfactory bulb section. Mice were infected intranasally with 10^6 pfu (~100 LD_{50s}) of wt VACV and treated 1 dpi with 10^7 pfu of v50ΔB13RMγ. All representative sections were obtained at 4 mm depth and were stained with polyclonal antibodies against VACV and 7/4 'anti neutrophil'. OB= olfactory bulb, CP=cribriform plate. (A) 100X magnification. (B) 400X magnification.

A

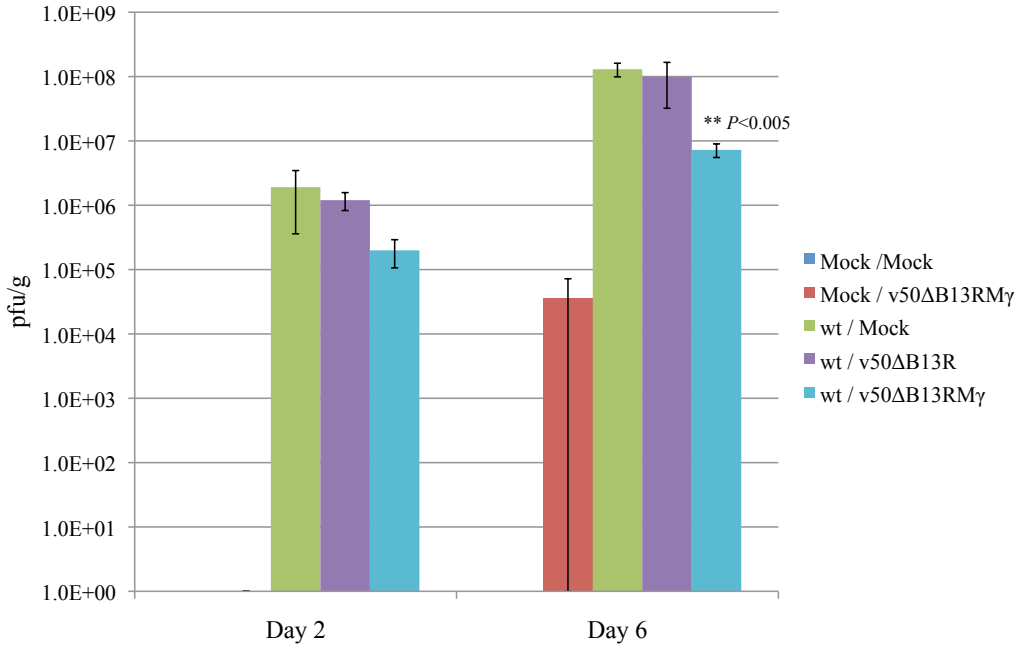

B

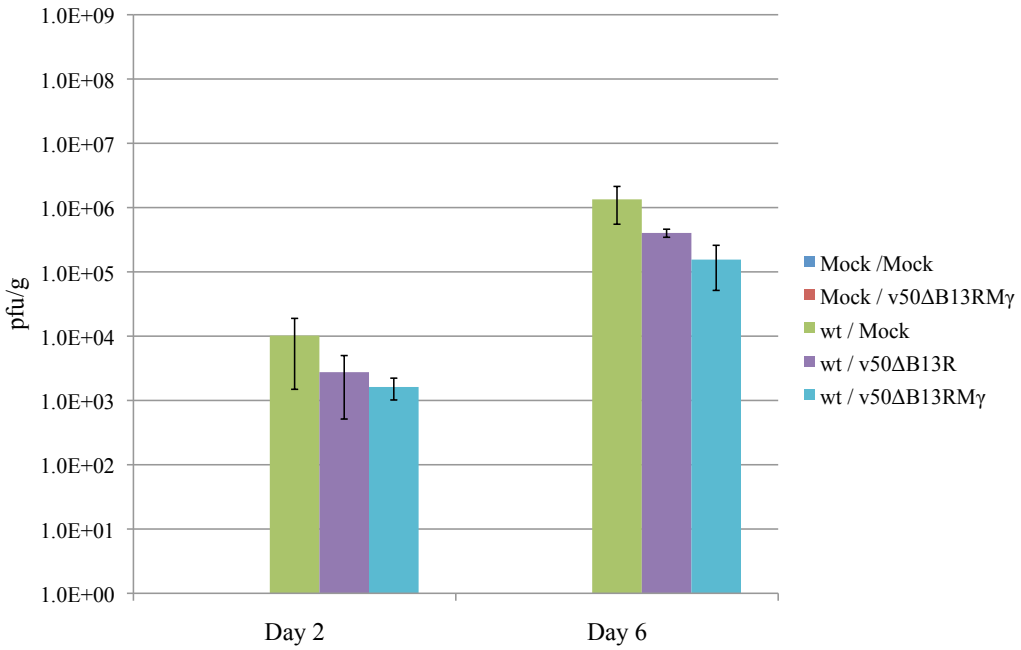

FIG. 20. Viral spread of wt VACV in the olfactory bulb and brain of infected animals. Groups of 5 C57BL/6 mice were mock-infected or infected intranasally with 10^6 pfu of wt VACV. Animals remained untreated or were treated one day post-infection with 10^7 pfu of v50ΔB13R or v50ΔB13RMγ. Samples were collected and analyzed at 2 and 6 dpi. (A) Replication in the olfactory bulb. (B) Replication in the brain. Error bars indicate the standard error of the mean.

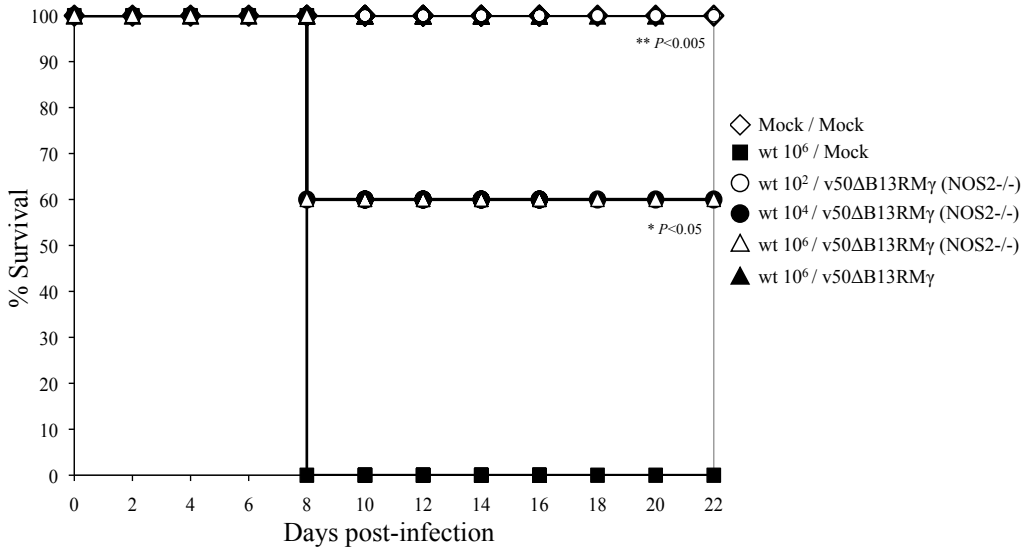

FIG. 21. Susceptibility of NOS2-/- mice after intranasal infection with different doses of wt VACV and subsequent treatment with v50ΔB13RMγ. Groups of 5 four-week-old NOS2-/- mice were infected intranasally with 10^2 pfu (<1 LD_{50s}), 10^4 pfu (1 LD_{50}) or 10^6 pfu (100 LD_{50s}) of wt VACV and treated one day post-infection with 10^7 pfu of v50ΔB13RMγ. A group of 5 four-week-old C57BL/6 mice served as control animals and included mock-treated (■), mock-infected and mock-treated (◊) and animals treated with v50ΔB13RMγ (▲).

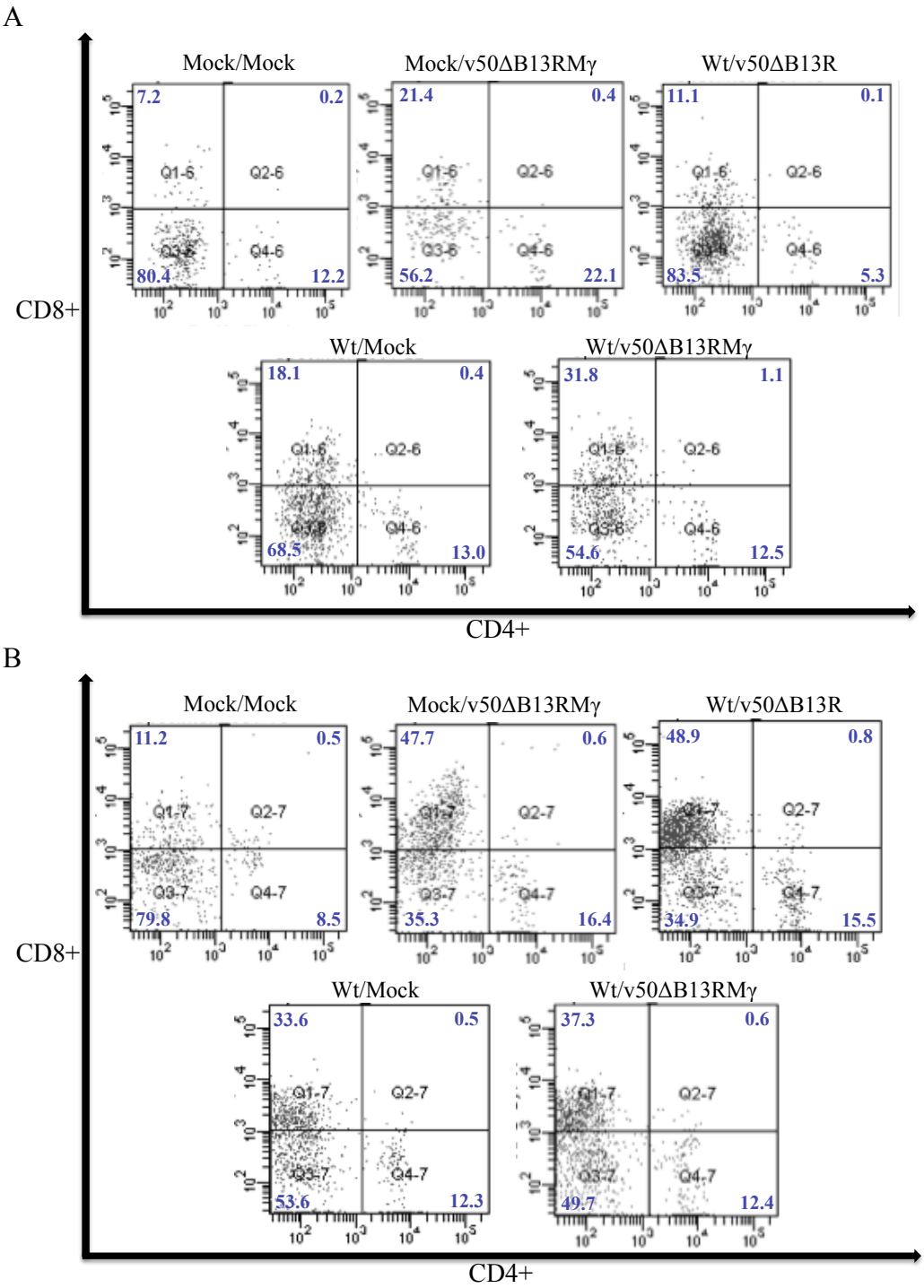

FIG. 22. Treatment of infected animals with v50ΔB13RMγ enhances proliferation of $CD8^+$ T cells. Groups of five C57BL/6 mice were either mock-infected or infected intranasally with 10^6 pfu (~100 LD_{50s}) wt VACV. Animals were treated with 10^7 pfu of v50ΔB13R, v50ΔB13RMγ or mock-treated at 1 dpi. On days 2 (A) and 6 (B) post-infection, nasal lavages were collected and analyzed for $CD3^+$ by flow cytometry. Data are representative of two independent experiments.

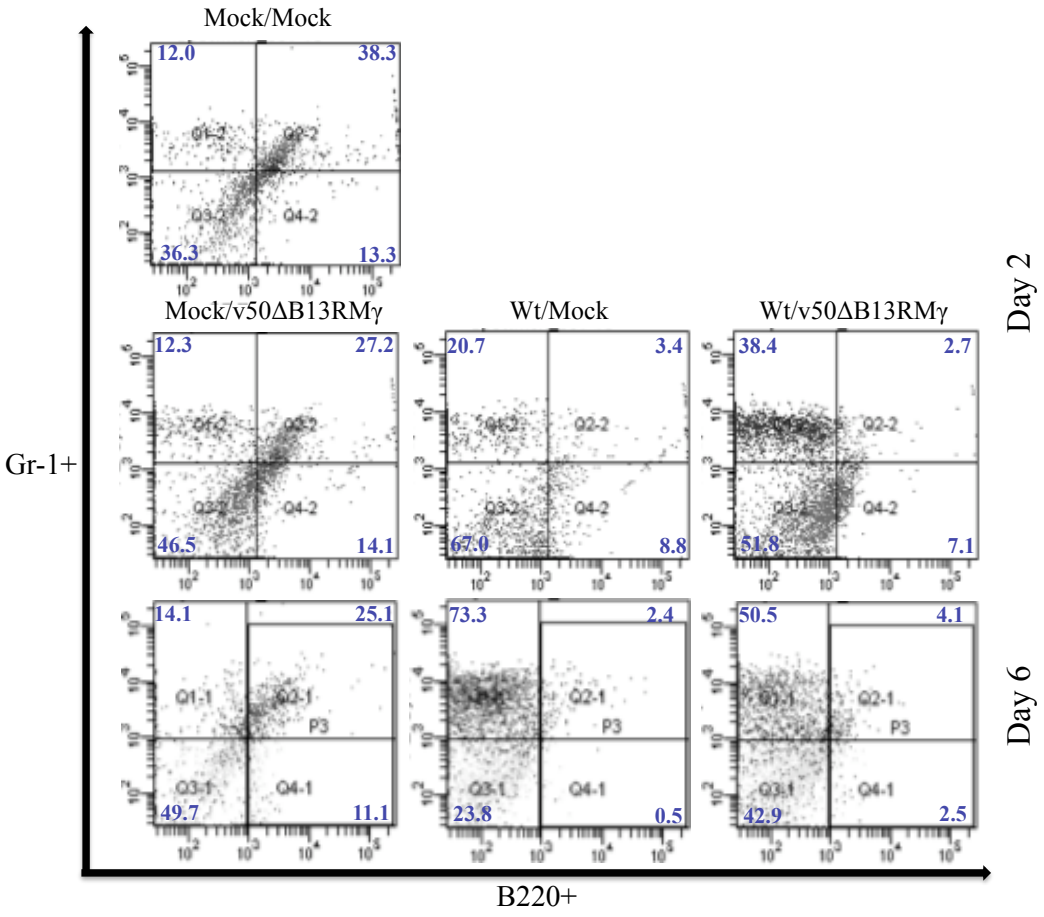

FIG. 23. Infection of animals with wt VACV reduces the $Gr1^+$ $B220^+$ cell population at the site of infection. Groups of five C57BL/6 mice were either mock infected or infected intranasally with 10^6 pfu (~100 LD_{50s}) wt VACV. Animals were treated with 10^7 pfu of v50ΔB13R, v50ΔB13RMγ or mock treated at 1 dpi. On days 2 and 6 post-infection, nasal lavages were collected, pooled and analyzed for Gr1 and B220 by flow cytometry. Data are representative of two independent experiments.

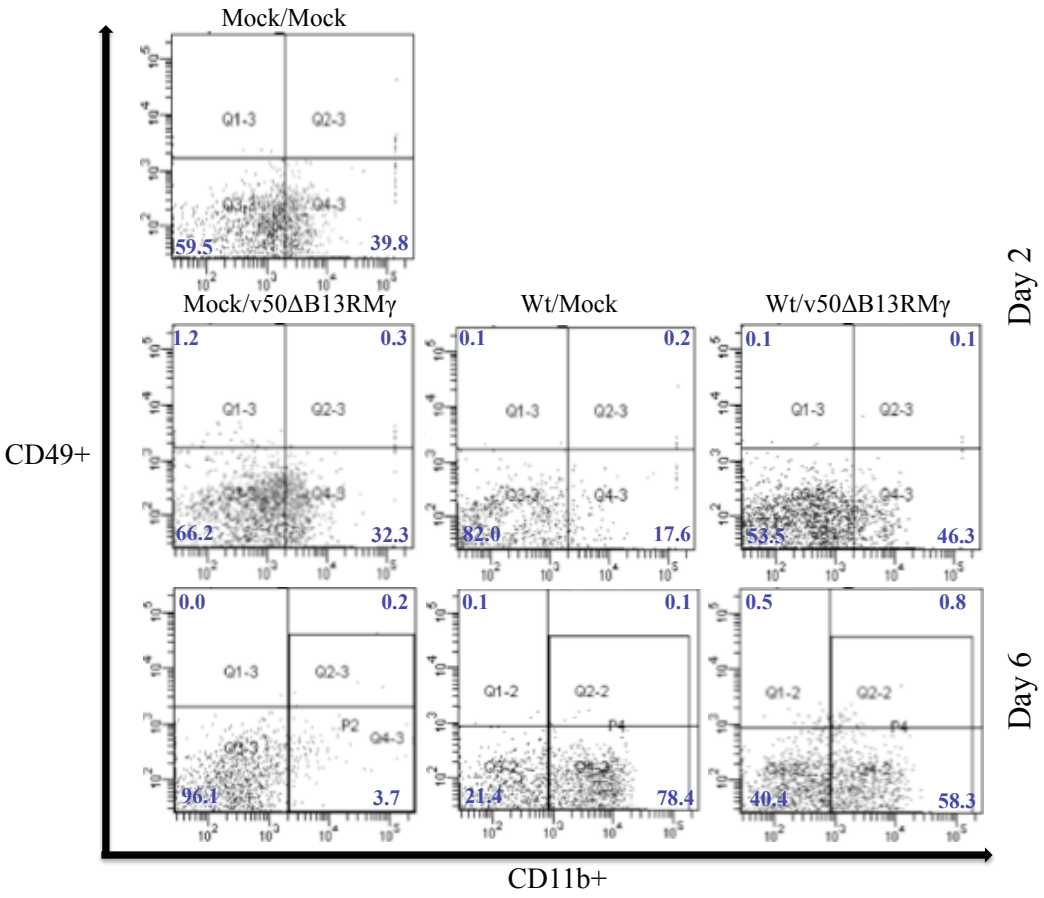

FIG. 24. Infection of animals with wt VACV does not affect the population of $CD49^+$ (NK) cells at the site of infection. Groups of five C57BL/6 mice were either mock infected or infected intranasally with 10^6 pfu (~100 LD_{50s}) wt VACV. Animals were treated with 10^7 pfu of v50ΔB13RMγ or mock treated at 1 dpi. On days 2 and 6 post-infection, nasal lavages were collected, pooled and analyzed for CD49 and CD11b by flow cytometry. Data are representative of two independent experiments.

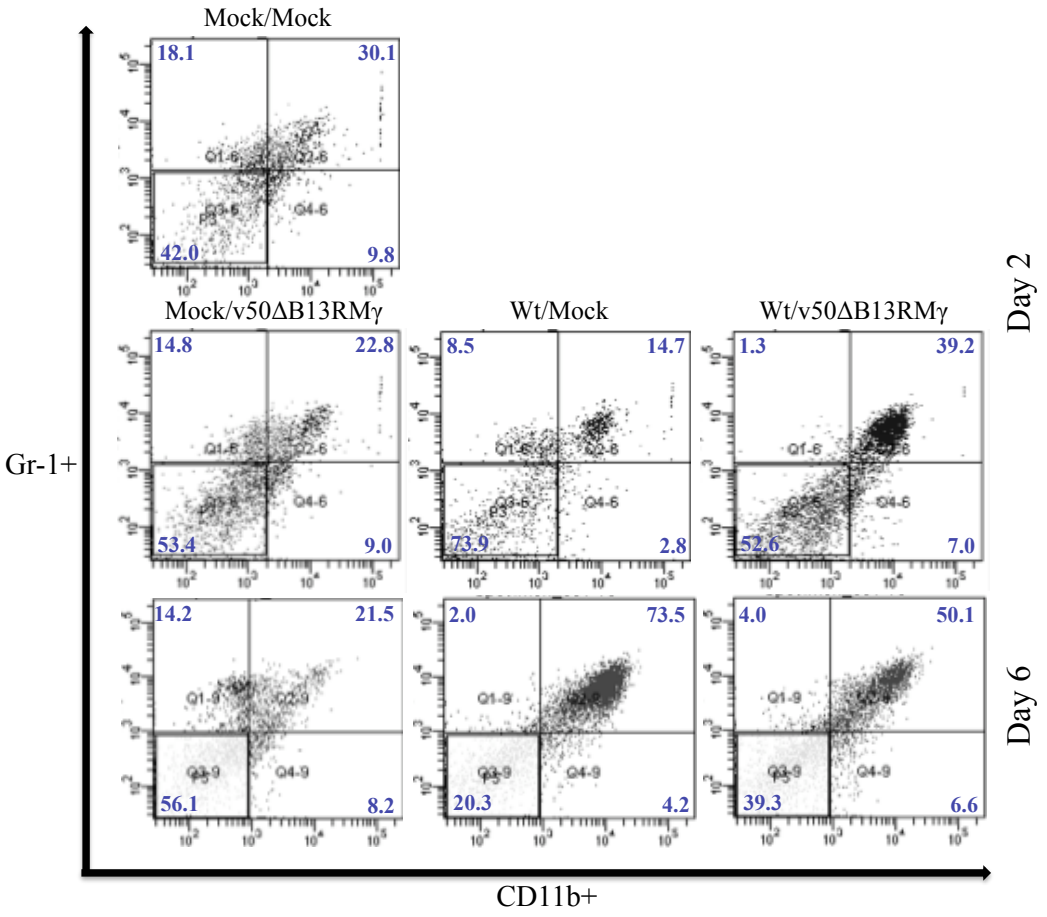

FIG. 25. Treatment of infected animals with v50ΔB13RMγ enhances proliferation of $Gr1^+$ $CD11b^+$ myeloid-derived suppressor cells by day 2 post-infection. Groups of five C57BL/6 mice were either mock infected or infected intranasally with 10^6 pfu (~100 LD_{50s}) wt VACV. Animals were treated with 10^7 pfu of v50ΔB13R, v50ΔB13RMγ or mock treated at 1 dpi. On days 2 and 6 post-infection, nasal lavages were collected, pooled and analyzed for Gr1 and CD11 by flow cytometry. Data are representative of two independent experiments.

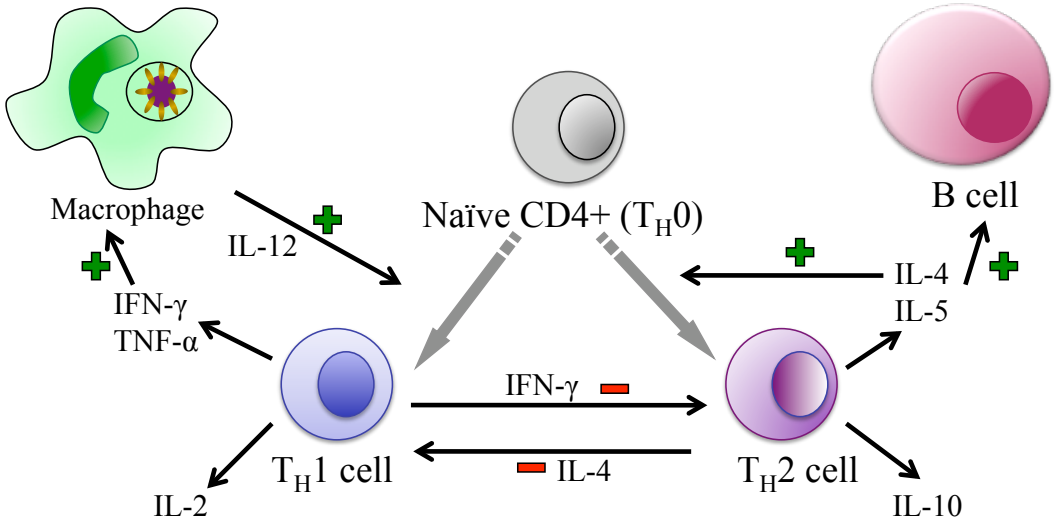

FIG. 26. Polarized T_H1 and T_H2 responses. Both T_H1 and T_H2 subsets produce distinct set of cytokines and have distinct effector functions. While T_H1 cells promote cell-mediated immunity and phagocyte-dependent inflammation, T_H2 cells enhance strong antibody responses and eosinophil accumulation (phagocyte-independent inflammation).

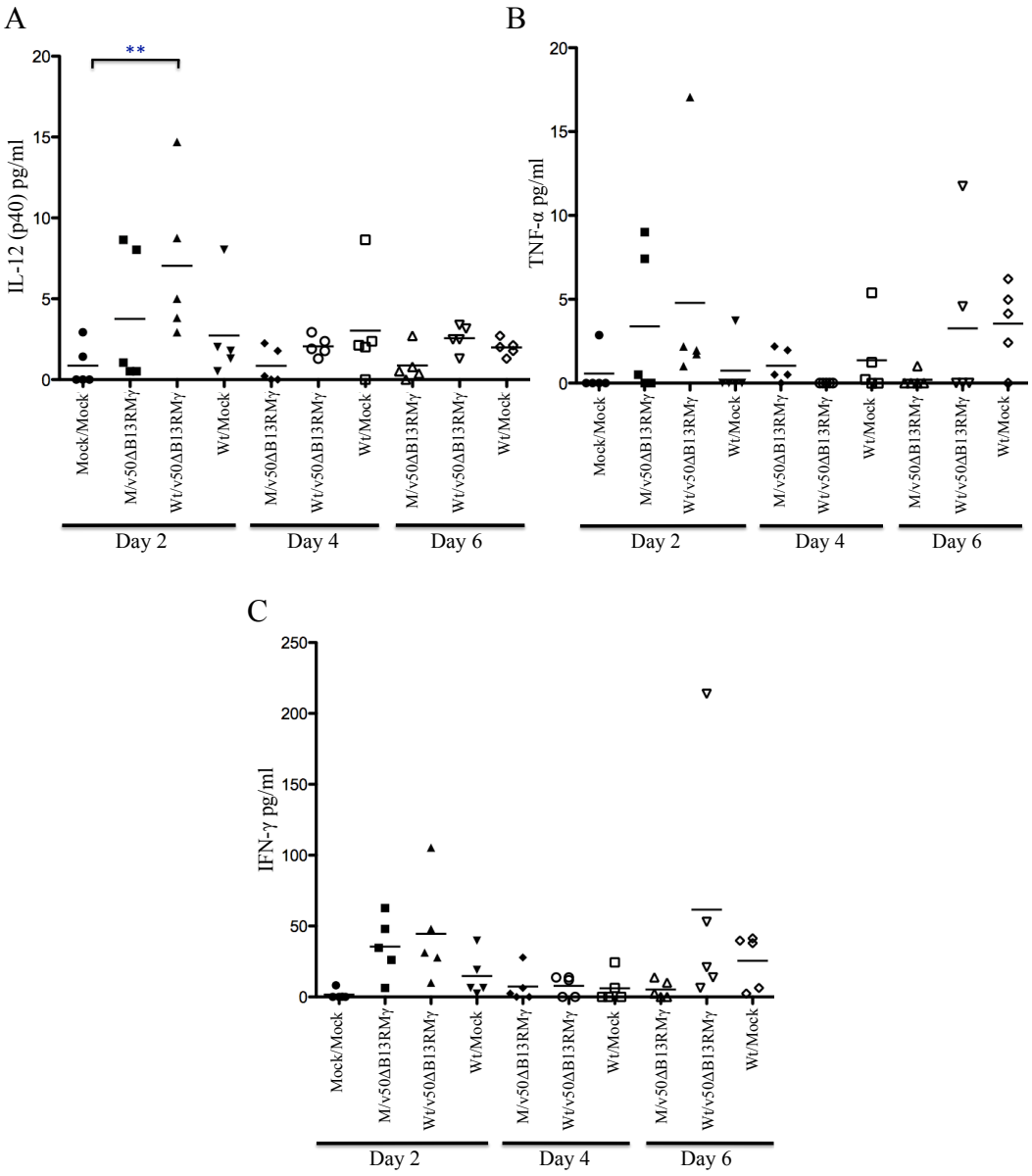

FIG. 27. Expression of Th1 cytokines in infected animals. Groups of five C57BL/6 mice were either mock infected or infected IN with 10^6 pfu (~100 LD_{50s}) wt VACV. Animals were treated with 10^7 pfu of v50ΔB13RMγ or mock treated at 1 dpi. Nasal lavages were collected and analyzed using the Bio-plex system. IL-12 (A), TNF-α (B) and IFN-γ (C). * P<0.05, ** P<0.01, *** P<0.0001.

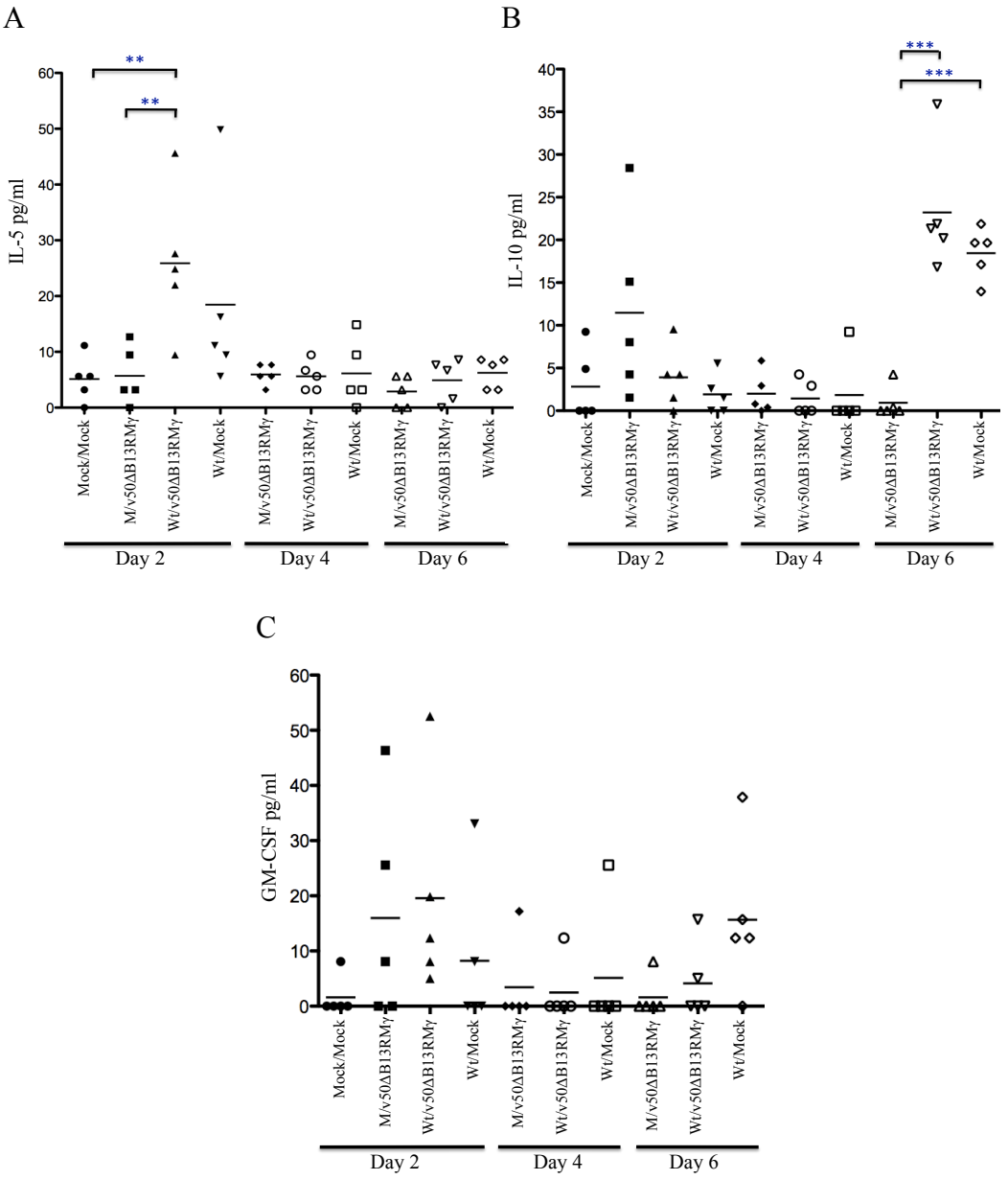

FIG. 28. Expression of Th2 cytokines in infected animals. Groups of five C57BL/6 mice were either mock infected or infected IN with 10^6 pfu (~100 LD_{50s}) wt VACV. Animals were treated with 10^7 pfu of v50ΔB13RMγ or mock treated at 1 dpi. Nasal lavages were collected and analyzed using the Bio-plex system. IL-5 (A), IL-10 (B) and GM-CSF (C). * P<0.05, ** P<0.01, *** P<0.0001.

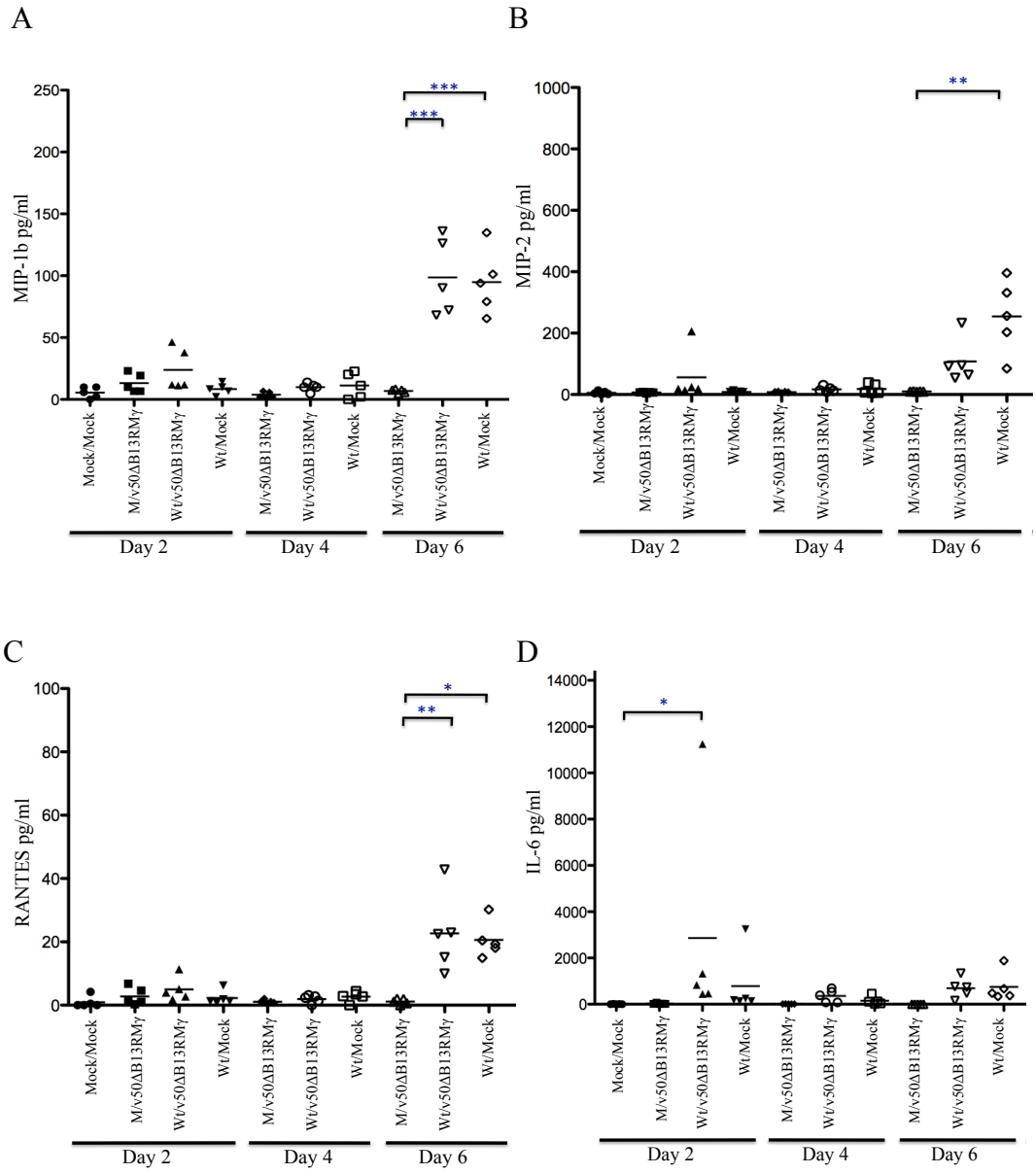

FIG. 29. Expression of chemoattractans and IL-6. Groups of five C57BL/6 mice were either mock infected or infected IN with 10^6 pfu (~100 LD_{50s}) wt VACV. Animals were treated with 10^7 pfu of v50ΔB13RMγ or mock treated at 1 dpi. Nasal lavages were collected and analyzed using the Bio-plex system. MIP-1β (A), MIP-2 (B), RANTES (C) and IL-6 (D). * P<0.05, ** P<0.01, *** P<0.0001.

CHAPTER 3

DUAL EXPRESSION OF THE VACCINIA VIRUS E3L PROTEIN Z-DNA AND DOUBLE-STRANDED RNA BINDING DOMAINS

ABSTRACT

Vaccinia virus (VACV) is a member of the genus *Orthopoxvirus* of the family *Poxviridae* and it is considered a highly effective vaccine against smallpox and other closely related viruses such as monkeypox and cowpox. VACV has a double stranded DNA genome approximately 190 Kbp in length and encodes for about 200 proteins. One of the main characteristics of this virus is that it is interferon (IFN) resistant as evidenced by replication of VACV in cultured cell lines treated with type I IFN. This effect is primarily mediated by the protein encoded by the E3L gene as deletion of the entire gene renders a VACV that is IFN sensitive. The E3L protein has two main domains: a Z-DNA binding domain contained in the amino terminus, and a double-stranded RNA binding domain in the carboxy terminus. Both domains have been shown to be necessary for pathogenesis as a VACV mutant lacking the Z-DNA binding domain is less pathogenic than wild type in intranasal infections. A virus that expresses both domains of E3L was constructed and compared to wild type VACV in cells in culture and for its ability to inactivate the IFN response. The dual expression virus was unable to replicate in JC cells, a cell line where E3L mutants lacking either the Z-DNA binding domain or the dsRNA binding domain are unable to replicate.

Moreover, phosphorylation of the dsRNA dependent protein kinase (PKR) was observed at late times post-infection. The present data support the hypothesis that both domains of E3L need to be linked together in order to block the IFN response suggesting that the Z-DNA binding domain of E3L could bind to dsRNA in its Z-form.

INTRODUCTION

Vaccinia virus (VACV) is a member of the genus *Orthopoxvirus* of the *Poxviridae* family. Other members from this family include variola virus (VARV), the causing agent of smallpox; monkeypox virus (MPXV), ectromelia virus (ECTV) and cowpox virus (CPXV) (66, 160). After an intensive vaccination strategy initiated in 1967, smallpox was declared eradicated from the world in 1980 and routine smallpox vaccination was discontinued in the U.S. in 1972 (237). Following September 11, 2001, the potential use of VARV as a bioterrorism agent is of particular concern, as it constitutes an ideal terrorist weapon of mass destruction (135). Moreover, there also remains a low but very real risk of VARV release, whether intentional or accidental (227).

Responsible for the eradication of the smallpox and able to induce antibodies that protect against monkeypox virus (56), VACV is also used as an expression vector for foreign genes and as a live recombinant vaccine for infectious diseases and cancer (144, 151). Unfortunately, inoculation in humans with VACV can lead to severe complications, especially in children and

immunocompromised individuals thus, a safer vaccine as well as a better understanding of the vaccine vector has become necessary (58).

One of the main characteristics of VACV is that it is interferon (IFN) resistant and the mechanisms by which this virus evades the host response (Fig. 30) are currently being investigated. In VACV, E3L is the major IFN resistance gene (106), which has also been associated with neurovirulence in mice (19, 122). E3L codes for two proteins, p25 (190 amino acids) and a smaller protein p20 (153 amino acids), which is generated due to leaky scanning during translation (36). E3L has two main defined domains, a C-terminal dsRNA binding domain (dsRNA BD) that is required for both replication in many cells in culture and pathogenesis in mice, and an N- terminal Z-DNA binding domain (Z-DNA BD) that is dispensable for replication in cells in culture, but required for pathogenesis (122) (Fig. 31). Moreover, the C-terminus has been associated with IFN resistance and PKR inhibition, although recent data show that the N-terminus is also necessary for both IFN resistance and PKR inhibition (235). These new data provide new insight into the function of the N-terminus *in vivo.* This N-terminus domain is highly conserved in poxviruses and in VACV has been proven to be necessary for neurovirulence in mice and its spread from the nose to the brain (neuroinvasion) in VACV infection in C57/BL6 mice (18, 122). Furthermore, the N-terminus is necessary to inhibit PKR activation at late times post-infection and eIF2α phosphorylation in HeLa cells as well as in nasal turbinates of C57/BL6 mice (132).

The N-terminus of E3L is a member of the Zα family of Z-DNA binding domains. Other members in this family include the human adenosine deaminase acting on RNA 1 (ADAR1), mouse Z-DNA binding protein 1 (ZBP1) and fish PKR like kinase, PKZ (122, 205) (Fig. 32). Each of these Zα domains, including the one from E3L, is characterized by a helix-turn-helix motif with an additional β-sheet (Fig. 33A). Although the structures are very similar, the amino acid sequence is not conserved, except for the residues that contact DNA (122). This was proven to be true when the Zα domain of E3L was substituted for other Zα domains. Indeed, both chimeric viruses $Z\alpha_{ADAR1}$-$E3L_c$ and $Z\alpha_{DLM1}$-$E3L_c$ retain the same pathogenicity as wt VACV after intracranial (IC) infection (122). Interestingly, the solution structures of the Zα domain of E3L, $Z\alpha_{ADAR1}$ and $Z\alpha_{DLM1}$ are very similar but differ in the side chain conformation of a key Z-DNA contacting residue Y48 (110, 122). This difference could explain why the Zα domain has a reduced affinity to Z-DNA *in vitro*, although *in vivo* other factors could render wt E3L as pathogenic as the $Z\alpha_{ADAR1}$-$E3L_c$ chimera (110, 122). The Zα domain of E3L has also proven to be important in the transcriptional activation of human IL-6, NF-AT and p53 as well as in the inhibition of hygromycin B-induced apoptosis in HeLa cells (129).

Both B-DNA and A-RNA helices can undergo a transition to left-handed double helical structures forming Z-DNA and Z-RNA respectively. In the case of Z-DNA, negative supercoiling and high-salt conditions have been previously shown to stabilize the structure (194). Nevertheless the transition of A-RNA to Z-

RNA seems to require higher salt concentrations and higher temperatures, although Z-RNA can also be formed at lower temperatures during longer transitions (92). In a more physiological-like environment a B to Z-DNA transition can be induced in alternating purine - pyrimidine sequences by adding the Zα domain from ADAR1 while mutations in the key residues that contact the DNA reduce the ability of the protein to convert B-DNA to Z-DNA as demonstrated by circular dichroism (122). Similarly, this domain has been proven to stabilize the Z-RNA conformation making both Z-DNA and Z-RNA targets of ADAR1 (23), which has been corroborated by the recent crystal structure of the $Z\alpha_{ADAR1}$/Z-RNA complex. The complex revealed that the same key residues are involved in binding both Z-DNA and Z-RNA (179) giving an insight into the new possible biological function of the Zα domain of E3L.

Transition of A-RNA to Z-RNA has been previously described at high salt concentrations (6M $NaClO_4$) and high temperatures (45°C) (92). The nuclear magnetic resonance (NMR) structure of Z-RNA has been obtained at this high salt concentration although at a lower temperature (30°C) (181). More recently, the crystal structure of $Z\alpha_{ADAR1}$ bound to Z-RNA has been obtained at a lower salt concentration (0.1 M Na^+ versus 6 M Na^+) (179). Moreover, although both structures depict Z-RNA, differences in the structures point to a Z_R (novel left-handed helix) and Z_D (Z-DNA-like conformation). These two distinct forms of Z-RNA have been previously observed using Raman spectroscopy at different at 35°C for Z_R-RNA (96). It is believed that ionic strength is the driving force

behind both conformations and that the A-to Z_D transition is followed by a Z_D to Z_R transition. It has also been noted that chemical bromination of poly[r(C-G)] has a profound effect on the conformation properties of the RNA duplex. A limited chemical bromination of poly[r(CG)] (32% br8G, 26% br5C) produces a 1:1 ratio mixture of A and Z-forms of RNA while a more extensive bromination of poly[r(CG)] (>49% br8G, 43% br5C) results in stabilization of the Z_D form (96, 153).

The C-terminus of E3L contains a dsRNA binding domain. Previous deletion analyses localized the domain necessary for binding dsRNA between amino acids 83 and 183 (34), although this domain is limited to amino acids 117 to 182 (102, 103) (Fig. 33B). Other proteins containing this dsRNA binding domain include PKR, ADAR1, *Drosophila melanogaster* staufen, and *Escherichia coli* RNase III (102). The presence of this domain in E3L is important, as dsRNA produced during viral infections is the alerting mechanism to initiate the type I IFN pathway (36). VACV evades this mechanism by binding to dsRNA via E3L and inhibiting the interferon induced effector molecules 2'-5-oligoadenylate synthetase and PKR. By doing this E3L prevents inhibition of both viral and host proteins synthesis as well as apoptosis (119). Participation of Zα domain of E3L in the inhibition of PKR activation by also masking dsRNA would constitute a novel biological function for this domain; thus, binding to dsRNA would not be limited to the C-terminal dsRNA binding domain of E3L.

MATERIAL AND METHODS

Cells and viruses. Baby hamster kidney (BHK-21) cells and Rabbit kidney cells (RK-13) were cultured in Eagle's Minimal Essential Medium (MEM, Gibco, BRL) containing 5% fetal bovine serum (FBS, Hyclone) and 50 µg/ml of gentamycin. Epithelial cells from the kidney of *Cercopithecus aethiops* also known as African green monkey kidney cells (BSC-40) were grown in Dulbecco's modified Eagle's medium (DMEM, Gibco, BRL) supplemented with 10% FBS (Hyclone) and 50 µg/ml of gentamycin. JC cells (ATCC CRL-2116) were grown in RPMI-1640 Medium containing 10% FBS. All cells were incubated at 37°C with 5% CO_2. The Western Reserve (WR) strain of VACV was used as the parental virus for these studies. The E3L VACV mutants were generated by standard methods routinely employed in Dr. Bertram Jacobs' laboratory. Construction of VACV mutants have previously been described (119). VACVΔE3LΔTK::GP-GNR has Gyrase PKR and the green fluorescent protein (GFP) fused to a neomycin resistant gene driven by a double synthetic promoter in the TK locus, *lacZ* is in place of E3L (James Jancovich, unpublished). All viruses were amplified in BHK-21 cells and partially purified by pelleting through a 36% sucrose pad, as previously described (15, 54).

Plasmids construction. Standard PCR techniques were employed in the construction of the plasmids with Platinum® *Pfx* DNA Polymerase (Invitrogen). In order to generate a plasmid where the entire sequence for the dsRNA binding domain was deleted, the E3L sequence for nucleotides 1 to 351 was amplified

from the plasmid pMKE3L (Jacobs' laboratory) using the primers Δ73C-FLAG$_F$ and Δ73C-FLAG$_R$ (Table 1), and cloned into the *BamH*I and *Pst*I restriction sites of the plasmid pJC1 producing the recombinant plasmid pJC1-Δ73C-FLAG. The parental pJC1 was previously constructed (Jason Cameron, unpublished) by altering pMPE3ΔGPT, a vector previously described (119). The plasmid pJC1 contains both the native promoter of E3L (preceding *BamH*I and *Hind*III sites) and a synthetic early-optimized promoter (EO$_P$) 5' AAAAATTGAAAAACTATTCTAATTTATTGCACGG 3' preceding the *Sal*I and *Pst*I restriction sites. The plasmid pJ1R-J3R was constructed in a two-step process using pUC19 as a backbone. Briefly, primers to generate a 478 bp J1R arm were designed using the VACV sequence for the WR strain (GenBank accession number AY243312). The primer J1R$_F$ containing an *Nde*I site and J1R$_R$ containing a *Sac*I site (Table 1) were used to amplify the J1R fragment using cDNA from wt VACV as a template. The J1R fragment was then cloned into pUC19 *Nde*I and *Sac*I sites resulting in plasmid pJ1R. A 488 bp J3R arm was then generated similarly using primers J3$_F$ with a *Xma*I site and J3R$_R$ with a *Pst*I site (Table 1). The resulting fragment was cloned into the *Xma*I and *Pst*I sites of pJ1R resulting in the recombinant plasmid pJ1R-J3R. A PCR product containing a deletion of the sequence coding for the N-terminus was then made by amplifying E3L nucleotides 250 to 573 from pJC1-AEIK using primers Δ83N-FLAG$_F$ with a *Sac*I site and Δ83N-FLAG$_R$ with a *Xma*I site (Table 1), resulting in a fragment with the EO$_P$ at the 5' end. pJC1-AEIK was previously constructed by cloning

E3L nucleotides 1 to 249 with a sequence coding for an N-terminus HIS-tag in the *BamH*I and *Hind*III sites and E3L nucleotides 250 to 573 with a sequence coding for an N-terminus FLAG sequence into the *Sal*I and *Pst*I restriction sites of pJC1. Another similar PCR product was made with using primers Δ83N-FLAGopp$_F$ with a *Sac*I site and Δ83N-FLAGopp$_R$ with a *Xma*I site (Table 1), the 3' end of this PCR product contains the EOp sequence reading at the opposite direction. The products were cloned into the *Sac*I and *Xma*I sites of pJ1-J3 resulting in pJ1R-FLAG-Δ83N-J3R and pJ1R-FLAG-Δ83Nopp-J3R. All the generated PCR products were purified using the Wizard® SV Gel and PCR Clean-Up system (Promega) according to manufacturer's protocol. Vectors were dephosphorylated with the enzyme Antarctic Phosphatase (New England Biolabs) and ligated to the PCR products using T4 DNA ligase (New England Biolabs). Ligation reactions were precipitated with glycogen overnight and transformed into Subcloning Efficiency™ DH5α™ chemically competent *E. coli* (Invitrogen). Following a standard alkaline lysis protocol, recombinant plasmids were verified by DNA sequencing.

Plasmid *In vivo* recombinations. Recombinant viruses were generated by plasmid *in vivo* recombination (PIVR). Plasmid pJC1-Δ73C-FLAG, which has a pMPE3Δgpt backbone, allows insertion of genes into the E3L locus of VACVΔE3LΔTK::GP-GNR by homologous recombination. Recombinant VACVE3LΔ73C$_F$ was selected due to their resistance to mycophenolic acid (MPA), an inhibitor of purine metabolism. Only recombinant viruses that inserted

the *ecogpt* gene in their genome are able to overcome the inhibition of purine metabolism by MPA (61) (107). After three rounds of plaque purification in RK-13 cells, the selection was removed allowing a second recombination event to occur. The insertion of the gene of interest into VACV was screened for by loss of *lacZ*; thus, colorless plaques were picked instead of blue plaques (107). The resulting virus, VACVE3LΔ73C_F, has GFP in the TK locus thus plaques fluoresce green. Plasmids pJ1R-FLAG-Δ83N-J3R and pJ1R-FLAG-Δ83Nopp-J3R allow insertion into the J2R (TK) locus by homologous recombination. PIVR reactions were done using VACVΔE3L virus (for controls) and VACVE3LΔ73C_F. Three rounds of selection were done in BSC-40 cells and white plaques instead of green were picked in each round. The resulting recombinant viruses were VACVE3LΔ73C_F-TK::$_F$E3LΔ83N and VACVE3LΔ73C_F-TK::$_F$E3LΔ83Nopp. All recombinant viruses were amplified in BHK-21 cells. An aliquot of the amplified virus was used for phenol/chloroform genomic DNA extraction and DNA sequencing.

Detection of the E3L domains by Western blot. Subconfluent cell monolayers in 60 mm dishes were infected at a multiplicity of infection (MOI) of 5 and processed at the indicated times. Samples were harvested by scraping the cells into 1X SDS sample buffer containing β-mercapto-ethanol and passing them through a QIAshredder homogenizer (QIAGEN) followed by a centrifugation step of two minutes at 16,000 g. Samples were heated at 95°C for five minutes and protein resolved on a 20% SDS-PAGE gel. Proteins were then transferred

overnight at 4°C to a Polyvinylidene fluoride (PVDF) membrane. The membrane was blocked with 1X TBS with Tween-20 containing 3% instant non-fat dry milk and probed with Anti-FLAG (clone M2) antibodies (Sigma) made in mouse or E3L antibodies (Jacobs' laboratory) made in rabbit. Proteins were detected by chemiluminescense (Pierce) and exposure to X-ray films.

Activated PKR and eIF2α phosphorylation assays. Subconfluent HeLa cells were infected at an MOI of 5. At 4 and 9 hours post-infection cell lysates were prepared as described in the previous section. Protein samples were resolved on a 10% SDS-PAGE gel. Separated proteins were then transferred for one hour at 100V to a nitrocellulose membrane, blocked with 1X TBS with Tween-20 containing 3% instant non-fat dry milk and probed with rabbit anti-eIF2α phospho (Ser 51) antibodies from Cell Signaling or rabbit anti-PKR phospho (Thr 446) antibodies from Epitomics. Proteins were detected by chemiluminescense (Pierce) and exposure to X-ray films. Following detection membranes were stripped using stripping buffer (62.5 mM Tris-HCl ph 6.8, 2% SDS, 100 mM beta mercaptoethanol) and probed with rabbit anti-PKR antibodies (Epitomics) or anti-eIF2α antibodies (Epitomics). Detection was done by chemiluminescense (Pierce) as described above. Membranes were then stripped and re-probed using rabbit anti-GAPDH antibodies (Abcam) in order to ensure that equal amounts of proteins were loaded.

Host range. Six well plates of BSC-40 and RK13 E3L cells were infected with several dilutions of virus in 1 mM Tris HCl pH 8.8. Plates were rocked every

10 minutes in order to keep the monolayers moist. After one hour the cells were overlaid with their appropriate media (DMEM 10%FBS for BSC-40 cells and MEM 5% FBS for RK13 cells). When plaques were visible (~30 hours), the monolayers were stained with crystal violet (0.5% in 20% ethanol). Plaques were counted and the titer was calculated for each virus. The efficiency of plaquing (EOP) was calculated by dividing the pfu/ml in BSC-40 cells by the pfu/ml in RK13 cells.

Multi-step growth curve. Four replicas of confluent JC cells seeded in 35 mm dishes were infected with the viruses described in Fig. 28 and the respective controls. The cells were rocked every 10 minutes for one hour. At one hour post-infection the inoculum was removed and the cells were washed three times with warm phosphate buffered saline (PBS). The cells were then overlaid with RPMI media containing 10% FBS. One set (two replicas) of the infected dishes was then harvested by scraping the cells into the media. Cells were then centrifuged at 2,000 g for 10 minutes at 4°C. The supernatant was discarded and the pellet resuspended in 1 mM Tris HCl pH 8.8, the samples were then subjected to three rounds of freeze/thaw (one hour at -80°C, 30 minutes on ice, two minutes at 37°C). Samples were then centrifuged and the supernatant was transferred to another tube. This first set of samples was considered the 0 hours post-infection time point. Another set of samples (two replicas) was harvested at 72 hours post-infection in a similar manner. Both set of samples were used to infect RK13 E3L

cells and the titers from the input virus (0 hours) with the titers were the virus went through multiple cycles of replication (72 hours) were compared.

RESULTS

Generation of recombinant viruses. In order to study the dual expression of both the Zα domain and the dsRNA binding domain of E3L, VACVE3LΔ73C_F-TK::$_F$E3LΔ83N and VACVE3LΔ73C_F-TK::$_F$E3LΔ83Nopp were constructed in the WR background by PIVR using the plasmid vectors pJ1-FLAGΔ83N-J3 and pJ1-FLAGΔ83Nopp-J3 as described in the material and methods section. In these viruses the native E3L promoter drives the region that codes for the Zα domain in the E3L locus while an early optimized promoter, EO_P, drives the region that codes for the dsRNA binding domain in the TK locus (Fig. 34). The sequence of EO_P was previously obtained by combining several mutations that resulted in having a greater effect on expression of β-galactosidase *in vitro* (44).

Confirmation of the dual expression of Zα domain (N-terminus) and the dsRNA binding domain (C-terminus) of VACV E3L. Preliminary results from Western blots have shown that viruses with the EO_P have the same relative amount of protein at early and late times post-infection indicating that both the native E3L promoter and EO_P function similarly (data not shown). The FLAG tag was added to the C-terminus of the Zα domain so this domain will retain the wild type Kozak sequence next to the first codon of the E3L protein. Similarly, the dsRNA binding domain has the FLAG tag in the N-terminus. In order to check for

functional protein expression, BHK cells were infected with the recombinant VACV viruses and controls made using the constructs depicted in Fig. 34. The infected cells were harvested at 6 hours post-infection and proteins resolved on a 20% SDS-PAGE gel. Proteins were then transferred overnight at 4°C to a PVDF membrane. Protein levels were compared among the different viruses by probing with antibodies specific for the FLAG tag. Equal expression of both domains can be observed for VACVE3LΔ73C$_F$-TK::$_F$E3LΔ83N (Fig. 35, lane 8) and VACVE3LΔ73C$_F$-TK::$_F$E3LΔ83Nopp (Fig. 35 lane 9). E3L antibodies were also used in order to detect both the Zα domain and the dsRNA binding domain of E3L (Fig. 36).

PKR activation and eiF2α phosphorylation. It has been previously demonstrated that the dsRNA binding domain of E3L is required to inhibit the activation of PKR (132). In order to determine the activation of PKR and the subsequent phosphorylation of eIF2α, HeLa cells were infected and cells were harvested at 4 and 9 hours post-infection. Proteins were then resolved in a 10% SDS-PAGE gel, transferred into a nitrocellulose membrane and probed with antibodies specific for the phosphorylated forms of PKR and eIF2α. Infection of HeLa cells with VACVΔE3L, VACVE3LΔ73C and VACVE3LΔ73C$_F$ (Fig. 37, lanes 2, 4 and 5 respectively) resulted in phosphorylation of PKR at 4 hours post-infection. PKR phosphorylation levels were higher in VACVΔE3L, VACVE3LΔ73C and VACVE3LΔ73C$_F$ (Fig. 37, lanes 2, 4 and 5 respectively) as well as in VACVE3LΔ73C$_F$-TK::$_F$E3LΔ83N (Fig. 37, lane 8) and

VACVE3LΔ73C$_F$-TK::$_F$E3LΔ83Nopp (Fig. 37, lane 9) by 9 hours post-infection, although less phosphorylation of PKR was observed in the VACVE3LΔ73C$_F$-TK::$_F$E3LΔ83N virus compared to VACVE3LΔ73C$_F$-TK::$_F$E3LΔ83Nopp. When PKR is phosphorylated it leads to the phosphorylation of eIF2α (Fig. 30). To determine if phosphorylation of PKR correlated with eIF2α phosphorylation, the protein-bound membranes were probed with antibodies specific for the phosphorylated form of eIF2α. Infection of HeLa cells with VACVΔE3L, VACVE3LΔ73C and VACVE3LΔ73C$_F$ (Fig. 38, lanes 2, 4 and 5 respectively) resulted in phosphorylation of eIF2α by 4 hours post-infection while eIF2α phosphorylation was observed in VACVΔE3L, VACVE3LΔ73C and VACVE3LΔ73C$_F$ (Fig. 38, lanes 2, 4 and 5 respectively) as well as in VACVE3LΔ73C$_F$-TK::$_F$E3LΔ83N (Fig. 38, lane 8) and VACVE3LΔ73C$_F$-TK::$_F$E3LΔ83Nopp (Fig. 38 lane 9) by 9 hours post-infection.

Host range phenotype of VACV E3L mutants. Wild type VACV has previously been shown to have a broad host range (213). Moreover, it has been demonstrated that E3L has a role in the host range by regulating PKR activity. VACVΔE3L is unable to grow in HeLa cells because the endogenous level of PKR is higher in the HeLa cells compared to BHK cells, which support the growth of the mutant VACV (133). Thus, the host range restriction of VACV is closely tied in with the anti-viral state of a cell and on the ability of the virus to disable the host response to infection. While VACV E3L C-terminal mutants are able to replicate in BHK and RK13 cells, they are not able to replicate in HeLa

cells (213) or BSC-40 cells (Jacobs' laboratory, unpublished data). On the other hand, VACV E3L N-terminal mutants are able to grow in BHK, RK13, HeLa and BSC-40 cells (broad host range) indicating that the amino terminus is dispensable for virus replication in these cell lines (14, 35, 241). Plaque assays in RK13 and BSC-40 cells using equal amounts of the recombinant viruses constructed were done in order to get data regarding the host range of these mutants. All viruses were able to replicate in RK13 cells while only the viruses that have the Zα domain of E3L intact were able to replicate in BSC-40 cells (Table 2).

E3L Zα domain needs to be linked to the dsRNA biding domain for replication in JC cells. Another cell line that was used in order to evaluate the mutants is the JC cell line. The JC cells are epithelial cells obtained from the mammary glands of mice with adenocarcinoma and have been useful in the characterization of amino terminal mutants (100, 228). JC cells were infected at an MOI of 0.05 and harvested at 0 hours and 72 hours post-infection in order to determine the input and resultant titer following several rounds of viral replication. As observed in Fig. 33 only wt VACV was able to replicate in this cell line indicating that both the Zα domain and the dsRNA binding domain of E3L need to be linked together in order for a virus to replicate. These findings correlate with previous results of a similar experiments that showed replication in the JC cells of the $Z\alpha_{ADAR1}$-$E3L_C$ chimera where both domains are fused (data not shown).

DISCUSSION

This chapter provides insights into the role of the N-terminal Z-DNA binding domain of E3L, a protein that is primarily responsible for making VACV IFN resistant (133). Although VACV, the agent used in the smallpox vaccine, is one of the most effective vaccines ever used, it can cause severe complications after vaccination especially in immunosuppressed individuals (66). In the last four decades safer and highly immunogenic candidate VACV vaccines have been developed for a variety of uses (47, 108, 118). Some of these safer effective alternatives focus on the modulation of immune evasion genes (136, 137). As it was previously mentioned, one of these VACV immune evasion genes is E3L. E3L contains two domains with apparently non-overlapping functions. The C-terminus binds to dsRNA and inhibits the activation of the IFN-inducible proteins, protein kinase R (PKR) and 2'-5' oligoadenylate synthase (OAS) (19). Binding to dsRNA also inhibits phosphorylation of a constitutively expressed transcription factor, IRF-3, which in turn leads to inhibition of IFN-β production (217). The N-terminus, on the other hand, contains a Z-DNA binding domain, which belongs to the Zα family (129). Deletion of this domain renders VACV apathogenic as demonstrated in previous studies indicating a role for Z-DNA binding in VACV pathogenesis and neurovirulence in infected mice (122).

The goal of this chapter was to elucidate the functions of the E3L domains in the evasion of the IFN response and to determine the possible interaction of both domains with dsRNA after viral infection**.** The specific hypothesis behind

this research is that the N-terminus of E3L inhibits PKR activation by interacting with dsRNA in its Z-form and that this interaction is mediated by binding of the C-terminus to the same molecule (Fig. 40). This hypothesis was based on the following observations: First, deletion of type I IFN receptors (IFNα/βR -/-) in mice restores the pathogenicity of VACVE3LΔ83N to wild type levels (235). Second, in mouse embryo fibroblasts (MEFs) from the parental strain (129SV) of the IFNα/βR -/- mice, E3LΔ83N is IFN sensitive and this is mediated by phosphorylation of the PKR substrate, eIF2α (235). Third, this sensitivity is reversed in MEFs from PKR-/- mice, as well as in MEFs transfected with siRNA targeting PKR (235). Fourth, the recent crystal structure of $Z\alpha_{ADAR1}$ bound to Z-RNA indicate that binding of both Z-DNA and Z-RNA is possible through this domain, suggesting that the Zα domain could target dsRNAs containing purine-pyrimidine repeats, possibly of viral origin (179). Based on these observations, the experimental focus of this chapter was on the N-terminus of E3L, which contains a Z-DNA binding domain (121).

Preliminary studies have shown that the chimeric virus $Z\alpha_{ADAR1}$- $E3L_C$ previously described (164) is able to retain its lethality after intracranial inoculation (122) suggesting not only that the ability to bind Z-DNA is essential to E3L activity but also that both domains need to be linked together in order to work. Moreover, studies done in the JC cell line, where N-terminus mutants of E3L are unable to replicate, have shown that both wt VACV as well as the $Z\alpha_{ADAR1}$- $E3L_C$ chimera replicate to similar titers by 72 hours post-infection (data

not shown). The present study demonstrates that both the Z-DNA binding domain and the dsRNA binding domain of E3L need to be linked together in order to inhibit PKR phosphorylation and in order to replicate in JC cells. This was assessed by constructing two forms of a dual expression virus, which express equally amount of both the Zα domain in the E3L locus and the dsRNA binding domain of E3L in the TK locus. These viruses were first tested for their ability to rescue a wild-type VACV phenotype in cells in culture as well as activation of PKR and subsequent eIF2α phosphorylation. VACVΔE3L, VACVE3LΔ73C and VACVE3LΔ73C$_F$ were unable to replicate in BSC-40 cells indicating that the dsRNA binding domain is necessary for replication in this cell line. Interestingly, when comparing the efficiency of plaquing between VACVΔE3LTK::$_F$E3LΔ83N and VACVE3LΔ73C$_F$-TK::$_F$E3LΔ83N it was observed that the dual expression virus had an EOP value comparable to wt VACV while the EOP of VACVΔE3L-TK::$_F$E3LΔ83N was comparable to the control virus VACVE3LΔ83N (Table 2). This difference could indicate that the Zα domain could be indeed partially rescuing replication in the BSC-40 cell line although further analyses are needed. Moreover, VACVE3LΔ73C$_F$-TK::$_F$E3LΔ83Nopp was unable to replicate as efficiently as VACVE3LΔ73C$_F$-TK::$_F$E3LΔ83N in this cell line. These results correlate with the PKR activation observed at 9 hours post-infection in the HeLa cell line where late phosphorylation of PKR was observed for VACVE3LΔ73C$_F$-TK::$_F$E3LΔ83N and VACVE3LΔ73C$_F$-TK::$_F$E3LΔ83Nopp with levels of phosphorylation higher for VACVE3LΔ73C$_F$-TK::$_F$E3LΔ83Nopp (Fig. 37). The

lower replication levels in BSC-40 cells as well as higher phosphorylation levels of PKR at 9 hours post-infection in VACVE3LΔ73C$_F$-TK::$_F$E3LΔ83Nopp could be due to the fact that transcription in the TK locus with the TK promoter and the early optimized promoter going in the opposite direction may be generating more dsRNA. These higher levels of dsRNA would not be able to be masked effectively by the dsRNA binding domain, activating the IFN-inducible PKR protein and affecting replication in the BSC-40 cell line.

Neither VACVE3LΔ73C$_F$-TK::$_F$E3LΔ83N nor VACVE3LΔ73C$_F$-TK::$_F$E3LΔ83Nopp were able to replicate in the JC cell line, similar titers were observed in VACVΔE3L, viruses lacking a Zα domain (VACVE3LΔ83N and VACVTK::$_F$E3LΔ83N) and viruses lacking a dsRNA binding domain (VACVE3LΔ73C and VACVE3LΔ73C$_F$) suggesting that both domains have to be linked together for replication in the JC cells (Fig. 39). Based on these and previous results a model (Model 1, Fig. 40) that could explain the role of the Zα domain of E3L in the activation of the PKR would be that the binding of the dsRNA binding domain of E3L to dsRNA causes a torsional strain that generates a transient Z-form which would be then bound by the Zα domain of E3L. On the other hand, following binding to dsRNA by the dsRNA binding domain of E3L, the Zα domain could as well recognize a specific sequence and facilitate and A to Z transition (Model 2, Fig. 40). A model indicating PKR activation when using the dual expression virus from this study is depicted in Fig. 41. When both E3L domains are not linked together, only the dsRNA binding domain would be able

to bind to dsRNA, PKR which have been induced by IFN secreted from neighboring infected cells would then compete with E3L and bind to dsRNA. Binding of two PKR molecules to the same dsRNA will lead to a stable dimer which will in turn be phosphorylated rendering PKR active (250).

In models 1 and 2, binding of the dsRNA binding domain of E3L to dsRNA would increase the affinity of the Zα domain towards dsRNA in its Z-form. In order to determine the affinity of the Zα domain of E3L towards Z-RNA, some biochemical assays can be performed. One of them would include the expression on the Zα domain using a bacterial expression vector. The purified expressed protein could then be exposed to chemically synthetic Z-RNA, to be obtained through bromination and specific salt concentrations, and their binding affinity measure using surface plasmon resonance. Moreover, both Z-forms of RNA (Z_D and Z_L) could be tested in order to evaluate the binding affinities of the Zα domain of E3L towards both forms. Because binding of $Z\alpha_{ADAR1}$ to Z-RNA has been confirmed using X-ray crystallography (179), binding of the Zα domain of E3L to Z-RNA is feasible and would constitute a novel role for this protein.

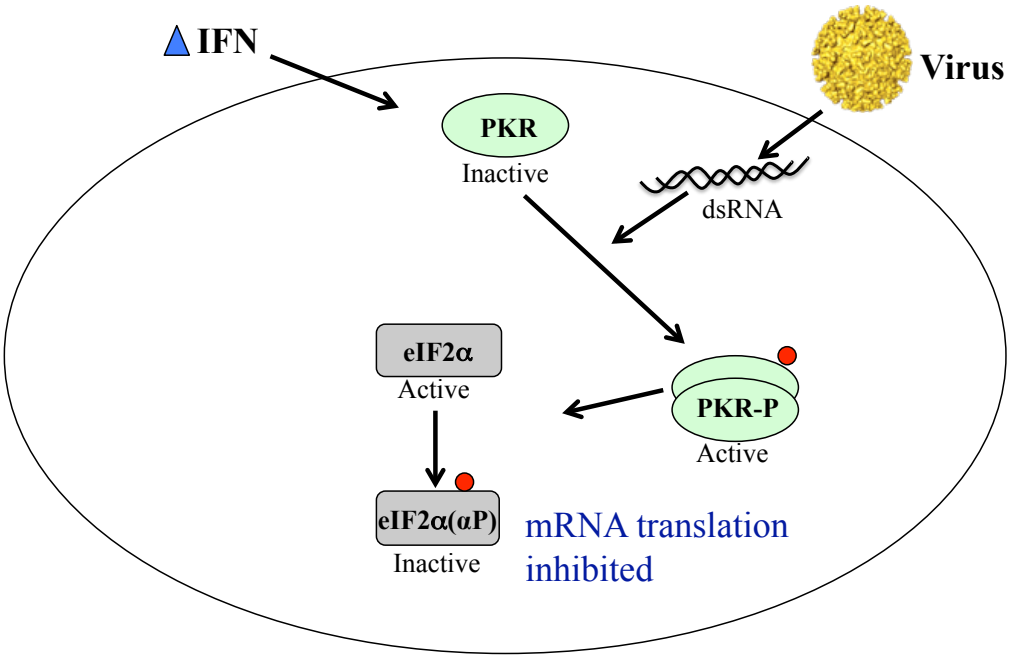

FIG. 30. Double stranded RNA dependent kinase pathway. A virus infected cell secretes IFN as a warning signal for nearby cells that are uninfected. IFN induces the synthesis of many genes. One of these genes encodes for the protein PKR which becomes activated by dsRNA produced as a byproduct of viral infection in the host cell. Activated PKR then phosphorylates eIF2α, this inhibits cellular mRNA translation, thereby preventing viral protein synthesis. VACV E3L protein binds to the dsRNA molecules and prevents binding and activation of PKR allowing for viral protein synthesis and replication of the virus.

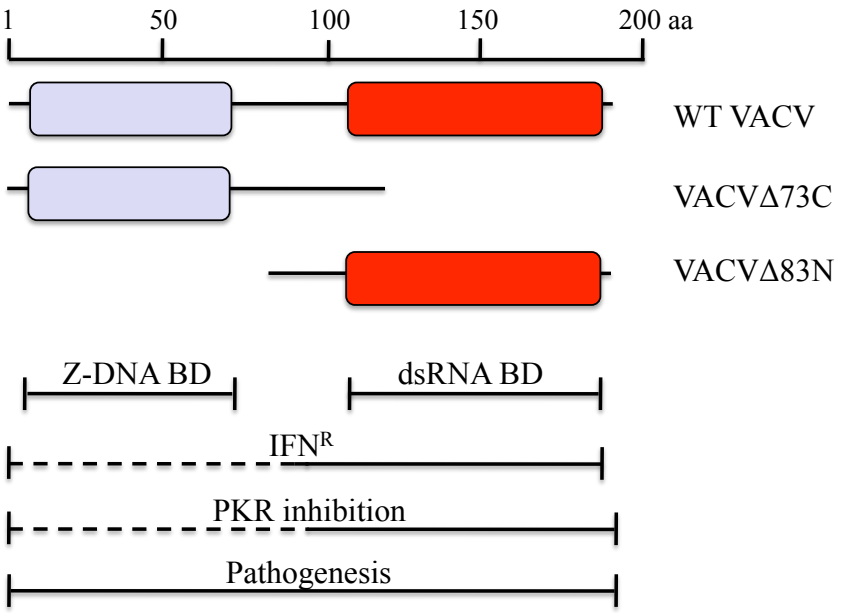

FIG. 31. Schematic representation of the E3L protein. The wild type VACV expresses an E3L protein that contains a Z-DNA binding domain (Z-DNA BD) in the N-terminus and a dsRNA binding domain (dsRNA BD) in the C-terminus. IFN^R= interferon resistant.

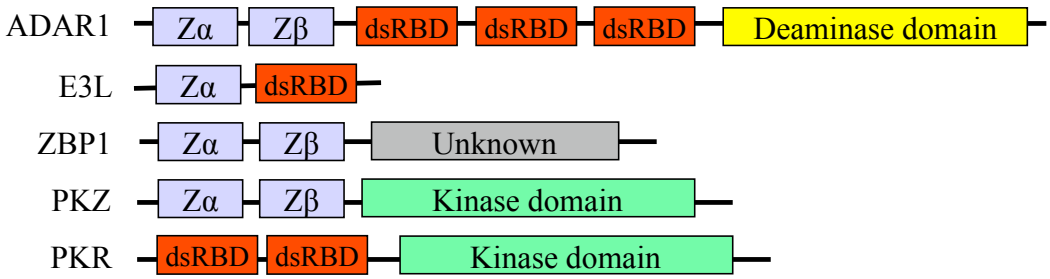

FIG. 32. Domain organization of some proteins with a Zα domain. The following proteins are represented: human ADAR1, VACV E3L, mouse ZBP1 and zebrafish PKZ. Human PKR is shown as a comparison with PKZ as PKZ has a PKR-like kinase activity but has two Zα domains instead of two dsRNA binding domains (dsRBD).

A

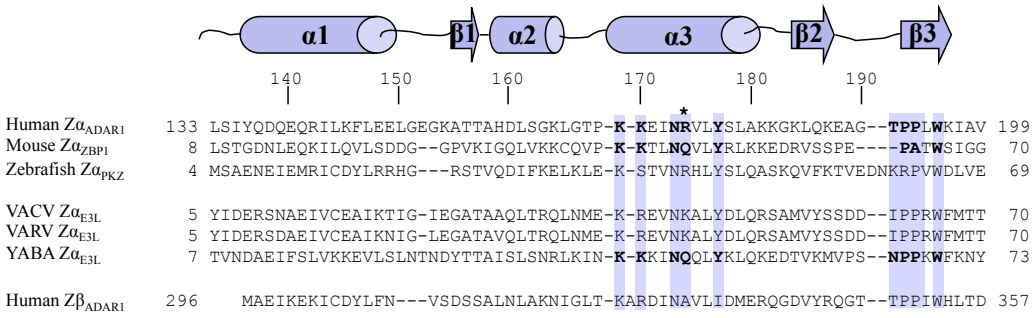

B

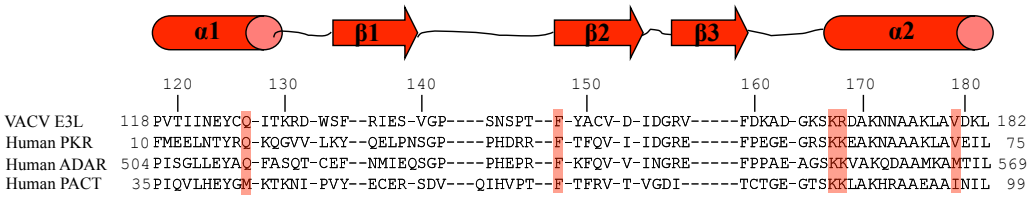

FIG. 33. Comparison of the amino acid sequence of the Zα domain and dsRNA binding domain in VACV E3L and various species with related proteins. (A) Zα domains. Residues interacting with Z-DNA based on X-ray crystal structures are in bold and highlighted. Homologous residues in proteins whose structure has not been determined are highlighted. Sequence of the related human $Z\beta_{ADAR1}$ is also shown as comparison. The recent crystal structure of $Z\alpha_{ADAR1}$ bound to Z-RNA indicates that the same residues that participate in Z-DNA binding are involved in Z-RNA binding with the exception of R 174 (*). (B) Double stranded RNA binding domains. Alignment of VACV E3L double stranded RNA binding domain with human proteins known to bind dsRNA. Highlighted residues are known to interact with either dsRNA or PKR.

TABLE 1. Oligonucleotide primers utilized in plasmid constructions

Name	Sequence (5' → 3')[a]
Δ73C-FLAG$_F$	GAATTCGGATCCCCCGGGCTGCCTGAAAAATGTCTAAGATCTATATCG
Δ73C-FLAG$_R$	GAATTCCTGCAGTCA*CTTGTCGTCGTCGTCCTTGTAGTC*GTTAGCACCTTTCC
Δ83N-FLAG$_F$	GAATTCGAGCTCAAAAATTGAAAAACTATTCTAATTTATTGCACGGGTTAACG
Δ83N-FLAG$_R$	GAATTCCCCGGGTCAGAATCTAATGATGACGTAACCAAGAAGTTTATC
Δ83N-FLAGopp$_F$	GAATTCGAGCTCATAAAAACTGCAGTCAGAATCTAATGATGACGTAACCAAG
Δ83N-FLAGopp$_R$	GAATTCCCCGGGAAAAATTGAAAAACTATTCTAATTTATTGCACGGG
J1R$_F$	GAATTCCATATGGATCACAACCAGTATCTCTTAACGATGTTCTTCG
J1R$_R$	GAATTCGAGCTCGATGACAATAAAGAATTAATTATTGTTCACTTTATTC
J3R$_F$	GAATTCCCCGGGTATTATATTTTTTATCTAAAAAACTAAAAATAAACATTG
J3R$_R$	GAATTCCTGCAGTGGATCTCACATCAGAAATTAAAATAATCTTAGAAGGATG

[a] Engineered restriction sites are underlined on the primer sequence.

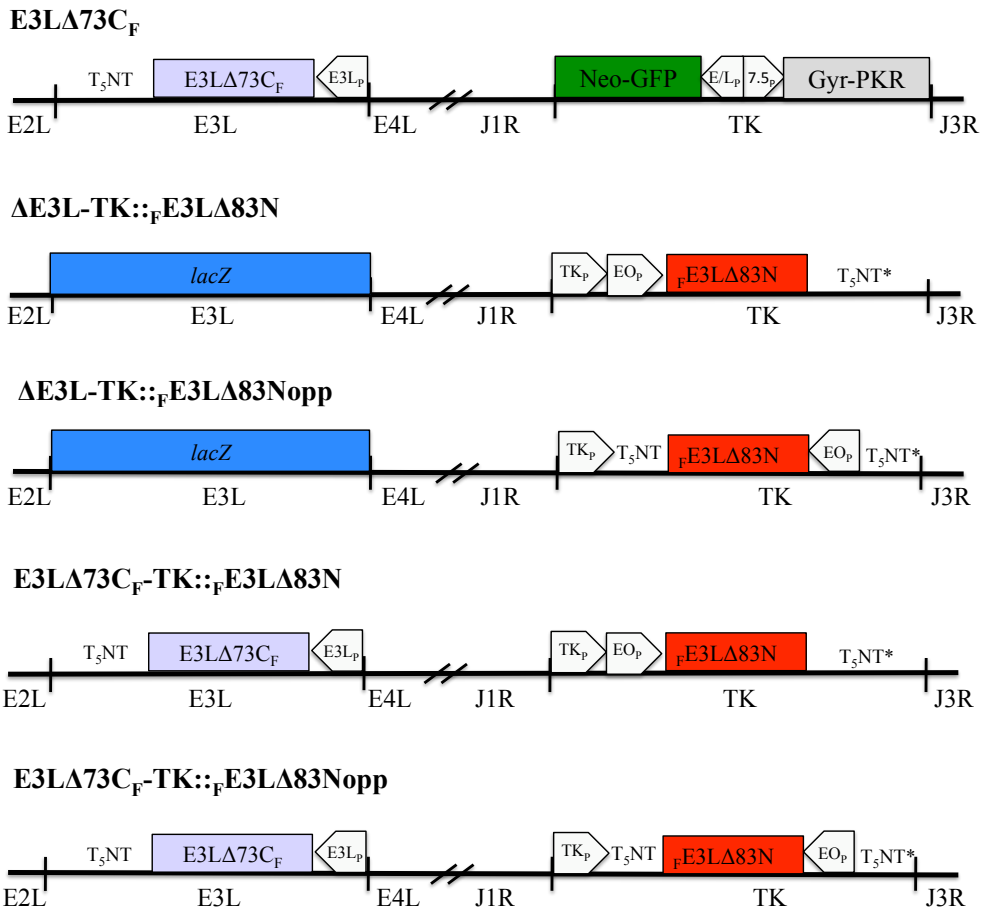

FIG. 34. Schematic representation of the constructs engineered to make the viruses analyzed in this study. The sequence coding for the Zα domain of E3L is driven by the natural E3L promoter ($E3L_P$) in the E3L locus while the sequence that codes for the dsRNA binding domain is driven by the early optimized promoter (EO_P) in the TK locus. The transcriptional stop is denoted by T_5NT while T_5NT* denotes the transcriptional stop for TK. The $_F$ denotes the position of the FLAG in the construct.

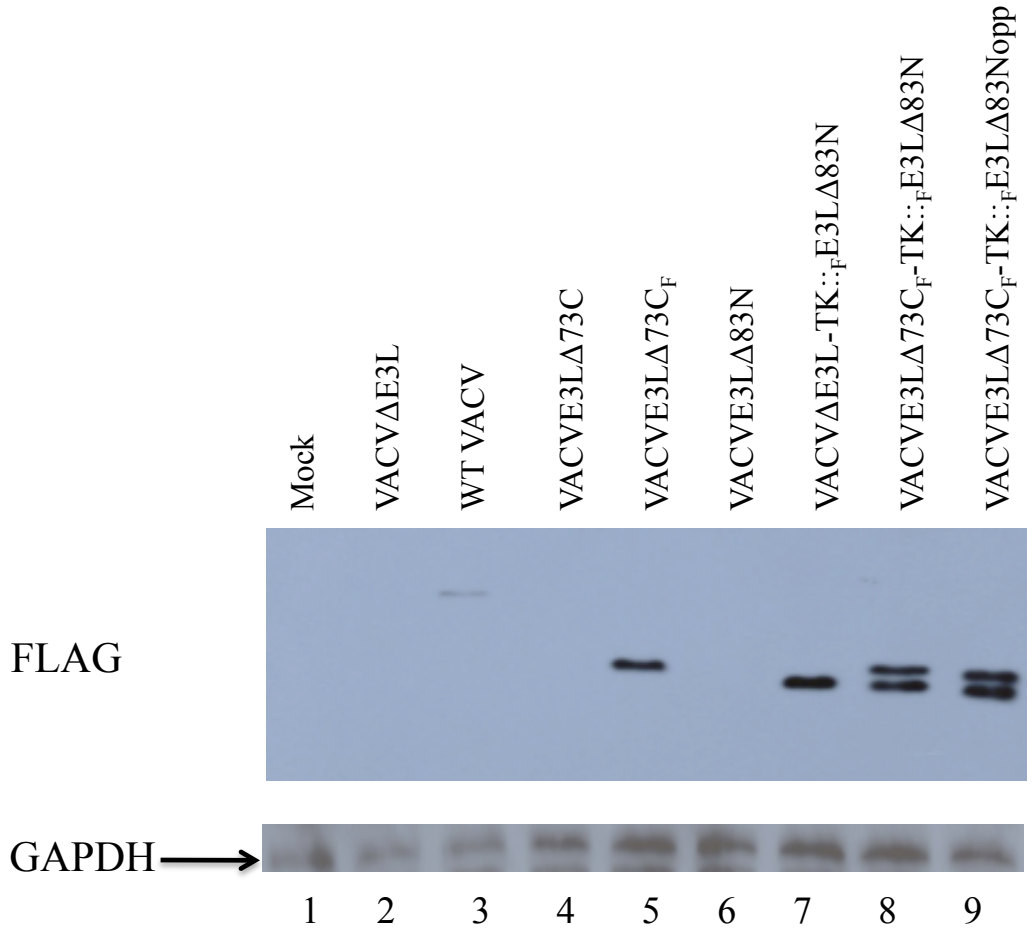

FIG. 35. Equal levels of expression of both the Zα domain and the dsRNA binding domain of VACVE3LΔ73C$_F$-TK::$_F$E3LΔ83N and VACVE3LΔ73C$_F$-TK::$_F$E3LΔ83Nopp. BHK cells were either mock-infected (lane 1) or infected with the indicated E3L mutants at an MOI of 5. At 6 hours post-infection, the infected monolayers were harvested, separated on a 20% SDS-PAGE gel and analyzed by Western blot analysis using antibodies specific for FLAG. Results represent three independent assays.

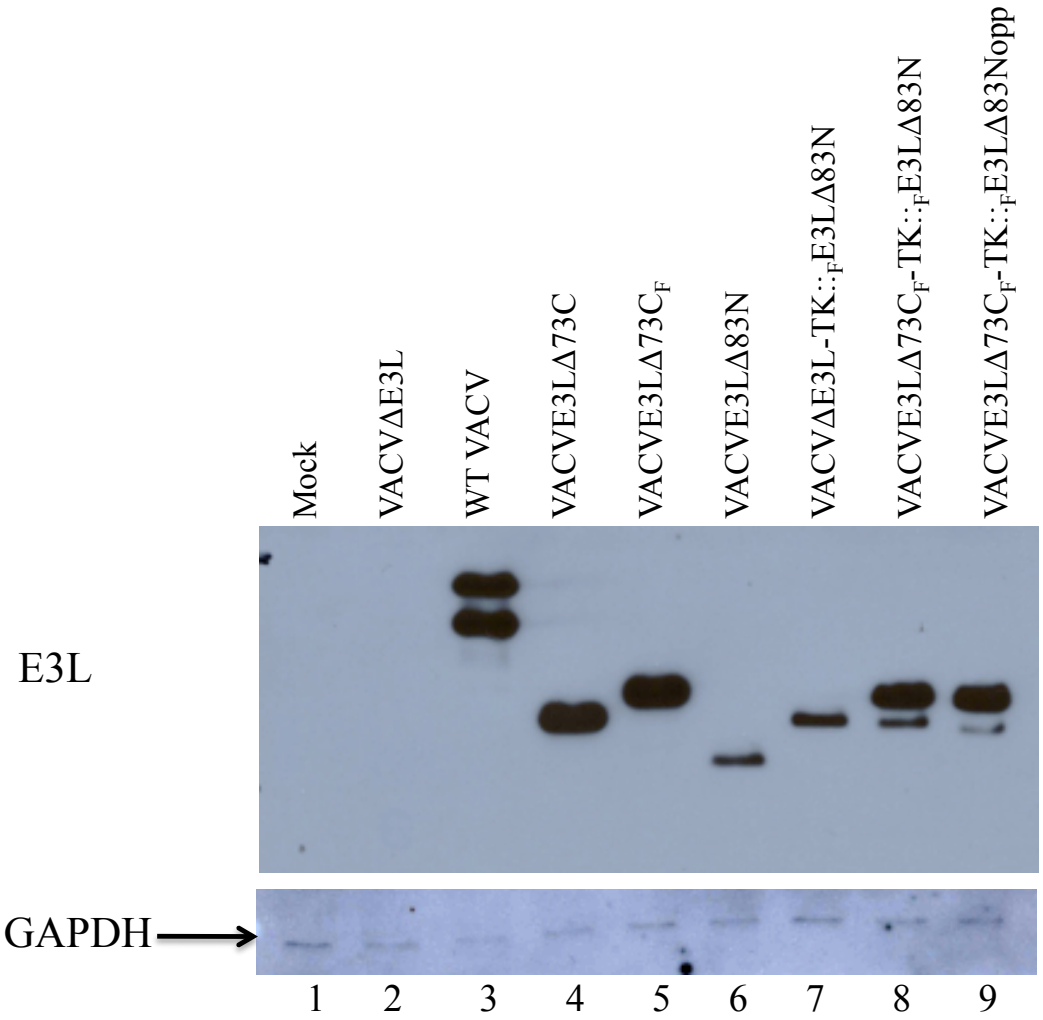

FIG. 36. Expression o the Zα domain and the dsRNA binding domain of E3L. BHK cells were either mock-infected (lane 1) or infected with the indicated E3L mutants at an MOI of 5. At 6 hours post-infection, the infected monolayers were harvested, separated on a 20% SDS-PAGE gel and analyzed by Western blot analysis using rabbit antiserum against E3L. Results represent three independent assays.

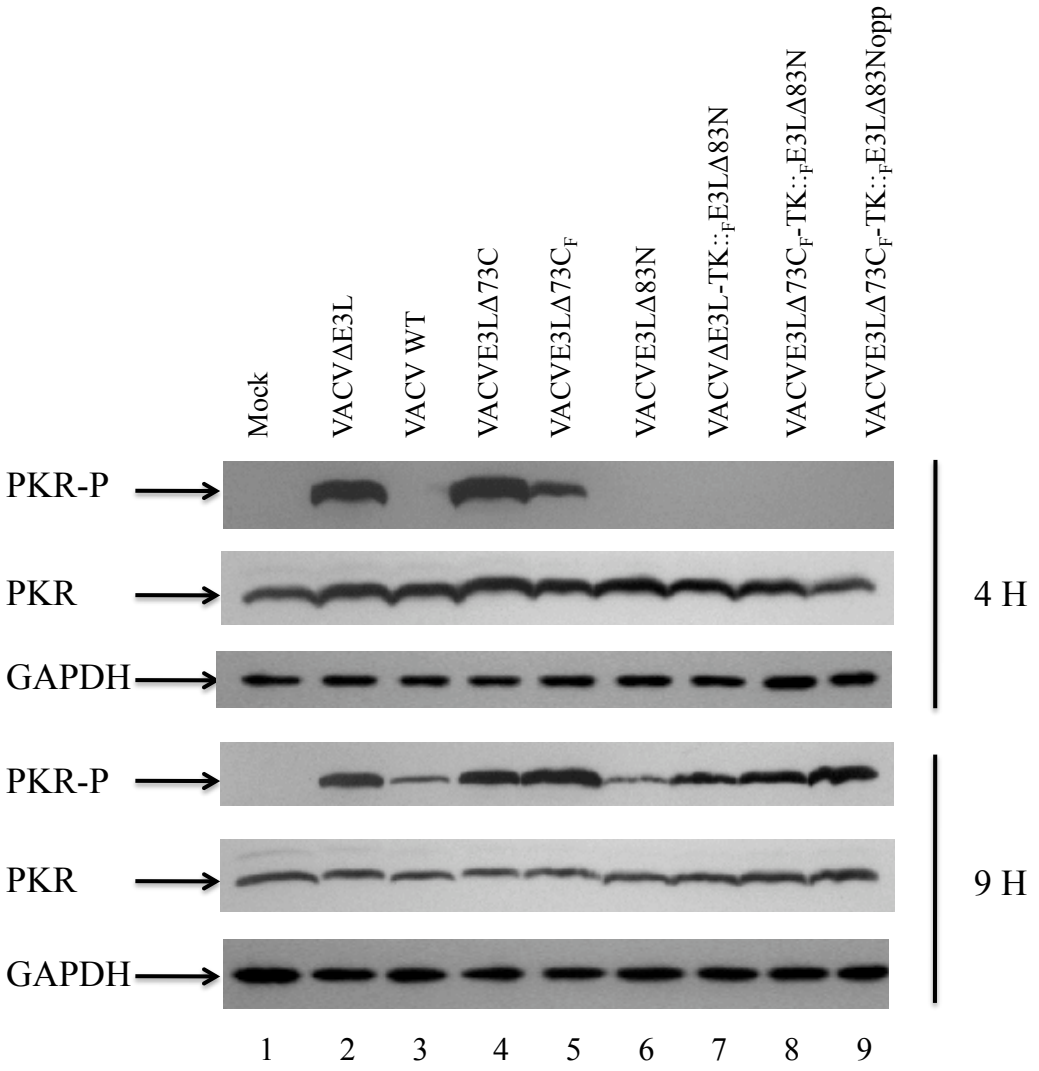

FIG. 37. PKR phosphorylation assay. HeLa cells were either mock-infected (lane 1) or infected with the indicated E3L mutants at an MOI of 5. At 4 and 9 hours post-infection, the infected monolayers were harvested, separated on a 10% SDS-PAGE gel and analyzed by Western blot analysis using specific antibodies against the phosphorylated form of PKR (PKR-P). The membranes were then stripped for proteins and reprobed with antibodies against PKR. Results represent two independent assays.

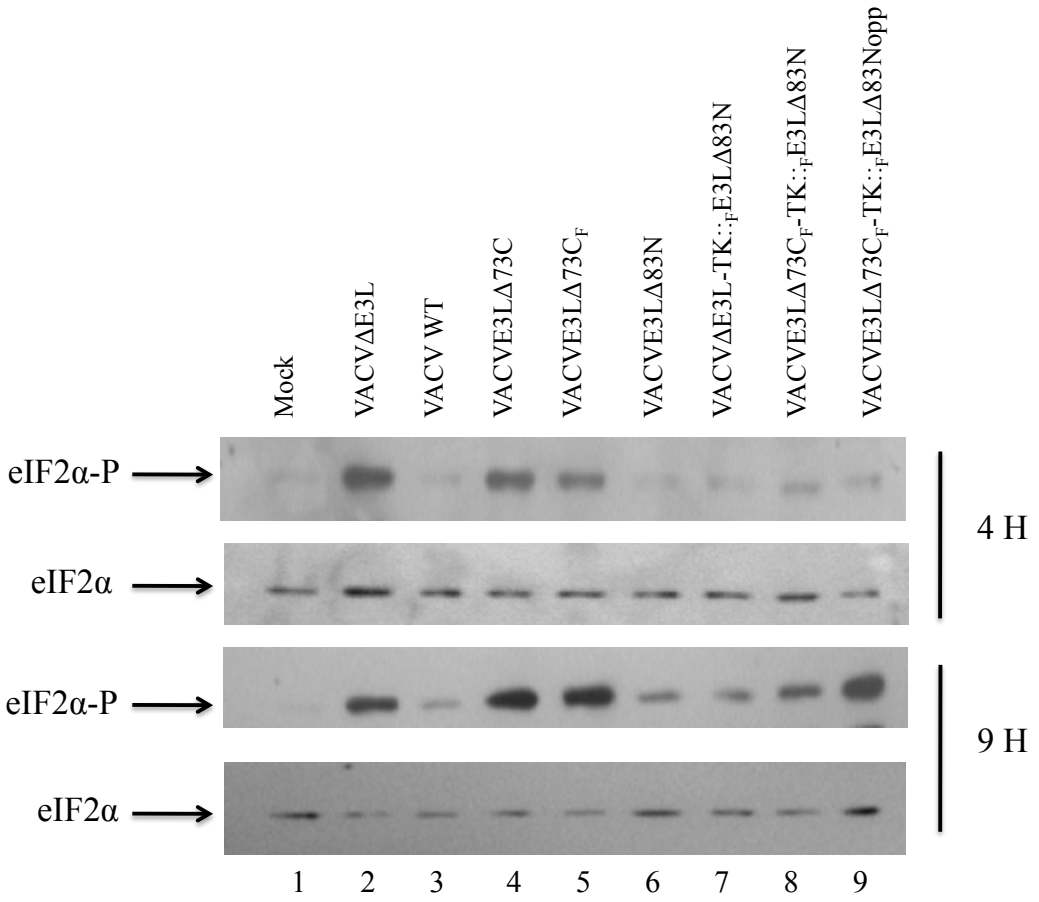

FIG. 38. eIF2α phosphorylation assay. HeLa cells were either mock infected (lane 1) or infected with the indicated E3L mutants at an MOI of 5. At 4 and 9 hours post-infection, the infected monolayers were harvested, separated on a 10% SDS-PAGE gel and analyzed by Western blot analysis using specific antibodies against the phosphorylated form of eIF2α (eIF2α-P). The membranes were then stripped for proteins and reprobed with antibodies against total eIF2α. Results represent two independent assays.

TABLE 2. Determination of host range in BSC-40 cells. The efficiency of plaquing (EOP) is calculated by dividing the pfu/ml in BSC-40 cells by the pfu/ml in RK13 cells.

Virus	RK13 cells (pfu/ml)	BSC40 cells (pfu/ml)	EOP
WT VACV	$9.5x10^9$ +/- $5.5x10^8$	$1.39x10^{10}$ +/- $9.03x10^8$	1.47
VACVΔE3L	$4.4x10^9$ +/- $6.0x10^8$	<10	<0.001
VACVE3LΔ73C	$2.6x10^8$ +/- $4.0x10^7$	<10	<0.001
VACVE3LΔ73C_F	$1.6x10^8$ +/- $6.0x10^7$	<10	<0.001
VACVE3LΔ83N	$1.1x10^{10}$ +/- $3.4x10^9$	$1.02x10^{10}$ +/- $3.5x10^9$	0.96
VACVΔE3L-TK::$_F$E3LΔ83N	$1.55x10^9$ +/- $7.5x10^7$	$1.27x10^9$ +/- 1.8510^8	0.82
VACVE3LΔ73C_F-TK::$_F$E3LΔ83N	$3.1x10^9$ +/- $1.0x10^8$	$4.94x10^9$ +/- $4.38x10^8$	1.59
VACVE3LΔ73C_F-TK::$_F$E3LΔ83Nopp	$1.49x10^9$ +/- $3.5x10^7$	$5.35x10^8$ +/- $4.23x10^7$	0.36

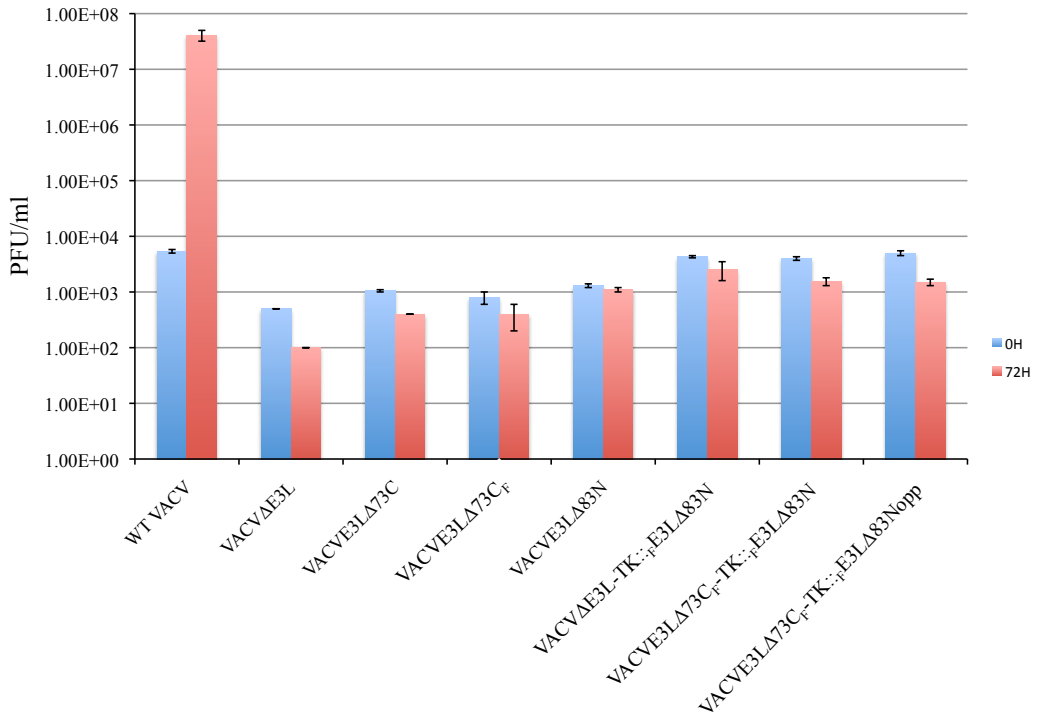

FIG. 39. Replication of the dual expression viruses in JC cells. Two sets of confluent 35 mm dishes with confluent JC cells were infected at an MOI of 0.05 with the indicated viruses. Following one hour of incubation the inoculum was removed and the cells rinsed with PBS and overlay with the corresponding media. At 0 hours and 72 hours post-infection the dishes was harvested and the titer was determined in RK13 cells. Error bars indicate the standard error of the mean.

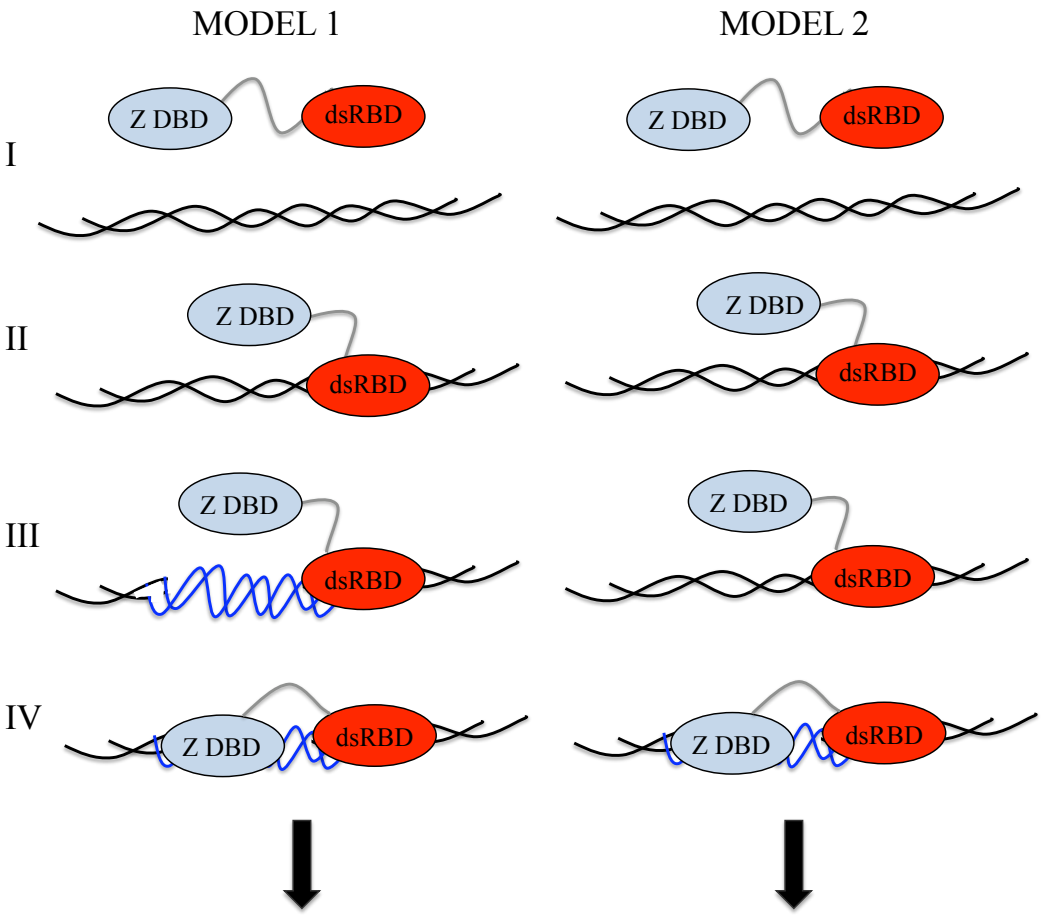

FIG. 40. Possible role of the E3L Zα binding domain in the activation of the PKR system. In model 1, binding of the dsRNA binding domain causes a torsional strain that generates a transient Z-form, which is stabilized by the Zα binding domain. In model 2, the Z-DNA binding domain recognizes a specific sequence and facilitates the A to Z transition. Z-DNA binding domain=Z DBD, dsRNA binding domain=dsRBD.

FIG. 41. Model indicating PKR activation in the presence of independent expressed proteins made by a dual expression virus from this study. Steps I to III: Binding of the dsRNA binding domain to dsRNA, in its A-form, causes a torsional strain that generates a transient Z-form (blue). Step IV: In the absence of the Z-DNA binding domain in the proximity, the Z-form returns to its original configuration. Step V: PKR, which was induced by IFN, will be able to successfully compete with the dsRNA binding domain of E3L and bind to dsRNA using both of its dsRBD. Binding of two PKR molecules to the same molecule of dsRNA leads to formation of stable PKR dimers and dissociation of the inhibitory interaction between PKR dsRBD II and its kinase domain. Z DBD= Z-DNA binding domain, dsRBD=dsRNA binding domain, K_N and K_C=N-terminal and C-terminal domain of PKR kinase domain respectively.

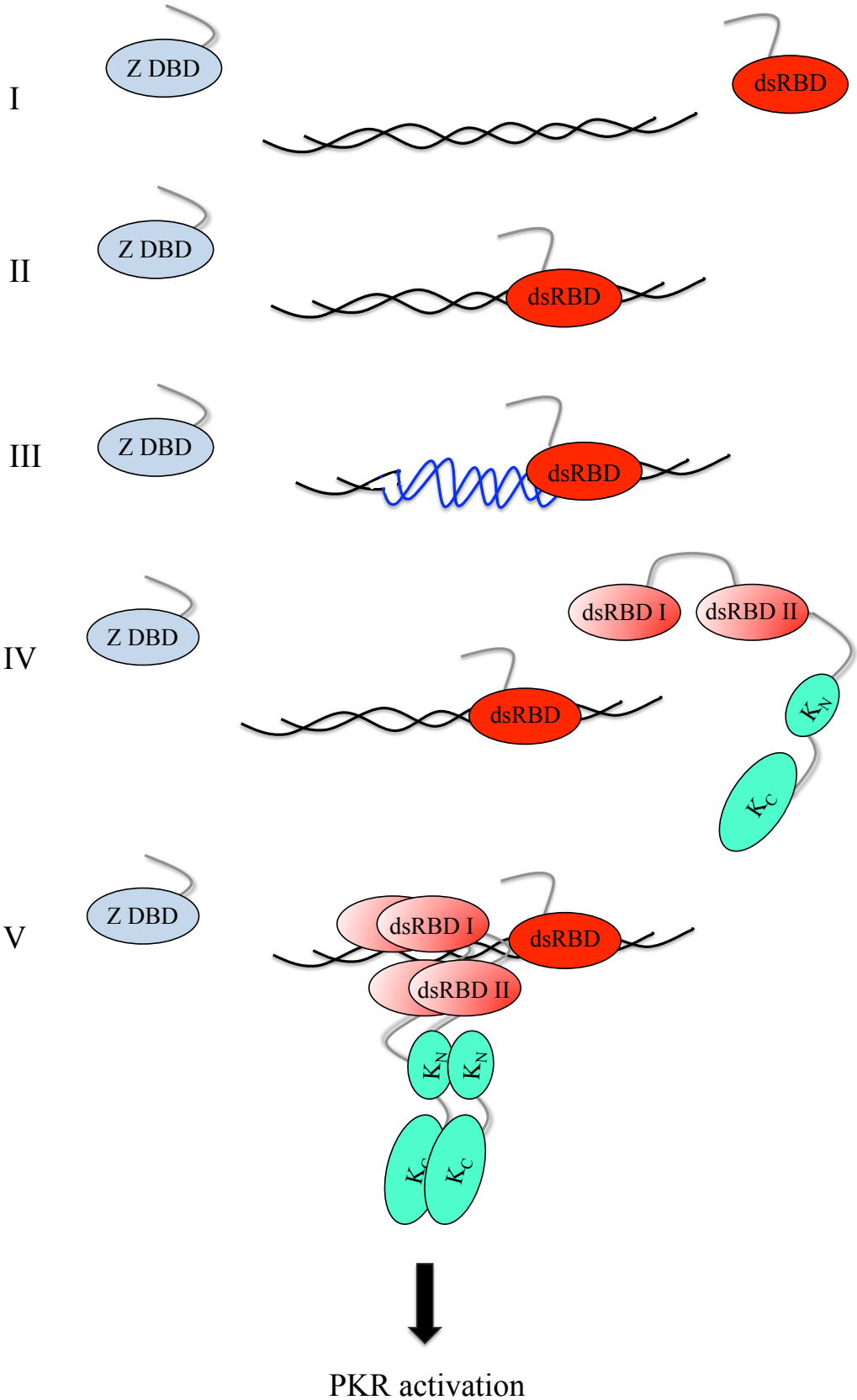
I
Z DBD
dsRBD
II
Z DBD
dsRBD
III
Z DBD
dsRBD
IV
Z DBD
dsRBD I
dsRBD II
dsRBD
K_N
K_C
V
Z DBD
dsRBD I
dsRBD
dsRBD II
K_N
K_N
K_C
K_C
PKR activation

CHAPTER 4

USE OF MATHEMATICAL MODELS AS TOOLS FOR DENGUE RESEARCH

ABSTRACT

Dengue is one of the most severe and under-diagnosed vector-borne diseases in the world threatening two-fifths of the world population. That is, there are 2.5 billion individuals at risk including individuals living in some regions of the U.S. World statistics put a range of 50 to 100 million documented infections every year including approximately 500,000 severe cases and 22,000 deaths, involving mostly children (236). Dengue is a primarily epidemic disease where prior strain-specific infections may lead to increased susceptibility to the severe potential fatal Dengue Hemorrhagic Fever (DHF) and Dengue Shock Syndrome (DSS). There is not yet a vaccine for dengue due to unresolved challenges in the development of candidate vaccines (223). While other challenges such as education and vector control are also important, attention should be also directed towards the understanding of other parameters such as the vector and host interactions, vaccine candidates' effectiveness, dynamics of circulating dengue serotypes, vectors life history dynamics, geographical and demographical factors as well as the pathogens' evolution. Identifying, implementing and evaluating "optimal" solutions that diminish or prevent the spread of dengue, given our knowledge and resources, are being explored systematically through the use of

mathematical models (38-40, 208) and Murillo, D., Holechek, S., Sanchez, F. & Castillo-Chavez, C., manuscript in preparation. This chapter highlights my personal perspective as a non-mathematical scientist on the importance of the interactions between lab/field scientists and mathematical modelers and collaborative efforts that may allow for the best use of "lab" results in addressing public health policies over multiple spatial and temporal scales. Modeling involves the establishment of quantitative theories and the simulation of "realistic" scenarios and in the process one must identify key transmission biological parameters (20). A personal review of the mathematical theory and its connections to its use in the study of transmission dynamics and control of dengue will be reviewed. Data pertinent to the Luciano Castillo Colonna (LCC) region in Peru, the region where dengue virus 2 (DENV-2) Asian genotype, dengue virus 3 (DENV-3) and dengue virus 4 (DENV-4) first entered the country during the 2000-2001 outbreak will be used as a platform and a preliminary analysis of the basic reproductive number will be presented.

INTRODUCTION

Infectious diseases have played an important role in the evolution of civilizations around the world and are still a prevalent problem for humans specially with the continuous travelling within cities (41, 50, 178). Understanding the spatio-temporal dynamics of diseases such as dengue, one of the most important emerging and re-emerging infectious diseases in the last few decades

(93, 98, 178, 236) over multiple scales, requires multidisciplinary and transdisciplinary efforts.

My personal experience with dengue started while I was working in the Molecular Biology Division at the National Institute of Health in Peru. As a molecular biologist in charged of the molecular diagnosis of dengue and member of the dengue multi-disciplinary team I had the opportunity to witness first hand what this disease can do to a country when there is not a prevention plan in place.

Walking through the hospitals in Sullana (Piura, LCC region, Peru) filled with patients being treated intravenously and children being tested for hemorrhagic symptoms was a life changing experience. While many lessons were learned as a country during that first dengue outbreak in Peru with hemorrhagic cases (154), more questions were raised. Dengue is now endemic in the LCC region and in many other areas in Peru, and is an impacting health challenge especially with the introduction of new strains into susceptible populations that need to be understood and quantified. Here at Arizona State University I had the opportunity to interact and collaborate with mathematical modelers with vast experience modeling dengue and have come to the conclusion that both fields can benefit from each other when trying to understand the larger scale implications of dengue as a disease. This is the rationale for adding a chapter to my dissertation on the challenges and opportunities posed by the study of complex adaptive systems given by the human-vector-dengue dynamics, using mathematical models.

I will first review the epidemiology of dengue in order to identify the nature of the assumptions that are commonly made by mathematical modelers. Different classes of dengue models will be also reviewed and classified in the Materials and Methods section according to specific perspectives.

The etiological agent of the disease, dengue virus, is a single-stranded, positive-sense RNA virus that belongs to the genus *Flavivirus*, family *Flaviviridae* (49). Dengue has four antigenically different serotypes (DENV-1, DENV-2, DENV-3 and DENV-4), each one with the potential of causing disease. The pathogenicity of the disease can range from asymptomatic to mild dengue fever (DF) to dengue hemorrhagic fever (DHF) and dengue shock syndrome (DSS), which affect primarily children (49, 93). According to the World Health Organization, 40% of the global population is in risk for dengue infection with an estimate of 50 to 100 million infections yearly including 500,000 cases of DHF and 22,000 deaths, mostly among children (236).

Although dengue has historically been a tropical disease, it now has a foothold in the U.S. Dozens of cases have been reported in Florida and it is believed that over 5% of the Key West population has been exposed (32). Hence, dengue represents a real threat to the U.S., especially considering the amount of international travel and high DF prevalence in many regions (156) including Southeast Asia, with a 70% increase in cases during the last decade (128).

Infection with one dengue serotype does not usually protect against the others, and while a secondary infection with a heterologous serotype increases the

probability of DHF and DSS (25, 94), there are also reports that indicate that a primary infection may be also responsible of severe dengue cases (85, 202, 249). The antibody-dependent enhancement (ADE) mechanism also known as the immune enhancement theory, explains in part the phenomena observed with heterologous infection and it has been observed *in vitro* for dengue and other viruses (95) as well as in the observation of pre-existing immunity to other serotypes (155, 226).

Another concern about dengue is that differences in severity have been associated with particular serotypes and genotypes posing the question that some specific genotypes from a determined serotype are more pathogenic than others (130). Out of the four dengue serotypes, DENV-2 has been the most frequently associated with dengue outbreaks as well as with DHF and DSS (154, 196, 216, 249), followed by DENV-1 and DENV-3 viruses (11, 98, 154). DENV-4 has been associated to milder cases of dengue although it is also capable of causing severe infections (170).

Heterogeneity in severity is also prevalent within each serotype. For example, not all genotypes of DENV-2 are equally virulent. DENV-2 American has been the most predominant strain in the Americas prior the early 1980s and has not been associated with DHF cases (124, 154). On the other hand, studies show the association between DENV-2 Asian and DHF or DSS in young children. Thus, the identification of specific DENV-2 genotypes is one of the priorities in the study of the epidemiology of the disease (139, 154, 195, 196, 216, 249).

Unfortunately, there is evidence that the more virulent DENV-2 Asian has replaced DENV-2 American in certain countries and factors associated with the life history of DENV-2 Asian infected vectors seem to be central to this observed outcome (154, 195, 216, 249).

Dengue is transmitted primarily by the mosquito vector *Aedes aegypti*, which has spread to a vast majority of countries in the tropics and sub-tropics (98, 193). The secondary vector, *Aedes albopictus*, has a range that reaches farther north than *Ae. aegypti* and there are reports that its eggs adapt better to subfreezing temperatures which increases the risk of a dengue outbreak in the U.S. (101, 156). This risk could also be increased due to vertical transmission from infected females to eggs. Although previous studies suggested that vertical transmission of dengue was not possible (199), recent findings have demonstrated that vertical transmission involving *Ae. aegypti* and *Ae. albopictus* species is feasible in captivity and in the wild (9, 17, 33, 89, 126, 203). While data indicate that the percentage of transovarial transmission observed in *Ae. aegypti* is low (105, 198), certain strain of mosquitoes from determined geographic areas appear to be more susceptible to dengue infection and transmission of specific dengue serotypes (9, 123, 225). Moreover, data collected from pooled and individual mosquitoes from regions where dengue is endemic in Peru strongly suggest that *Ae. aegypti* could be carrying two dengue serotypes simultaneously (26). These results corroborate Lorono-Pino's studies in Asia and Mexico where viremic samples from patients were shown to contain more than one serotype (141)

matching data obtained from a dengue outbreak in Northwestern Peru in 2008 (145).

There are up to date many dengue vaccine candidates including live, attenuated, and vaccines created using recombinant DNA technology such as those developed at the U.S. National Institutes of Allergy and Infectious Diseases, InViragen, Walter Reed Army Institute of Research/GlaxoSmithKline and Sanofi Pasteur, as well as subunit vaccines like those developed by Merck/Hawaii Biotech (90). Of these vaccines, the tetravalent dengue vaccine from Sanofi Pasteur is currently in Phase III trials in Thailand and results are expected by the end of 2012 (91). This vaccine was constructed using the yellow fever vaccine 17D as a backbone with substitution of the prM and E genes from each dengue serotype. This chimeric yellow fever dengue tetravalent dengue vaccine (CYD TDV) is a combination of four CYD viruses, one for each dengue serotype, into one single vaccine (88, 91).

Unfortunately, although there are many dengue epidemiological studies that use mathematical and statistical approaches, they are not as widely discussed with dengue or field specialists as one would like to see (171). Mathematical models with well-determined biological parameters can assess the risk for the spreading of dengue and suggest appropriate vector control measures. The following section provides a non-expert account of some of the most widely used mathematical dengue models into different categories and collects some relevant dengue literature that could serve as a starting point for the identification of

biological parameters that are key to the development of mathematical dynamical models.

MATERIAL AND METHODS

Mathematical and epidemiological models. While there are several theoretical models for the study of dengue epidemiology (171) their approach as well as the biological assumptions that are made are different depending on the specific problems that are addressed. Although dengue models differ from each other, most share a population dynamics starting point in (51) which has its origins in the seminal work of Sir Ronal Ross a British doctor who studied the dynamics of malaria at a population level (204) following his extraordinary discovery of *Plasmodium sp.* in the *Anopheles* mosquito for which he received the Nobel Prize in Physiology or Medicine in 1902 (172). Ross' theoretical work in mathematical epidemiology was followed by Kermack and McKendrick (116, 117) and later formalized by MacDonald (143).

Mathematical models consider the members of a population (humans or mosquitoes) to belong to a specific compartment or classes according to the health status of the individuals (20, 55, 104, 232). Moreover, a very interesting phenomena called the threshold effect or tipping point rules the dynamics of the transition in disease epidemiology and it is associated to biological variables such as biting rate of the mosquito (28).

Determining the basic reproductive number (R_0). The basic reproductive number or R_0 is one of the most important concepts when it comes to determine the transmission potential of a disease. An R_0 equal to 2 indicates for example, that a typical single infectious individual will infect on the average two individuals if released in a completely susceptible population (104, 232). Thus, R_0 quantifies the strength of an outbreak and is one of, if not the most, important number or ratio that needs to be estimated when modeling a disease. There are many factors that make difficult to quantify the R_0 , i.e. What constitutes a typical individual in a heterogeneous population? In many instances, it turns out that these models support two types of equilibrium (long-term dynamical outcomes), one where there is no disease ($R_0<1$) and one where the disease is endemic ($R_0>1$), with $R_0=1$ the threshold or tipping point (28). The value of the effective reproductive number or R_{0e} will change over time. Its value will depend on the immunity of the population, the heterogeneity of susceptible individuals. Generally, if control measures are put in place, for example through the use of vaccination campaigns, R_{0e} will decrease. If $R_{0e}<1$ then the transmission of the disease will not be sustained and the outbreak will promptly cease, on the other hand if $R_{0e}>1$, the disease will remain endemic (104).

Choosing a model structure. There are three main questions that need to be addressed when choosing an appropriate model (232): (1) the natural history of the infection, (2) the time period that is going to be modeled and (3) the research question that needs to be answered. One of the simplest models is the Susceptible-

Infectious (SI) model which can be used to describe for example an HIV infection as once a person is infected by another person, he/she will remain infectious for life (114). The Susceptible-Infectious-Susceptible (SIS) model is commonly used to describe diseases that can be cured but do not provide immunity (81) while both the Susceptible-Infectious-Recovered (SIR) and the Susceptible-Exposed (Pre-infectious)-Infectious-Recovered (SEIR) models are used for diseases with immunizing infections (232) (Fig. 42). Current dengue models usually fall into the latest two categories when describing just the infection in the human population while a more simple SI coupled model is commonly used when classifying the mosquito population (171). More complex models divide the mosquito population into four classes: Aquatic, Susceptible, Exposed and Infectious, being the last three classes composed of the female adult mosquito (247). Moreover, the possibility of vertical transmission in dengue has led to the formulation of other models were vertical transmission could be the key for the success of a specific strain over another one (Murillo, D., Holechek, S., Sanchez, F. & Castillo-Chavez, C., manuscript in preparation).

(i) Stochastic vs. deterministic models. Models can also be divided into stochastic or deterministic. A deterministic model captures what happens on average in a population with a fixed set of parameters while an stochastic model allows for a random variation in the number of individuals who go from one compartment to another (232). Current dengue models fall into both of these categories (62, 171, 178).

(ii) Models with emphasis in the vector. While earlier approaches highlight the importance of the use of stochastic models in the study of large-scale epidemics (13) the deterministic Container-Inhabiting Mosquito Simulation Model (CIMSiM) is one of the most widely known for vector control strategies (239). CIMSiM is a dynamic life table simulation model that accounts for multiple parameters such as temperature, artificial vs. natural containers, development rates of each mosquito stage, gonotrophic cycle, and larval weight gain and food depletion. This model uses historical weather data, larval habitat and population density in order to produce a simulation that can be tailored to a specific region (72, 73, 239).

(iii) Models with emphasis in the virus.

(a) Sequential models. One of the first models that studied the possible acquisition of DHF is the sequential model of which two different scenarios are accounted for. The first one assumes that DHF is caused by infection with a different dengue serotype (double sequential model), while the second scenario assumes infection with two serotypes in the same year and a third different serotype in a the following year (triple sequential model) (68).

(b) Dengue simulation model (DENSiM). This transmission model builds on CIMSiM and accounts for virus development in an infected individual and the passage of the virus between human and mosquito populations. It also takes into consideration the geographic area, age-specific birth and death rates. The temperature and the titer of the virus in the host help determine the extrinsic

incubation period in the vector. The virus titer is also use as a measurement of the probability for virus transfer between host and vector (71).

(iv) Models with emphasis in two dengue strains. There are several models that account for the circulation of two dengue serotypes.

(a) Competitive exclusion model. The competitive exclusion model by Feng & Velasco-Hernandez takes into consideration the co-circulation of two strains with temporary cross-immunity, assuming that both strains have a different disease progression pattern. This temporary coexistence of these two strains in the host population is later disturbed with a resulting competitive exclusion of one strain (64) .

(b) Coexistence model. This deterministic compartmental model was described by Esteva and Vargas where the coexistence of two dengue serotypes was feasible for a large range of parameters in contrast to the competitive exclusion model described above (60).

(c) Antibody-dependent enhancement (ADE) models. There are several models that account for the ADE phenomenon. The model by Ferguson *et al.* explores dengue transmission dynamics with the co-circulation of multiple dengue strains. As a result, a complex and persistent cyclical or chaotic epidemic behavior is generated (67). On the other hand, Kawaguchi's *et al.* model explores genetic and immunological distances among serotypes and how they contribute to stable viral communities that allow for a stable coexistence in the population (115). While the models above are deterministic in nature, a hybrid stochastic

approach has been also formulated where a short period of cross-immunity could explain the periodical phenomena of DHF (234).

(v) Models with emphasis in control measures. Back in 1975, Dietz presented a deterministic compartmental model with vaccination strategies (51). In 2003, Derouich *et al.,* proposed a model where both environmental and vaccination strategies are discussed in an scenario where one epidemic with a virus follows another one with a different one (48). The same year a continuous-time Markov chain model for uncertainty analysis was proposed by Luz *et al.* which incorporates vector density spatial heterogeneity, using this model they conclude that spatial heterogeneity of the mosquito population makes the risk of an epidemic higher and the control measures more complicated (142).

Case study: Luciano Castillo Colonna (LCC) dengue outbreaks 2000-2010. Data for all the dengue epidemics in the Luciano Castillo Colonna region, Piura, Peru were kindly provided by Edwar Pozo, Director of Epidemiology (LCC region-Ministry of Health). This data represent the weekly reports of clinically confirmed dengue cases by the medical staff based on the World Health Organization criteria as well as serological confirmed cases (154, 162).

The epidemiological curves for the distribution of dengue cases from 2000-2010 was done by plotting the number of the epidemiological week in the x axis and the number of cases in that week in the y axis and represent a good visualization of the dengue status in this endemic region.

Geographic distribution of cases in the LCC region. The total number of cases in each province from LCC was converted to a logarithmic scale and colors were assigned accordingly in order to provide an easy visualization of the number of cases. Similarly, the attack rate (Number of positive cases/Total number of the population) per 10,000 individuals was converted to a color scale for easier visualization.

Age distribution. The age distribution and the attack rate of the confirmed cases from 2000-2010 were also analyzed. Of interest is the 0-15 years old population as this has been declared by the World Health Organization as the one being more at-risk for DHF and DSS (236).

Early determination of the reproductive number (R_0). The R_0 was determined by using the following equation previously described by Favier *et al*. (62):

$$R_0 = \left(1 + \frac{\Lambda}{\gamma}\right)\left(1 + \frac{\Lambda}{\lambda}\right)\exp\left[\Lambda\left(\tau_e + \tau_i\right)\right] \qquad (1)$$

The force of infection, Λ, is computed by plotting the weekly number of cases against the cumulative number of cases. The phase of exponential growth in the number of cases can be visualized by a linear growth of the curve. The slope of this phase is Λ and its calculated by a least-square linear fit. The parameter corresponding to the mortality rate of the (λ), is obtained using the following equation:

$$\lambda = -\ln\left[0.91\lambda_1(T)\lambda_2(P_{vd})\right] \qquad (2)$$

where T is the average temperature in Celsius degrees for the epidemiological weeks that form the linear phase and P_{vd} is the vapor pressure deficit in mbar, which can be determined using T and relative humidity (RH) data:

$$P_{vd} = 6.11\exp\left[17.3\frac{T}{T+237.3}\right]\left(1-\frac{RH}{100}\right) \qquad (3)$$

The parameters λ_1 and λ_2 are:

$$\lambda_1(T) = \begin{cases} (T-5)/5 & \text{if } 5 < T < 10 \\ 1 & \text{if } 10 \leq T < 41 \\ 1-(T-41)/2 & \text{if } 41 < T < 43 \\ 0 & \text{for other temperatures} \end{cases} \qquad (4)$$

and

$$\lambda_2(P_{vd}) = \begin{cases} 1 & \text{if } P_{vd} < 10 \\ 1-40(P_{vd}-10)/20 & \text{if } 10 \leq P_{vd} \leq 30 \\ 0.6 & \text{if } P_{vd} > 30 \end{cases} \qquad (5)$$

RESULTS

Analysis of the dengue outbreaks from 2000-2010. The weekly number of cases was plotted against the epidemiological weeks for the years 2000-2010. As it can be observed in Fig. 43, the 2000-2001 dengue outbreak constitutes the

outbreak with more number of cases in the LCC region in Piura, Peru. It is know that during this outbreak DENV-2 Asian genotype invaded the LCC region and replaced the endemic DENV-2 American genotype as evidenced by the genomic analysis of the virus extracted from the serum of patients (154). Moreover, it was the first time that DENV-3 and DENV-4 also entered the Peruvian territory (154).

Other significant outbreaks can be observed in 2003, 2008 and 2010 (Fig. 43). The number of dengue cases by district was converted to a logarithmic scale and colors assigned accordingly (Fig. 44). As it can be observed from 2000 to 2010, only the districts located in the East side of the region have not registered any positive cases for dengue, this is presumably due to colder temperatures and higher altitudes which do not favor *Aedes aegypti* development. Because case numbers do not reflect the severity of an outbreak, the attack rates by district were also calculated and converted into a color scale (Fig. 45).

The age distribution is another important parameter to consider when analyzing outbreaks specially because the more severe forms of dengue disease, DHF and DSS, have been associated with children under 15 (12, 84, 86, 93). As it can be observed in figure 46 the 15-29 age group was the most affected throughout 2000-2010. When analyzing the attack rate per age groups, proportional attack rates were observed among the groups (Fig. 47).

Estimation of the R_0 and the force infection (Λ) for the 2000-2001 dengue outbreak. The 2000-2001 outbreak in LCC was chosen as this represents the first reported dengue outbreak in Peru with confirmed DHF cases as well as

the introduction of the DENV-2 Asian genotype and the DENV-3 and DENV-4 (154). There are many methods to estimate the R_0 for vector-borne diseases using real epidemics data (147). The method used in this chapter is a preliminary attempt to estimate the R_0 based on the initial cumulative number of cases and has previously been adapted to vector-borne diseases (62, 178). This method is based on the assumption that at the beginning of an outbreak the hypothesis of homogeneous mixing can be satisfied (63). When plotting the number of new cases per week against the cumulative number of cases, the phase of exponential growth of the cumulative number of cases can be evidenced by a linear growth of the curve. The slope of this line is the force of infection (Λ) and is obtained by computing a least-square linear fit of this linear phase (62, 178). When analyzing the initial exponential growth of the 2000-2001-dengue outbreak the Λ was found to be 0.462 (Fig. 48). Based on Λ, R_0 was estimated by only using two parameters for the host (1) γ = inverse duration of the host viremia and (2) τ_i = intrinsic incubation period and two parameters for the vector (1) λ = mortality rate of vectors and (2) τ_e = extrinsic incubation period (62). The host parameters have been previously described (149). The parameters for the mosquito population are dependent on the temperature and have been modeled by Favier *et al.* (62) based on previous models (71, 72). By using the formulas 2, 3, 4 and 5 described in the materials and methods section, the parameters needed to solve equation 1 were found and are described in Table 3. The R_0 for the 2000-2001 dengue outbreak in the LCC region calculated using equation 1 was 6.24.

DISCUSSION

The use of mathematical models have proved to be useful in the analysis of vector-borne diseases such as dengue and has evolved over time to encompass complex models that take into consideration the interaction between the human and vector populations on complex environmental landscapes (171). While there is not a gold standard for a dengue model, the current approaches are tailored to specific needs with respect to the virus (60, 64, 67, 115, 234), the vector (72, 73, 239) and the dynamics of an epidemic (48, 51, 142). From a biological perspective mathematical models could help us understand dengue at a bigger scale. One of the questions that modeling can help answer is for example what would be the effect of the invasion of a specific dengue strain into an area where an endemic strain is already circulating. In this scenario two broad categories of invasion could be observed. First, an area will be endemic with a strain other than DENV-2. Then, either DENV-2 Asian or American may attempt to invade. Secondly, a susceptible mosquito will become infected with either DENV-2 Asian or American genotype and vertical transmission of one of the DENV-2 genotypes in the vector could be considered. This model could explain the displacement of DENV-2 American genotype by the Asian genotype as well as the speed and severity of dengue outbreaks in countries like Peru where the DENV-2 Asian genotype was first introduced during the 2000-2001 epidemic (154). Prior to the appearance of DENV-2 Asian genotype in northwestern Peru, only DENV-1 and DENV-2 American genotype were circulating (124, 154). The absence of DHF

and DSS in the northeastern Peruvian city of Iquitos prior 2000 could be due to the cross-immunity conferred by DENV-1 against DENV-2 American genotype but not to the DENV-2 Asian genotype suggesting that the American genotype may have a DENV-1 like antigen (124). Moreover, there are data that indicates the presence of genetic variability between *A. aegypti* mosquitoes from the coast and the ones from the Peruvian northeast area (138), indicating that there could be a specific genetic variant responsible for the dissemination of DENV during the 2000-2001 dengue outbreak in Peru.

A model that includes vertical transmission, and its association with a more virulent strain like DENV-2 Asian genotype, should be taken into consideration for the prediction of dengue outbreak outcomes. Of all the 2000-2010 dengue outbreaks in the LCC region, the 2000-2001 outbreak is of significant importance as it marks the invasion of DENV-2 Asian genotype, DENV-3 and DENV-4 to the Peruvian territory (154). When determining the early reproductive number of this outbreak it was found to be 6.24, an estimate that is comparable to what has previously been found by modelers when analyzing real epidemiological data including previous work done in Peru involving the study of the spatial and temporal dynamics of dengue fever between 1994 and 2006 (R_0= 0.1 to 112.8) (40). Other estimates of the R_0 using the same method described in this chapter with real epidemics data from different Brazilian regions during 1996 to 2003 gave R_0 values from 2.1 to 103 (62). Further analyses of other outbreaks using this method and other methods are necessary in order to

validate if the early determination of the R_0 using the initial exponential growth of an outbreak is indeed more valuable than other approaches.

In the absence of an effective vaccine, worldwide efforts should be made to monitor *Aedes* mosquitoes, both males and females, and the DENV serotypes and genotypes that are being carried and transmitted. A mathematical model of this nature would be used to not only highlight the importance of vertical transmission in a dengue outbreak but also the importance of epidemiological surveillance incorporating molecular genotyping. Routine detection of the virus in both mosquitoes and hosts in endemic areas with dengue will be valuable in efforts to prevent major outbreaks. Interdisciplinary efforts should be encouraged in order to validate theoretical models with real life data.

Another aspect where models can be helpful is in the evaluation of implementation policies. Despite massive campaigns to eradicate dengue, results so far have been short-lived and many countries support control programs that are not very successful. Among the factors to be blamed are the limited government resources, increased growth of urban areas, inadequate trained personnel, reliance on insecticides, resistance to insecticides, reliance on government intervention and lack of education with respect to dengue (193). Moreover, failure of dengue control campaigns has also been attributed to the misconception that reduction of the *Aedes* population would stop transmission altogether. Large government-led programs are costly and become difficult to maintain, particularly if they have been successful for a long time (193). It has been observed that the dengue

surveillance program in Puerto Rico, one of the best in the world, is ineffective because of the lack of community involvement (83). Creating sustainable dengue control strategies require an innovative approach, one that moves away from the centralized top-down model into a decentralized bottom-up community-based model. A great example of a powerful community-based program is Project HOPE which trained community leaders in early disease detection and increased awareness in the population (183).

Many countries have implemented several prevention and awareness programs after they were affected by a dengue outbreak. In 2000, for example, although familiar with dengue, local Peruvian health officials were unprepared for the threat of DHF, and many severe cases developed before hospitals were able to successfully diagnose the disease. Evidence indicates that the outbreak was caused mainly by the introduction of a virulent strain from Asia where many DHF cases are reported (154). Following this outbreak, several educational resources have been put in place including marches, dengue-related games, yearly calendars showing months were dengue is expected, street performers and dissemination of dengue information through theater, radio campaigns and press (182). Currently all four dengue serotypes are endemic to Peru, including the LCC region where it has rapidly expanded (182). It is still too early to evaluate how effective these measures have been in the affected population. Other countries such as Singapore have adopted new strategies to get rid of dengue involving children in environmental campaigns and using the cyberspace to launch platform games

such as M.A.C.E. (Monster Annihilation and Control Enforcement) that are designed to create awareness of dengue prevention among the young population (215). Moreover, Ministry of Health leaders from some small communities in Costa Rica have observed that despite knowledge of the disease and its transmission, failure will be in the horizon if there is not a sense of community where leaders work together to reinforce the Ministry of Health suggestions and regulations regarding dengue (1).

All these reasons provide great opportunities for the evaluation of dengue prevention strategies, which can be evaluated using models that reflect the need and resources of each country as well as the biological fingerprint of the disease endemic to each region. Moreover, the relatively fast and inexpensive nature of working *in silico* provides a great tool for building models that examine problems at large scales. The need exists for expanding the interaction between biologists and mathematical modelers and bring the best of their expertise to better understand and ameliorate diseases like dengue which threatens two fifths of our world population (236).

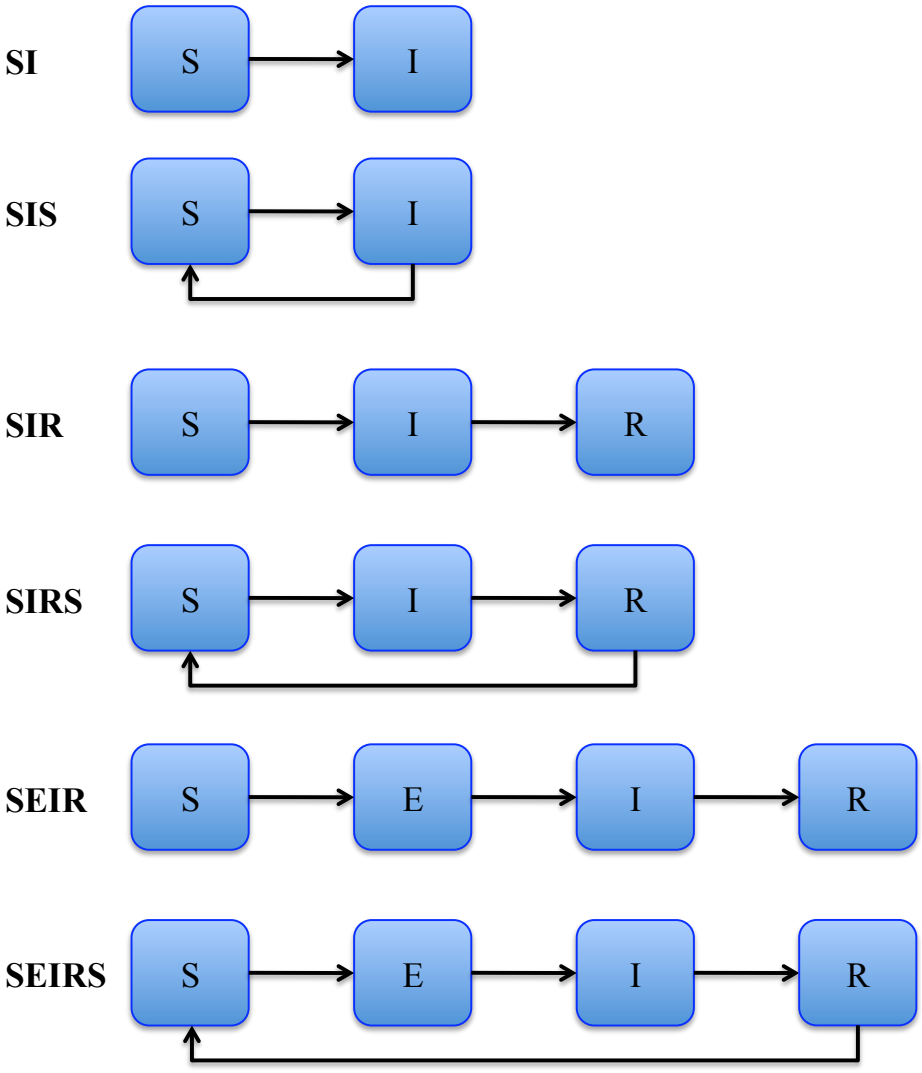

FIG. 42. Common model structures used to describe the transmission of diseases. S=Susceptible, E=Exposed/Pre-infectious, I=Infectious, R=Recovered/Immune.

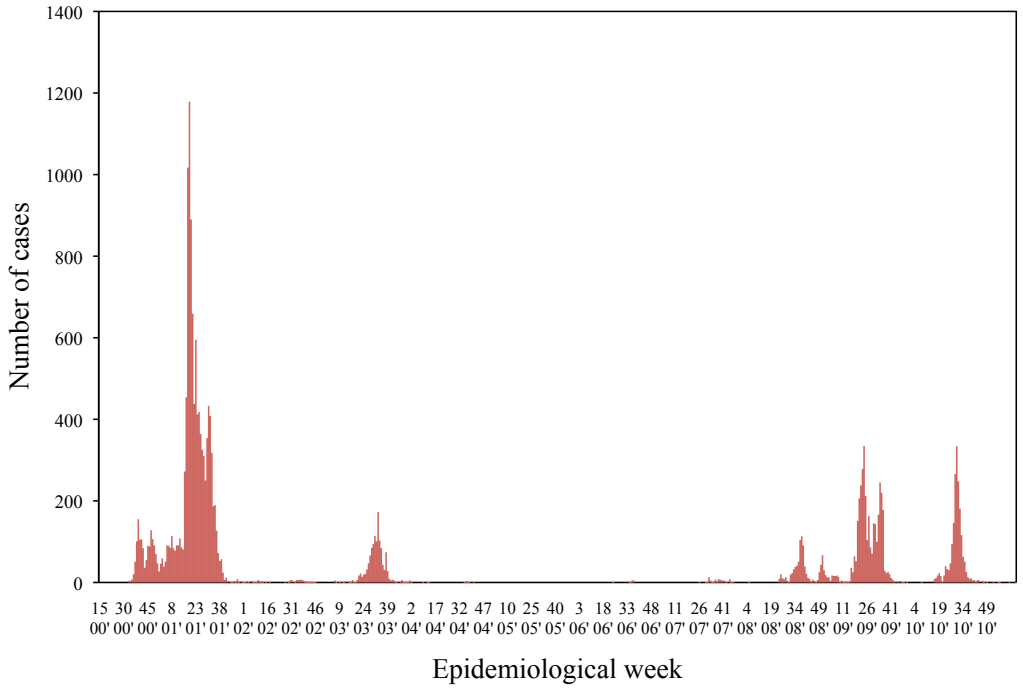

FIG. 43. Weekly numbers of dengue fever cases during 2000-2010 in the Luciano Castillo Colonna region, Piura, Peru.

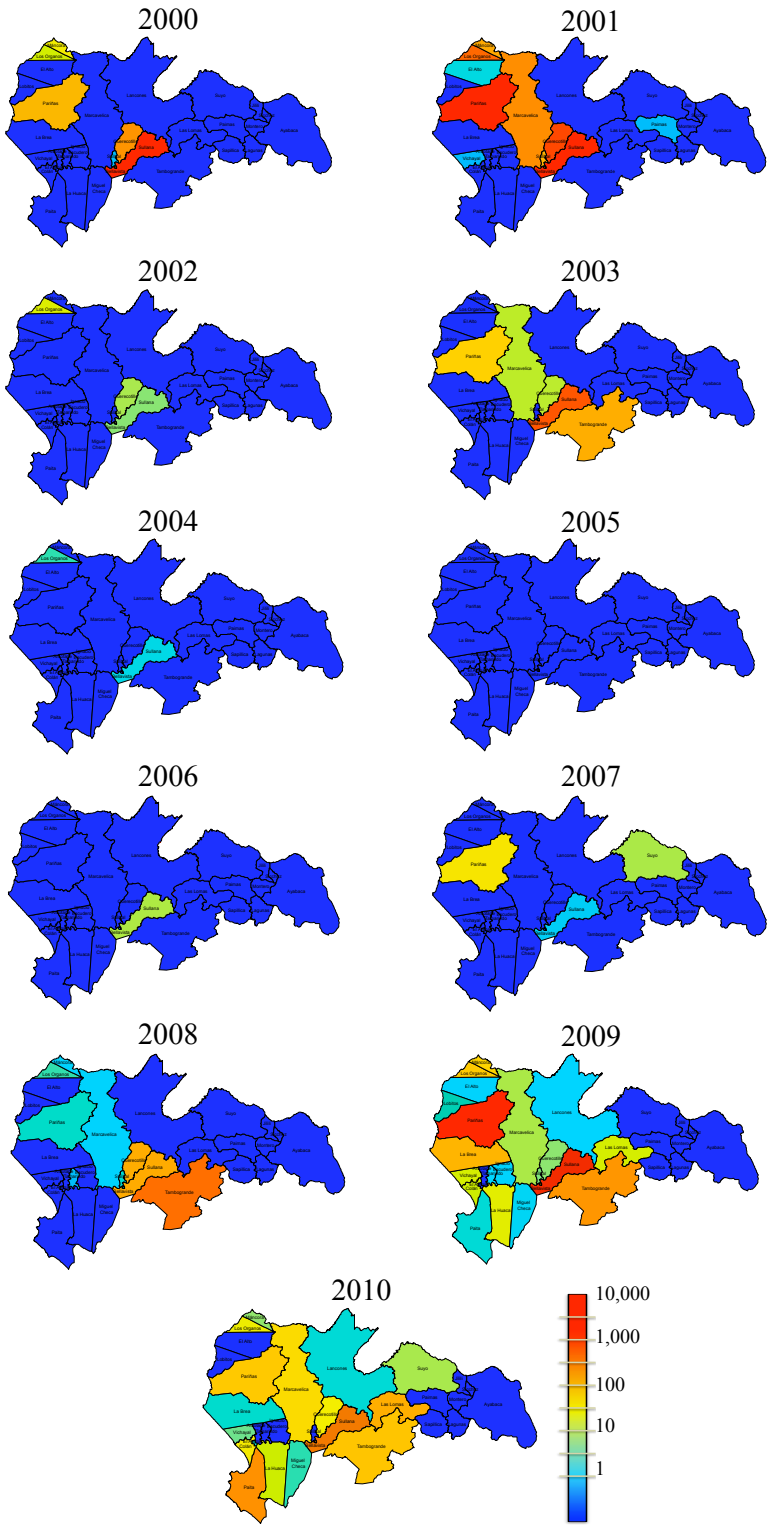

FIG. 44. Number of dengue cases by district in the Luciano Castillo Colonna region, Piura, Peru (2000-2010). A colored logarithmic scale was created in order to highlight areas with more concentration of cases.

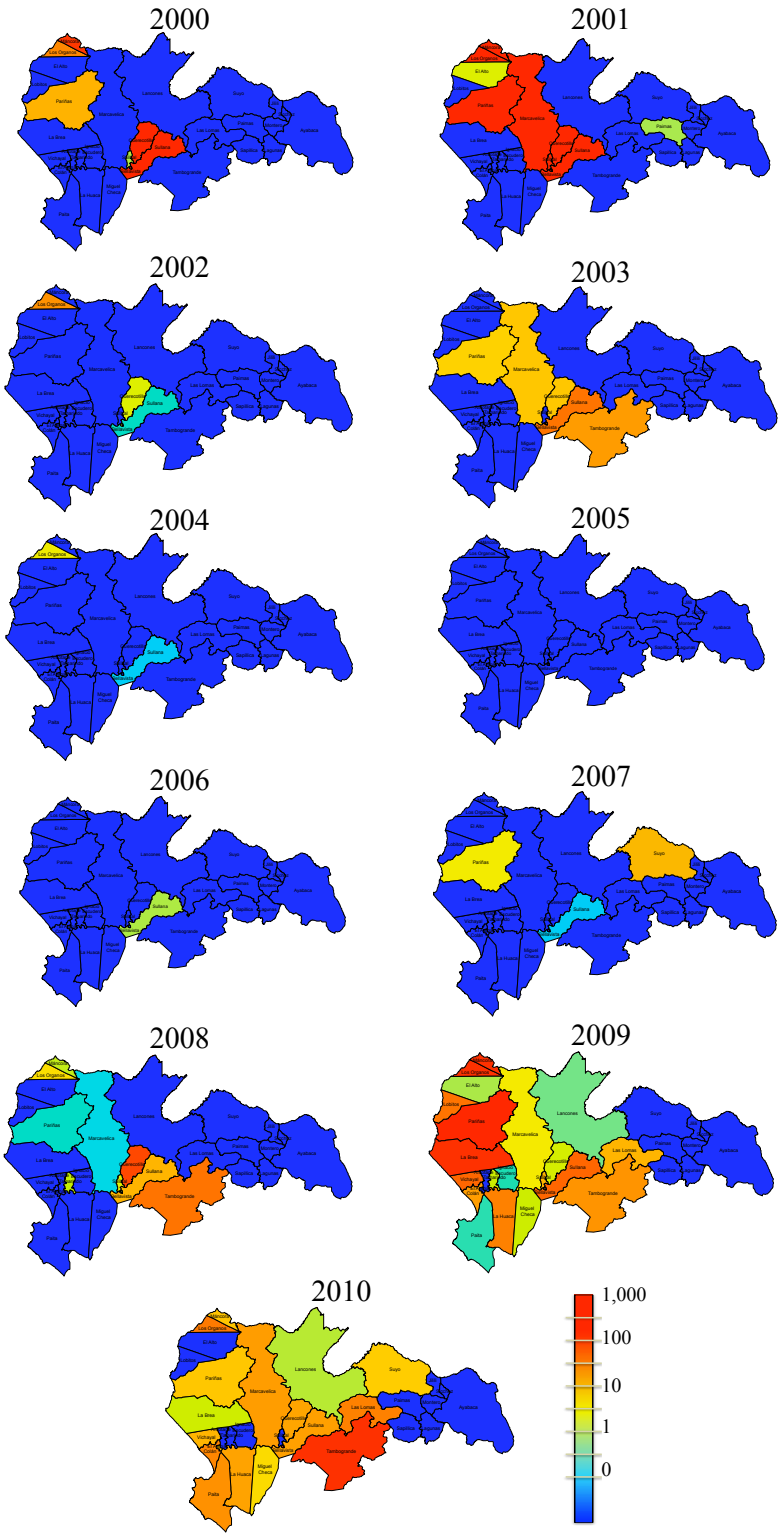

FIG. 45. Dengue attack rates by district in the Luciano Castillo Colonna region, Piura, Peru (2000-2010). Colors indicate the number of positive cases per 10,000 individuals.

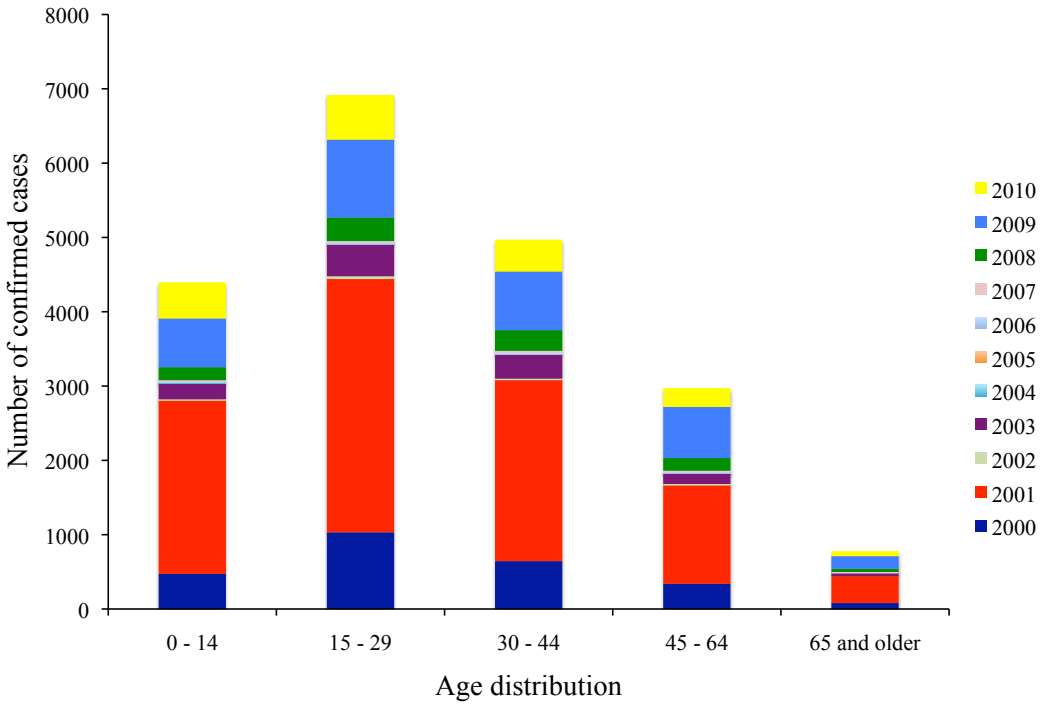

FIG. 46. Age distribution of dengue cases in the Luciano Castillo Colonna region, Piura, Peru (2000-2001).

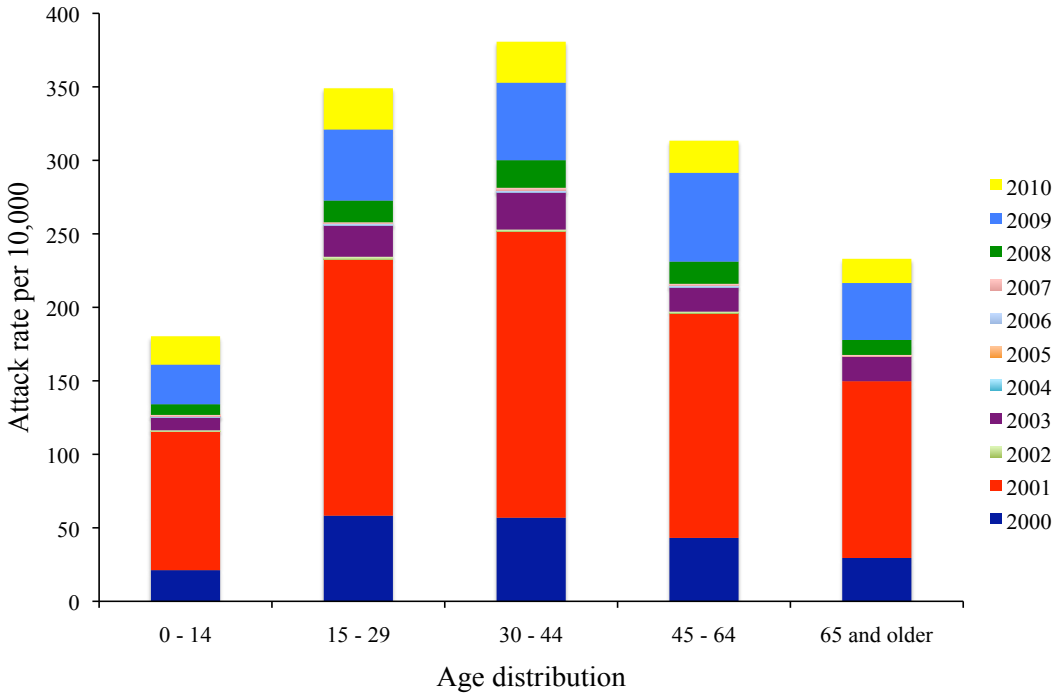

FIG. 47. Dengue attack rates by age groups in the Luciano Castillo Colonna region, Piura, Peru (2000-2010).

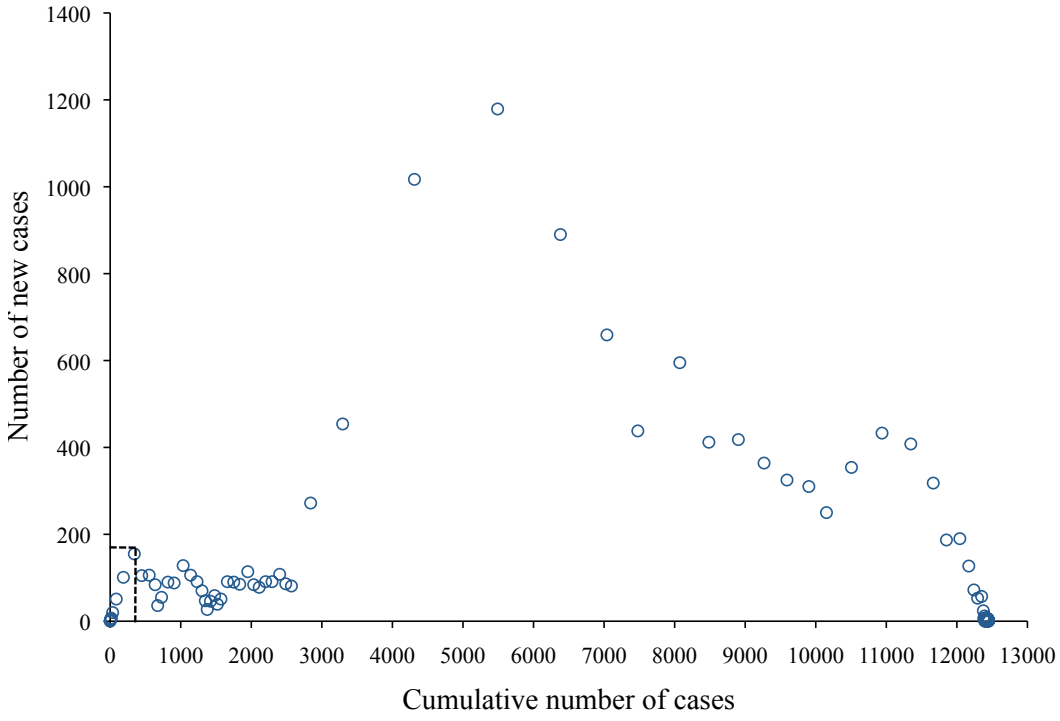

FIG. 48. Weekly number of cases against the cumulative number of cases for the 2000-2001 dengue outbreak in the Luciano Castillo Colonna region, Piura, Peru. The dashed box indicates the growing linear part of the plot corresponding to the initial exponential growth of the outbreak. The least-square linear fit of the linear phase gives $\Lambda=0.462\pm0.02$ with correlation coefficient $R\approx1.0$.

TABLE 3. Parameters used to estimate the basic reproduction number (R_0) for the 2000-2001 dengue outbreak in the Luciano Castillo Colonna region, Piura, Peru.

Parameter	Description	Value
Λ (day^{-1})[a]	Force of infection	0.066
T (°C)[b]	Average temperature	23.70
RH (%)[b]	Percentage of relative humidity	56.42
P_{vd} [b]	Vapor pressure deficit	12.8
γ[c]	Inverse of the duration of host viraemia	0.167
λ (day^{-1})[c]	Mortality rate of the vectors	0.2
τ_e (day)[b]	Extrinsic (vector) incubation period	13.2
τ_i (day)[c]	Intrinsic (host) incubation period	5

[a] Force of infection found using the slope in Fig. 48 was divided by 7 in order to obtain the daily value.
[b] Parameters calculated by using epidemiological and climatological data from weeks 18 to 24 (2000).
[c] Parameters established by Favier *et al.* (62)

OVERALL DISCUSSION

Since the pioneering work by Edwar Jenner and the establishment of the field of vaccinology back in 1796 (46), numerous efforts have been made in the lab and *in silico* to eradicate several diseases that impact not only the affected individuals but also the local and global economy. Although thanks to Jenner smallpox has been declared eradicated by the World Health Organization (4, 237), there is still the need to continue studying VACV, a virus that has been used as a vaccine for smallpox as it confers immunity to the disease (108). Moreover, VACV is also used as a recombinant vector for its potential to provide protection against other diseases (77, 108, 120, 158, 176, 248).

Unfortunately, inoculation in humans with VACV can cause mild to, in some cases, life-threatening reactions (58, 127, 206). After September 11, 2001, the concern arose for the use of VARV or monkeypox virus (MPXV) as a bioterrorism agent and the risk of an accidental VARV release (134, 169, 227). For all these reasons the developing and optimization of a post-exposure prophylaxis vaccine against smallpox was necessary. Chapter 1 describes the optimization of a recombinant VACV, v50ΔB13RMγ, as a post-exposure prophylactic agent in a VACV animal model. This virus is able to protect mice following exposure to $100LD_{50s}$ of wt VACV when is administered 1 dpi with 100% survival. This protection is dose and time dependent as treatment at 2 or 3 dpi increases morbidity and diminishes survival. When looking at the mechanism of action of this virus it was observed that although the mice survived and

obtained a health status comparable to uninfected mice by day 18 post-infection, viral replication was similar in the organs from wt VACV infected animals as well as in the ones that were infected with wt VACV and then treated with v50ΔB13RMγ. These data suggest that v50ΔB13RMγ is acting as an immunoregulator rather than as an antiviral. In Chapter 2 the mechanisms that v50ΔB13RMγ could be using to prevent morbidity and mortality were explored. Preliminary data indicate that v50ΔB13RMγ has an effect in viral replication in the olfactory bulb but not in the rest of the brain. Although poxvirus replication has already been observed in the olfactory bulb (21, 146, 189) recent data form our lab (Karen Denzler, unpublished data) have shown that the blood brain barrier (BBB) permeability is affected following infection with wt VACV. While v50ΔB13RMγ seems to be halting replication in the olfactory bulb of treated animals, wt VACV could be crossing the BBB which plays an important role in post-vaccinal encephalitis (76).

IFN-γ induces a variety of immune responses, when examining the immune cells that were recruited at the site of infection, $CD8^+$ T cells and the heterogeneous $Gr1^+CD11b^+$ cells, also known as myeloid derived suppressor cells (MDSCs), were observed in more numbers in the mice treated with v50ΔB13RMγ which would indicate a potential role of these populations during post-exposure although more analyses are needed as subpopulations of MDSCs have been depicted to have several roles under healthy and pathological conditions (148, 165, 230, 251). Recent studies have identified that a subpopulation of

$Gr1^+Cd11b^+$ cells not only produce type I IFN but also exhibit tissue protective properties following peripheral virus infection by producing reactive oxygen species (69). Future studies include the depletion of $Ly6G^+$ cells in order to evaluate their role during post-exposure prophylaxis using v50ΔB13RMγ as they could be indeed protecting infected tissue from immune-mediated damage.

The reasons why a better understanding of VACV is important have previously been mentioned. One of VACV innate characteristics is that it is IFN-resistant. This is primarily due to the E3L gene (106) which is also important for pathogenesis in mice (19, 122). E3L produces a 25-kDa protein that has two domains; an N-terminal domain that belongs to the vertebrate Zα family of Z-DNA binding domains (110, 121, 122, 129), and a C-terminal domain with a typical double-stranded RNA (dsRNA) binding domain (34, 43, 133). Recent data suggest that not only the dsRNA binding domain but the Z-DNA binding domain play a role in evading the host IFN response (235). In Chapter 3 a virus was engineered containing both domains of E3L in different loci of the VACV. This virus was tested in the murine JC cell line, the only cell line so far available where the Z-DNA binding domain is necessary for VACV replication (228). If indeed both domains can work independently, replication was expected in this cell line comparable to wt VACV levels. When viral titers were analyzed after 72 hours of infection with the input virus, no changes were noticed with the exception of wt VACV. When looking at the activation of the dsRNA dependent protein kinase (PKR) at late times post-infection, PKR phosphorylation was observed in cells

infected with the dual-expression virus suggesting that it was unable to bind and mask dsRNA synthesized during VACV infection. These results indicate that both domains of E3L need to be linked together in order to inhibit the IFN response. Future studies will include expression of the Z-DNA binding domaing using a bacterial expression vector and evaluating its affinity to Z-RNA using surface plasmon resonance. Based on previous data obtained with ADAR1, which also has a Z-DNA binding domain and binds both Z-DNA and Z-RNA (179), it is possible that the N-terminus of E3L could bind to a transient Z-RNA that could result from a torsional strain following binding of dsRNA by the dsRNA binding domain.

Another strategy that is used in the scientific field to study viruses is mathematical modeling. Because smallpox has already been eradicated, the utility of mathematical modeling as a tool for predicting the outcomes of disease spread was explored in Chapter 4 using dengue as a disease model. Dengue is one of the most complex and important emerging and re-emerging infectious diseases in the world (93, 98, 178, 236). The most important challenge for dengue is that there is not yet a commercial available vaccine although many efforts are being made by diverse research groups (53, 90, 91). The last chapter looks into some of the current dengue models and uses data from the 2000-2001 dengue outbreak in Peru as an example of how important the biological parameters are in order to obtain preliminary data when a dengue outbreak strikes a susceptible population. While the current Phase III clinical trials for vaccine candidates is still in process, the

World Health Organization is looking into the use of mathematical modeling to predict vaccination strategies (238). This will not be feasible without the expertise not only from mathematical modelers but that of clinicians, vaccinologists, virologists, immunologists, entomologists and epidemiologists. Thus, the last chapter highlights the importance of interdisciplinary collaboration and how it benefits research on infectious diseases.

REFERENCES

1. 2011. Taller sobre el enfoque ecosistemico en salud humana con personal de instituciones en la region Brunca. Costa Rica.

2. **Abbas, A. K., A. H. Lichtman, and S. Pillai.** 2010. Cellular and molecular immunology, 6th ed. Saunders-Elsevier.

3. **Alcami, A., and G. L. Smith.** 1995. Vaccinia, cowpox, and camelpox viruses encode soluble gamma interferon receptors with novel broad species specificity. J Virol **69:**4633-9.

4. **Amorosa, V. K., and S. N. Isaacs.** 2003. Separate worlds set to collide: smallpox, vaccinia virus vaccination, and human immunodeficiency virus and acquired immunodeficiency syndrome. Clin Infect Dis **37:**426-32.

5. **Anderson, K. P., E. H. Fennie, and T. Yilma.** 1988. Enhancement of a secondary antibody response to vesicular stomatitis virus "G" protein by IFN-gamma treatment at primary immunization. J Immunol **140:**3599-604.

6. **Anstey, N. M., J. B. Weinberg, M. Y. Hassanali, E. D. Mwaikambo, D. Manyenga, M. A. Misukonis, D. R. Arnelle, D. Hollis, M. I. McDonald, and D. L. Granger.** 1996. Nitric oxide in Tanzanian children with malaria: inverse relationship between malaria severity and nitric oxide production/ nitric oxide synthase type 2 expression. J Exp Med **184:**557-67.

7. **Appay, V., P. R. Dunbar, V. Cerundolo, A. McMichael, L. Czaplewski, and S. Rowland-Jones.** 2000. RANTES activates antigen- specific cytotoxic T lymphocytes in a mitogen-like manner through cell surface aggregation. Int Immunol **12:**1173-82.

8. **Armstrong, D. A., J. A. Major, A. Chudyk, and T. A. Hamilton.** 2004. Neutrophil chemoattractant genes KC and MIP-2 are expressed in different cell populations at sites of surgical injury. J Leukoc Biol **75:**641-8.

9. **Arunachalam, N., S. C. Tewari, V. Thenmozhi, R. Rajendran, R. Paramasivan, R. Manavalan, K. Ayanar, and B. K. Tyagi.** 2008. Natural vertical transmission of dengue viruses by *Aedes aegypti* in Chennai, Tamil Nadu, India. Indian J Med Res **127:**395-7.

10. **Asselin-Paturel, C., G. Brizard, J. J. Pin, F. Briere, and G. Trinchieri.** 2003. Mouse strain differences in plasmacytoid dendritic cell frequency and function revealed by a novel monoclonal antibody. J Immunol **171:**6466-77.

11. **Balmaseda, A., S. N. Hammond, L. Perez, Y. Tellez, S. I. Saborio, J. C. Mercado, R. Cuadra, J. Rocha, M. A. Perez, S. Silva, C. Rocha, and E. Harris.** 2006. Serotype-specific differences in clinical manifestations of dengue. Am J Trop Med Hyg **74:**449-56.

12. **Barnes, W. J., and L. Rosen.** 1974. Fatal hemorrhagic disease and shock associated with primary dengue infection on a Pacific island. Am J Trop Med Hyg **23:**495-506.

13. **Bartlett, M. S.** 1964. The relevance of stochastic models for large-scale epidemiological phenomena. Applied Statistics **13:**2-8.

14. **Beattie, E., K. L. Denzler, J. Tartaglia, M. E. Perkus, E. Paoletti, and B. L. Jacobs.** 1995. Reversal of the interferon-sensitive phenotype of a vaccinia virus lacking E3L by expression of the reovirus S4 gene. J Virol **69:**499-505.

15. **Blasco, R., J. R. Sisler, and B. Moss.** 1993. Dissociation of progeny vaccinia virus from the cell membrane is regulated by a viral envelope glycoprotein: effect of a point mutation in the lectin homology domain of the A34R gene. J Virol **67:**3319-25.

16. **Bloom, D. C., K. M. Edwards, C. Hager, and R. W. Moyer.** 1991. Identification and characterization of two nonessential regions of the rabbitpox virus genome involved in virulence. J Virol **65:**1530-42.

17. **Bosio, C. F., R. E. Thomas, P. R. Grimstad, and K. S. Rai.** 1992. Variation in the efficiency of vertical transmission of dengue-1 virus by strains of *Aedes albopictus* (Diptera: *Culicidae*). J Med Entomol **29:**985-9.

18. **Brandt, T., M. C. Heck, S. Vijaysri, G. M. Jentarra, J. M. Cameron, and B. L. Jacobs.** 2005. The N-terminal domain of the vaccinia virus E3L-protein is required for neurovirulence, but not induction of a protective immune response. Virology **333:**263-70.

19. **Brandt, T. A., and B. L. Jacobs.** 2001. Both carboxy- and amino-terminal domains of the vaccinia virus interferon resistance gene, E3L, are required for pathogenesis in a mouse model. J Virol **75:**850-6.

20. **Brauer, F., and C. Castillo-Chavez.** 2001. Basic ideas of mathematical epidemiology. *In* I. Springer-Verlag New York (ed.), Mathematical models in population biology and epidemiology.

21. **Braun, E., T. Zimmerman, T. B. Hur, E. Reinhartz, Y. Fellig, A. Panet, and I. Steiner.** 2006. Neurotropism of herpes simplex virus type 1 in brain organ cultures. J Gen Virol **87:**2827-37.

22. **Bronte, V., M. Wang, W. W. Overwijk, D. R. Surman, F. Pericle, S. A. Rosenberg, and N. P. Restifo.** 1998. Apoptotic death of $CD8^+$ T lymphocytes after immunization: induction of a suppressive population of $Mac\text{-}1^+/Gr\text{-}1^+$ cells. J Immunol **161:**5313-20.

23. **Brown, B. A., 2nd, K. Lowenhaupt, C. M. Wilbert, E. B. Hanlon, and A. Rich.** 2000. The zalpha domain of the editing enzyme dsRNA adenosine deaminase binds left-handed Z-RNA as well as Z-DNA. Proc Natl Acad Sci U S A **97:**13532-6.

24. **Buller, R. M., G. Owens, J. Schriewer, L. Melman, J. R. Beadle, and K. Y. Hostetler.** 2004. Efficacy of oral active ether lipid analogs of cidofovir in a lethal mousepox model. Virology **318:**474-81.

25. **Burke, D. S., A. Nisalak, D. E. Johnson, and R. M. Scott.** 1988. A prospective study of dengue infections in Bangkok. Am J Trop Med Hyg **38:**172-80.

26. **Caceres, O.** 2003. Detección rápida de los serotipos del virus dengue en el mosquito *Aedes aegypti*. Rev Peru Med Exp Salud Publica **20:**156-158.

27. **Canono, B. P., M. H. Middleton, and P. A. Campbell.** 1989. Recombinant mouse interferon-gamma is not chemotactic for macrophages or neutrophils. J Interferon Res **9:**79-86.

28. **Castillo-Chavez, C., Z. Feng, and W. Huang.** 2002. On the computation of R_0 and its role in global stability, p. 229-250. *In* C. Castillo-Chavez, P. Blower, P. Van den Driessche, D. Kirschner, and A. A. Yakubu (ed.), Mathematical approaches for emerging and reemerging infectious diseases: an introduction, vol. 125. IMA.

29. **CDC.** 2007. Household transmission of vaccinia virus from contact with a military smallpox vaccinee - Illinois and indiana, 2007. MMWR Morb Mortal Wkly Rep **56:**478-81.

30. **CDC.** 2009. Human vaccinia infection after contact with a raccoon rabies vaccine bait - Pennsylvania, 2009. MMWR Morb Mortal Wkly Rep **58:**1204-7.

31. **CDC.** 2009. Progressive vaccinia in a military smallpox vaccinee - United States, 2009. MMWR Morb Mortal Wkly Rep **58:**532-6.

32. **CDC** 2010, posting date. Report Suggests Nearly 5 Percent Exposed to Dengue Virus in Key West. [Online].

33. **Cecilio, A. B., E. S. Campanelli, K. P. Souza, L. B. Figueiredo, and M. C. Resende.** 2009. Natural vertical transmission by Stegomyia albopicta as dengue vector in Brazil. Braz J Biol **69:**123-7.

34. **Chang, H. W., and B. L. Jacobs.** 1993. Identification of a conserved motif that is necessary for binding of the vaccinia virus E3L gene products to double-stranded RNA. Virology **194:**537-47.

35. **Chang, H. W., L. H. Uribe, and B. L. Jacobs.** 1995. Rescue of vaccinia virus lacking the E3L gene by mutants of E3L. J Virol **69:**6605-8.

36. **Chang, H. W., J. C. Watson, and B. L. Jacobs.** 1992. The E3L gene of vaccinia virus encodes an inhibitor of the interferon-induced, dsRNA-dependent protein kinase. Proc Natl Acad Sci U S A **89:**4825-9.

37. **Cheers, C., M. Janas, A. Ramsay, and I. Ramshaw.** 1999. Use of recombinant viruses to deliver cytokines influencing the course of experimental bacterial infection. Immunol Cell Biol **77:**324-30.

38. **Chowell, G., P. Díaz-Dueñas, D. Chowell, S. Hews, G. Ceja-Espíritu, J. M. Hyman, and C. Castillo-Chavez.** 2007. Clinical diagnostic delays and epidemiology of dengue fever during the 2002 outbreak in Colima, Mexico. Dengue Bulletin **31:**26-35.

39. **Chowell, G., P. Diaz-Duenas, J. C. Miller, A. Alcazar-Velazco, J. M. Hyman, P. W. Fenimore, and C. Castillo-Chavez.** 2007. Estimation of the reproduction number of dengue fever from spatial epidemic data. Math Biosci **208:**571-89.

40. **Chowell, G., C. A. Torre, C. Munayco-Escate, L. Suarez-Ognio, R. Lopez-Cruz, J. M. Hyman, and C. Castillo-Chavez.** 2008. Spatial and temporal dynamics of dengue fever in Peru: 1994-2006. Epidemiol Infect **136:**1667-77.

41. **Curtiss, R., III.** 2011. The impact of vaccines and vaccinations: Challenges and opportunities for modelers. Math Biosci Eng **8:**77-93.

42. **Dalton, D. K., S. Pitts-Meek, S. Keshav, I. S. Figari, A. Bradley, and T. A. Stewart.** 1993. Multiple defects of immune cell function in mice with disrupted interferon-gamma genes. Science **259:**1739-42.

43. **Davies, M. V., H. W. Chang, B. L. Jacobs, and R. J. Kaufman.** 1993. The E3L and K3L vaccinia virus gene products stimulate translation

through inhibition of the double-stranded RNA-dependent protein kinase by different mechanisms. J Virol **67:**1688-92.

44. **Davison, A. J., and B. Moss.** 1989. Structure of vaccinia virus early promoters. J Mol Biol **210:**749-69.

45. **De Clercq, E., and J. Neyts.** 2004. Therapeutic potential of nucleoside/nucleotide analogues against poxvirus infections. Rev Med Virol **14:**289-300.

46. **de Veer, M., and E. Meeusen.** 2011. New developments in vaccine research -- unveiling the secret of vaccine adjuvants. Discov Med **12:**195-204.

47. **Denzler, K. L., J. Schriewer, S. Parker, C. Werner, H. Hartzler, E. Hembrador, T. Huynh, S. Holechek, R. M. Buller, and B. L. Jacobs.** 2011. The attenuated NYCBH vaccinia virus deleted for the immune evasion gene, E3L, completely protects mice against heterologous challenge with ectromelia virus. Vaccine.

48. **Derouich, M., A. Boutayeb, and E. H. Twizell.** 2003. A model of dengue fever. Biomed Eng Online **2:**4.

49. **Deubel, V., R. M. Kinney, and D. W. Trent.** 1988. Nucleotide sequence and deduced amino acid sequence of the nonstructural proteins of dengue type 2 virus, Jamaica genotype: comparative analysis of the full-length genome. Virology **165:**234-44.

50. **Diamond, J.** 1997. Guns, germs and steel: the fates of human societies. W. W. Norton & Company, Inc., New York.

51. **Dietz, K.** 1975. Transmission and control of arbovirus diseases, p. 104-121. *In* D. Ludwig and K. L. Cooke (ed.), Epidemiology. SIAM, Philadelphia.

52. **Dittmer, U., K. E. Peterson, R. Messer, I. M. Stromnes, B. Race, and K. J. Hasenkrug.** 2001. Role of interleukin-4 (IL-4), IL-12, and gamma interferon in primary and vaccine-primed immune responses to Friend retrovirus infection. J Virol **75:**654-60.

53. **Durbin, A. P., and S. S. Whitehead.** 2010. Dengue vaccine candidates in development. Curr Top Microbiol Immunol **338:**129-43.

54. **Earl, P. L., and B. Moss.** 1991. Generation of recombinant vaccinia viruses, p. 16.16.1-16.16.7. *In* F. M. Ausubel, R. Brent, R. E. Kingston, D.

D. Moore, J. G. Seidman, J. A. Smith, and K. Struhl (ed.), Current Protocols in Molecular Biology. Wiley, New York.

55. **Edelstein-Keshet, L.** 2005. Applications of continuous models to population dynamics, Mathematical models in Biology. SIAM.

56. **Edghill-Smith, Y., H. Golding, J. Manischewitz, L. R. King, D. Scott, M. Bray, A. Nalca, J. W. Hooper, C. A. Whitehouse, J. E. Schmitz, K. A. Reimann, and G. Franchini.** 2005. Smallpox vaccine-induced antibodies are necessary and sufficient for protection against monkeypox virus. Nat Med **11:**740-7.

57. **Ellis, T. N., and B. L. Beaman.** 2004. Interferon-gamma activation of polymorphonuclear neutrophil function. Immunology **112:**2-12.

58. **Esposito, J. J., and F. Fenner.** 2001. Poxviruses, p. 2885-2921. *In* D. M. Knipe and P. M. Howley (ed.), Fields Virology. Lippincott Williams & Wilkings, Philadelphia.

59. **Esteban, D. J., and R. M. Buller.** 2005. Ectromelia virus: the causative agent of mousepox. J Gen Virol **86:**2645-59.

60. **Esteva, L., and C. Vargas.** 2003. Coexistence of different serotypes of dengue virus. J Math Biol **46:**31-47.

61. **Falkner, F. G., and B. Moss.** 1988. *Escherichia coli gpt* gene provides dominant selection for vaccinia virus open reading frame expression vectors. J Virol **62:**1849-54.

62. **Favier, C., N. Degallier, M. G. Rosa-Freitas, J. P. Boulanger, J. R. Costa Lima, J. F. Luitgards-Moura, C. E. Menkes, B. Mondet, C. Oliveira, E. T. Weimann, and P. Tsouris.** 2006. Early determination of the reproductive number for vector-borne diseases: the case of dengue in Brazil. Trop Med Int Health **11:**332-40.

63. **Favier, C., D. Schmit, C. D. Muller-Graf, B. Cazelles, N. Degallier, B. Mondet, and M. A. Dubois.** 2005. Influence of spatial heterogeneity on an emerging infectious disease: the case of dengue epidemics. Proc Biol Sci **272:**1171-7.

64. **Feng, Z., and J. X. Velasco-Hernandez.** 1997. Competitive exclusion in a vector-host model for the dengue fever. J Math Biol **35:**523-44.

65. **Fenner, F.** 1949. Mouse-pox; infectious ectromelia of mice; a review. J Immunol **63:**341-73.

66. **Fenner, F., R. Wittek, and K. R. Dumbell.** 1989. The Orthopoxviruses. Academic Press, California.

67. **Ferguson, N. M., C. A. Donnelly, and R. M. Anderson.** 1999. Transmission dynamics and epidemiology of dengue: insights from age-stratified sero-prevalence surveys. Philos Trans R Soc Lond B Biol Sci **354:**757-68.

68. **Fischer, D. B., and S. B. Halstead.** 1970. Observations related to pathogenesis of dengue hemorrhagic fever. V. Examination of ag specific sequential infection rates using a mathematical model. Yale J Biol Med **42:**329-49.

69. **Fischer, M. A., M. L. Davies, I. E. Reider, E. L. Heipertz, M. R. Epler, J. J. Sei, M. A. Ingersoll, N. Van Rooijen, G. J. Randolph, and C. C. Norbury.** 2011. CD11b, Ly6G Cells Produce Type I Interferon and Exhibit Tissue Protective Properties Following Peripheral Virus Infection. PLoS Pathog **7:**e1002374.

70. **Flexner, C., A. Hugin, and B. Moss.** 1987. Prevention of vaccinia virus infection in immunodeficient mice by vector-directed IL-2 expression. Nature **330:**259-62.

71. **Focks, D. A., E. Daniels, D. G. Haile, and J. E. Keesling.** 1995. A simulation model of the epidemiology of urban dengue fever: literature analysis, model development, preliminary validation, and samples of simulation results. Am J Trop Med Hyg **53:**489-506.

72. **Focks, D. A., D. G. Haile, E. Daniels, and G. A. Mount.** 1993. Dynamic life table model for *Aedes aegypti* (Diptera: *Culicidae*): analysis of the literature and model development. J Med Entomol **30:**1003-17.

73. **Focks, D. A., D. G. Haile, E. Daniels, and G. A. Mount.** 1993. Dynamic life table model for *Aedes aegypti* (Diptera: *Culicidae*): simulation results and validation. J Med Entomol **30:**1018-28.

74. **Fulginiti, V. A., A. Papier, J. M. Lane, J. M. Neff, and D. A. Henderson.** 2003. Smallpox vaccination: a review, part II. Adverse events. Clin Infect Dis **37:**251-71.

75. **Gabrilovich, D. I., and S. Nagaraj.** 2009. Myeloid-derived suppressor cells as regulators of the immune system. Nat Rev Immunol **9:**162-74.

76. **Garcel, A., W. Fauquette, R. Cecchelli, J.-M. Crance, D. Garin, and A.-L. Favier.** 2008. Smallpox post-vaccinal encephalitis: vaccinia virus interaction with the blood brain barrier. BMC Proceedings 2(Suppl 1):P20.

77. **Gherardi, M. M., J. L. Najera, E. Perez-Jimenez, S. Guerra, A. Garcia-Sastre, and M. Esteban.** 2003. Prime-boost immunization schedules based on influenza virus and vaccinia virus vectors potentiate cellular immune responses against human immunodeficiency virus Env protein systemically and in the genitorectal draining lymph nodes. J Virol **77:**7048-57.

78. **Gherardi, M. M., J. C. Ramirez, and M. Esteban.** 2003. IL-12 and IL-18 act in synergy to clear vaccinia virus infection: involvement of innate and adaptive components of the immune system. J Gen Virol **84:**1961-72.

79. **Giavedoni, L., S. Ahmad, L. Jones, and T. Yilma.** 1997. Expression of gamma interferon by simian immunodeficiency virus increases attenuation and reduces postchallenge virus load in vaccinated rhesus macaques. J Virol **71:**866-72.

80. **Giavedoni, L. D., L. Jones, M. B. Gardner, H. L. Gibson, C. T. Ng, P. J. Barr, and T. Yilma.** 1992. Vaccinia virus recombinants expressing chimeric proteins of human immunodeficiency virus and gamma interferon are attenuated for nude mice. Proc Natl Acad Sci U S A **89:**3409-13.

81. **Goldman, S. M., and J. Lightwood.** 2002. Cost optimization in the SIS model of infectious disease with treatment. Topics in Economic Analysis & Policy **2**.

82. **Goni, O., P. Alcaide, and M. Fresno.** 2002. Immunosuppression during acute *Trypanosoma cruzi* infection: involvement of Ly6G (Gr1($^{+}$))CD11b($^{+}$) immature myeloid suppressor cells. Int Immunol **14:**1125-34.

83. **Gubler, D.** 2005. The emergence of epidemic dengue fever and dengue hemorrhagic fever in the Americas: a case of failed public health policy. Rev Panam Salud Publica **17:**221-4.

84. **Gubler, D. J.** 1987. Dengue and dengue hemorrhagic fever in the Americas. P R Health Sci J **6:**107-11.

85. **Gubler, D. J., D. Reed, L. Rosen, and J. R. Hitchcock, Jr.** 1978. Epidemiologic, clinical, and virologic observations on dengue in the Kingdom of Tonga. Am J Trop Med Hyg **27:**581-9.

86. **Gubler, D. J., and D. W. Trent.** 1993. Emergence of epidemic dengue/dengue hemorrhagic fever as a public health problem in the Americas. Infect Agents Dis **2:**383-93.

87. **Guerra, S., M. Aracil, R. Conde, A. Bernad, and M. Esteban.** 2005. Wiskott-Aldrich syndrome protein is needed for vaccinia virus pathogenesis. J Virol **79:**2133-40.

88. **Guirakhoo, F., R. Weltzin, T. J. Chambers, Z. X. Zhang, K. Soike, M. Ratterree, J. Arroyo, K. Georgakopoulos, J. Catalan, and T. P. Monath.** 2000. Recombinant chimeric yellow fever-dengue type 2 virus is immunogenic and protective in nonhuman primates. J Virol **74:**5477-85.

89. **Gunther, J., J. P. Martinez-Munoz, D. G. Perez-Ishiwara, and J. Salas-Benito.** 2007. Evidence of vertical transmission of dengue virus in two endemic localities in the state of Oaxaca, Mexico. Intervirology **50:**347-52.

90. **Guy, B., J. Almond, and J. Lang.** 2011. Dengue vaccine prospects: a step forward. Lancet **377:**381-2.

91. **Guy, B., B. Barrere, C. Malinowski, M. Saville, R. Teyssou, and J. Lang.** 2011. From research to phase III: Preclinical, industrial and clinical development of the Sanofi Pasteur tetravalent dengue vaccine. Vaccine **29:**7229-41.

92. **Hall, K., P. Cruz, I. Tinoco, Jr., T. M. Jovin, and J. H. van de Sande.** 1984. 'Z-RNA'--a left-handed RNA double helix. Nature **311:**584-6.

93. **Halstead, S. B., N. T. Lan, T. T. Myint, T. N. Shwe, A. Nisalak, S. Kalyanarooj, S. Nimmannitya, S. Soegijanto, D. W. Vaughn, and T. P. Endy.** 2002. Dengue hemorrhagic fever in infants: research opportunities ignored. Emerg Infect Dis **8:**1474-9.

94. **Halstead, S. B., S. Nimmannitya, and S. N. Cohen.** 1970. Observations related to pathogenesis of dengue hemorrhagic fever. IV. Relation of disease severity to antibody response and virus recovered. Yale J Biol Med **42:**311-28.

95. **Halstead, S. B., E. J. O'Rourke, and A. C. Allison.** 1977. Dengue viruses and mononuclear phagocytes. II. Identity of blood and tissue leukocytes supporting in vitro infection. J Exp Med **146:**218-29.

96. **Hardin, C. C., D. A. Zarling, J. D. Puglisi, M. O. Trulson, P. W. Davis, and I. Tinoco, Jr.** 1987. Stabilization of Z-RNA by chemical bromination and its recognition by anti-Z-DNA antibodies. Biochemistry **26:**5191-9.

97. **Harrington, L. E., R. Most Rv, J. L. Whitton, and R. Ahmed.** 2002. Recombinant vaccinia virus-induced T-cell immunity: quantitation of the response to the virus vector and the foreign epitope. J Virol **76:**3329-37.

98. **Harris, E., E. Videa, L. Perez, E. Sandoval, Y. Tellez, M. L. Perez, R. Cuadra, J. Rocha, W. Idiaquez, R. E. Alonso, M. A. Delgado, L. A. Campo, F. Acevedo, A. Gonzalez, J. J. Amador, and A. Balmaseda.** 2000. Clinical, epidemiologic, and virologic features of dengue in the 1998 epidemic in Nicaragua. Am J Trop Med Hyg **63:**5-11.

99. **Harris, N., R. M. Buller, and G. Karupiah.** 1995. Gamma interferon-induced, nitric oxide-mediated inhibition of vaccinia virus replication. J Virol **69:**910-5.

100. **Hauns, K.** 2008. Expression of cellular anti-viral antagonists from vaccinia virus to study the innate immune response and Z-DNA. Arizona State University.

101. **Hawley, W. A., P. Reiter, R. S. Copeland, C. B. Pumpuni, and G. B. Craig, Jr.** 1987. *Aedes albopictus* in North America: probable introduction in used tires from northern Asia. Science **236:**1114-6.

102. **Ho, C. K., and S. Shuman.** 1996. Mutational analysis of the vaccinia virus E3 protein defines amino acid residues involved in E3 binding to double-stranded RNA. J Virol **70:**2611-4.

103. **Ho, C. K., and S. Shuman.** 1996. Physical and functional characterization of the double-stranded RNA binding protein encoded by the vaccinia virus E3 gene. Virology **217:**272-84.

104. **Horsburgh Jr., C. R., and B. E. Mahon.** 2008. Infectious disease epidemiology. *In* K. J. Rothman, S. Greenland, and T. L. Lash (ed.), Modern epidemiology, 3rd ed. Wolter Kluwer Lippincott Williams & Wilkins Philadelphia.

105. **Hutamai, S., W. Suwonkerd, N. Suwannchote, P. Somboon, and L. A. Prapanthadara.** 2007. A survey of dengue viral infection in *Aedes aegypti* and *Aedes albopictus* from re-epidemic areas in the north of Thailand using nucleic acid sequence based amplification assay. Southeast Asian J Trop Med Public Health **38:**448-54.

106. **Jacobs, B. L., and J. O. Langland.** 1996. When two strands are better than one: the mediators and modulators of the cellular responses to double-stranded RNA. Virology **219:**339-49.

107. **Jacobs, B. L., J. O. Langland, and T. Brandt.** 1998. Characterization of viral double-stranded RNA-binding proteins. Methods **15:**225-32.

108. **Jacobs, B. L., J. O. Langland, K. V. Kibler, K. L. Denzler, S. D. White, S. A. Holechek, S. Wong, T. Huynh, and C. R. Baskin.** 2009. Vaccinia virus vaccines: past, present and future. Antiviral Res **84:**1-13.

109. **Jentarra, G. M., M. C. Heck, J. W. Youn, K. Kibler, J. O. Langland, C. R. Baskin, O. Ananieva, Y. Chang, and B. L. Jacobs.** 2008. Vaccinia viruses with mutations in the E3L gene as potential replication-competent, attenuated vaccines: scarification vaccination. Vaccine **26:**2860-72.

110. **Kahmann, J. D., D. A. Wecking, V. Putter, K. Lowenhaupt, Y. G. Kim, P. Schmieder, H. Oschkinat, A. Rich, and M. Schade.** 2004. The solution structure of the N-terminal domain of E3L shows a tyrosine conformation that may explain its reduced affinity to Z-DNA in vitro. Proc Natl Acad Sci U S A **101:**2712-7.

111. **Kaplan, C.** 1989. Vaccinia virus: a suitable vehicle for recombinant vaccines? Arch Virol **106:**127-39.

112. **Karupiah, G., J. H. Chen, C. F. Nathan, S. Mahalingam, and J. D. MacMicking.** 1998. Identification of nitric oxide synthase 2 as an innate resistance locus against ectromelia virus infection. J Virol **72:**7703-6.

113. **Karupiah, G., Q. W. Xie, R. M. Buller, C. Nathan, C. Duarte, and J. D. MacMicking.** 1993. Inhibition of viral replication by interferon-gamma-induced nitric oxide synthase. Science **261:**1445-8.

114. **Kasang, C., S. Kalluvya, C. Majinge, A. Stich, J. Bodem, G. Kongola, G. B. Jacobs, M. Mlewa, M. Mildner, I. Hensel, A. Horn, W. Preiser, G. van Zyl, H. Klinker, E. Koutsilieri, A. Rethwilm, C. Scheller, and B. Weissbrich.** 2011. HIV Drug Resistance (HIVDR) in antiretroviral therapy-naive patients in Tanzania not eligible for WHO threshold HIVDR survey is dramatically high. PLoS One **6:**e23091.

115. **Kawaguchi, I., A. Sasaki, and M. Boots.** 2003. Why are dengue virus serotypes so distantly related? Enhancement and limiting serotype similarity between dengue virus strains. Proc Biol Sci **270:**2241-7.

116. **Kermack, W. O., and A. G. McKendrick.** 1927. A contribution to the mathematical theory of epidemics. Proc R Soc A. Series A, containing papers of Mathematical and Physical character **115:**700-721.

117. **Kermack, W. O., and A. G. McKendrick.** 1932. A contribution to the mathematical theory of epidemics. II. The problem of endemicity. Proc R Soc London. Series A, containing papers of Mathematical and Physical character.

118. **Kibler, K. V., C. E. Gomez, B. Perdiguero, S. Wong, T. Huynh, S. Holechek, W. Arndt, V. Jimenez, R. Gonzalez-Sanz, K. Denzler, E. K. Haddad, R. Wagner, R. P. Sekaly, J. Tartaglia, G. Pantaleo, B. L. Jacobs, and M. Esteban.** 2011. Improved NYVAC-based vaccine vectors. PLoS One **6:**e25674.

119. **Kibler, K. V., T. Shors, K. B. Perkins, C. C. Zeman, M. P. Banaszak, J. Biesterfeldt, J. O. Langland, and B. L. Jacobs.** 1997. Double-stranded RNA is a trigger for apoptosis in vaccinia virus-infected cells. J Virol **71:**1992-2003.

120. **Kieny, M. P., J. Blancou, R. Lathe, P. P. Pastoret, J. P. Soulebot, P. Desmettre, and J. P. Lecocq.** 1988. Development of animal recombinant DNA vaccine and its efficacy in foxes. Rev Infect Dis **10 Suppl 4:**S799-802.

121. **Kim, Y. G., K. Lowenhaupt, D. B. Oh, K. K. Kim, and A. Rich.** 2004. Evidence that vaccinia virulence factor E3L binds to Z-DNA in vivo: Implications for development of a therapy for poxvirus infection. Proc Natl Acad Sci U S A **101:**1514-8.

122. **Kim, Y. G., M. Muralinath, T. Brandt, M. Pearcy, K. Hauns, K. Lowenhaupt, B. L. Jacobs, and A. Rich.** 2003. A role for Z-DNA binding in vaccinia virus pathogenesis. Proc Natl Acad Sci U S A **100:**6974-9.

123. **Knox, T. B., B. H. Kay, R. A. Hall, and P. A. Ryan.** 2003. Enhanced vector competence of *Aedes aegypti* (Diptera: *Culicidae*) from the Torres Strait compared with mainland Australia for dengue 2 and 4 viruses. J Med Entomol **40:**950-6.

124. **Kochel, T. J., D. M. Watts, S. B. Halstead, C. G. Hayes, A. Espinoza, V. Felices, R. Caceda, C. T. Bautista, Y. Montoya, S. Douglas, and K. L. Russell.** 2002. Effect of dengue-1 antibodies on American dengue-2 viral infection and dengue haemorrhagic fever. Lancet **360:**310-2.

125. **Kohonen-Corish, M. R., N. J. King, C. E. Woodhams, and I. A. Ramshaw.** 1990. Immunodeficient mice recover from infection with vaccinia virus expressing interferon-gamma. Eur J Immunol **20:**157-61.

126. **Kow, C. Y., L. L. Koon, and P. F. Yin.** 2001. Detection of dengue viruses in field caught male *Aedes aegypti* and *Aedes albopictus* (Diptera:*Culicidae*) in Singapore by type-specific PCR. J Med Entomol **38:**475-9.

127. **Kretzschmar, M., J. Wallinga, P. Teunis, S. Xing, and R. Mikolajczyk.** 2006. Frequency of adverse events after vaccination with different vaccinia strains. PLoS Med **3:**e272.

128. **Kwok, Y.** 2010. Across Asia, dengue fever cases reach record highs. TIME.

129. **Kwon, J. A., and A. Rich.** 2005. Biological function of the vaccinia virus Z-DNA-binding protein E3L: gene transactivation and antiapoptotic activity in HeLa cells. Proc Natl Acad Sci U S A **102:**12759-64.

130. **Kyle, J. L., and E. Harris.** 2008. Global spread and persistence of dengue. Annu Rev Microbiol **62:**71-92.

131. **Langland, J. O., J. M. Cameron, M. C. Heck, J. K. Jancovich, and B. L. Jacobs.** 2006. Inhibition of PKR by RNA and DNA viruses. Virus Res **119:**100-10.

132. **Langland, J. O., and B. L. Jacobs.** 2004. Inhibition of PKR by vaccinia virus: role of the N- and C-terminal domains of E3L. Virology **324:**419-29.

133. **Langland, J. O., and B. L. Jacobs.** 2002. The role of the PKR-inhibitory genes, E3L and K3L, in determining vaccinia virus host range. Virology **299:**133-41.

134. **LeDuc, J. W., I. Damon, D. A. Relman, J. Huggins, and P. B. Jahrling.** 2002. Smallpox research activities: U.S. interagency collaboration, 2001. Emerg Infect Dis **8:**743-5.

135. **LeDuc, J. W., and P. B. Jahrling.** 2001. Strengthening national preparedness for smallpox: an update. Emerg Infect Dis **7:**155-7.

136. **Legrand, F. A., P. H. Verardi, K. S. Chan, Y. Peng, L. A. Jones, and T. D. Yilma.** 2005. Vaccinia viruses with a serpin gene deletion and expressing IFN-gamma induce potent immune responses without detectable replication in vivo. Proc Natl Acad Sci U S A **102:**2940-5.

137. **Legrand, F. A., P. H. Verardi, L. A. Jones, K. S. Chan, Y. Peng, and T. D. Yilma.** 2004. Induction of potent humoral and cell-mediated immune responses by attenuated vaccinia virus vectors with deleted serpin genes. J Virol **78:**2770-9.

138. **Leiva, N., and O. Caceres.** 2004. Variabilidad genética de *Aedes aegypti* en algunas áreas del Perú usando Single Stranded Conformational Polymorphism (SSCP). Rev Peru Med Exp Salud Publica **21:**157-166.

139. **Lewis, J. A., G. J. Chang, R. S. Lanciotti, R. M. Kinney, L. W. Mayer, and D. W. Trent.** 1993. Phylogenetic relationships of dengue-2 viruses. Virology **197:**216-24.

140. **Liu, G., Q. Zhai, D. J. Schaffner, A. Wu, A. Yohannes, T. M. Robinson, M. Maland, J. Wells, T. G. Voss, C. Bailey, and K. Alibek.** 2004. Prevention of lethal respiratory vaccinia infections in mice with interferon-alpha and interferon-gamma. FEMS Immunol Med Microbiol **40:**201-6.

141. **Lorono-Pino, M. A., C. B. Cropp, J. A. Farfan, A. V. Vorndam, E. M. Rodriguez-Angulo, E. P. Rosado-Paredes, L. F. Flores-Flores, B. Beaty, and D. J. Gubler.** 1999. Common occurrence of concurrent infections by multiple dengue virus serotypes. Am J Trop Med Hyg **61:**725-30.

142. **Luz, P. M., C. T. Codeco, E. Massad, and C. J. Struchiner.** 2003. Uncertainties regarding dengue modeling in Rio de Janeiro, Brazil. Mem Inst Oswaldo Cruz **98:**871-8.

143. **MacDonald, G.** 1957. The epidemiology and control of malaria. Oxford University Press, Oxford.

144. **Mackett, M., T. Yilma, J. K. Rose, and B. Moss.** 1985. Vaccinia virus recombinants: expression of VSV genes and protective immunization of mice and cattle. Science **227:**433-5.

145. **Mamani, E., D. Figueroa, M. Garcia, M. Garaycochea, and E. Pozo.** 2010. Infecciones concurrentes por dos serotipos del virus dengue durante un brote en el noroeste de Peru, 2008. Rev Peru Med Exp Salud Publica **27:**16-21.

146. **Martinez, M. J., M. P. Bray, and J. W. Huggins.** 2000. A mouse model of aerosol-transmitted orthopoxviral disease: morphology of experimental aerosol-transmitted orthopoxviral disease in a cowpox virus-BALB/c mouse system. Arch Pathol Lab Med **124:**362-77.

147. **Massad, E., F. A. Coutinho, M. N. Burattini, and M. Amaku.** 2010. Estimation of R_0 from the initial phase of an outbreak of a vector-borne infection. Trop Med Int Health **15:**120-6.

148. **Mazzoni, A., V. Bronte, A. Visintin, J. H. Spitzer, E. Apolloni, P. Serafini, P. Zanovello, and D. M. Segal.** 2002. Myeloid suppressor lines inhibit T cell responses by an NO-dependent mechanism. J Immunol **168:**689-95.

149. **McBride, W. J., and H. Bielefeldt-Ohmann.** 2000. Dengue viral infections; pathogenesis and epidemiology. Microbes Infect **2:**1041-50.

150. **McCall, T. B., R. M. Palmer, and S. Moncada.** 1991. Induction of nitric oxide synthase in rat peritoneal neutrophils and its inhibition by dexamethasone. Eur J Immunol **21:**2523-7.

151. **Meitin, C. A., B. S. Bender, and P. A. Small, Jr.** 1991. Influenza immunization: intranasal live vaccinia recombinant contrasted with parenteral inactivated vaccine. Vaccine **9:**751-6.

152. **Melkova, Z., and M. Esteban.** 1995. Inhibition of vaccinia virus DNA replication by inducible expression of nitric oxide synthase. J Immunol **155:**5711-8.

153. **Moller, A., A. Nordheim, S. A. Kozlowski, D. J. Patel, and A. Rich.** 1984. Bromination stabilizes poly(dG-dC) in the Z-DNA form under low-salt conditions. Biochemistry **23:**54-62.

154. **Montoya, Y., S. Holechek, O. Caceres, A. Palacios, J. Burans, C. Guevara, F. Quintana, V. Herrera, E. Pozo, E. Anaya, E. Mamani, V. Gutierrez, A. Ladron de Guevara, E. Fernandez, P. Asmat, V. Alva-Davalos, C. Hoguin, V. A. Laguna, A. M. Morales, P. Minaya, and T. Kochel.** 2003. Circulation of dengue viruses in North-western Peru, 2000-2001. Dengue Bulletin **27:**52-62.

155. **Morens, D. M.** 1994. Antibody-dependent enhancement of infection and the pathogenesis of viral disease. Clin Infect Dis **19:**500-12.

156. **Morens, D. M., and A. S. Fauci.** 2008. Dengue and hemorrhagic fever: a potential threat to public health in the United States. JAMA **299:**214-6.

157. **Mortimer, P. P.** 2003. Can postexposure vaccination against smallpox succeed? Clin Infect Dis **36:**622-9.

158. **Moss, B.** 1996. Genetically engineered poxviruses for recombinant gene expression, vaccination, and safety. Proc Natl Acad Sci U S A **93:**11341-8.

159. **Moss, B.** 2001. Poxviridae: the viruses and their replication, p. 2849-2883. *In* B. N. Fields, D. M. Knipe, and P. M. Howley (ed.), Fields Virology, 4th ed, vol. 2. Lippincott-Raven Publishers, Philadelphia.

160. **Moss, B., and P. L. Earl.** 1991. Expression of proteins in mammalian cells using vaccinia virus vectors. Overview of the vaccinia virus expression system, p. 16.16.1.-16.16.7. *In* F. M. Ausubel, R. Brent, R. E. Kingston, D. D. Moore, J. G. Seidman, J. A. Smith, and K. Struhl (ed.), Current protocols in molecular biology.

161. **Mossman, K., C. Upton, R. M. Buller, and G. McFadden.** 1995. Species specificity of ectromelia virus and vaccinia virus interferon-gamma binding proteins. Virology **208:**762-9.

162. **Mostorino, R., A. Rosas, V. Gutierrez, E. Anaya, M. Cobos, and M. Garcia.** 2002. Manifestaciones clínicas y distribución geográfica de los serotipos del dengue en el Perú - año 2001. Rev Peru Med Exp Salud Publica **19:**171-180.

163. **Muller, U., U. Steinhoff, L. F. Reis, S. Hemmi, J. Pavlovic, R. M. Zinkernagel, and M. Aguet.** 1994. Functional role of type I and type II interferons in antiviral defense. Science **264:**1918-21.

164. **Muralinath, M.** 2003. The role of the amino terminus of E3L in vaccinia virus pathogenesis. Arizona State University, Tempe.

165. **Nagaraj, S., M. Collazo, C. A. Corzo, J. I. Youn, M. Ortiz, D. Quiceno, and D. I. Gabrilovich.** 2009. Regulatory myeloid suppressor cells in health and disease. Cancer Res **69:**7503-6.

166. **Najarro, P., P. Traktman, and J. A. Lewis.** 2001. Vaccinia virus blocks gamma interferon signal transduction: viral VH1 phosphatase reverses Stat1 activation. J Virol **75:**3185-96.

167. **Nalca, A., J. M. Hatkin, N. L. Garza, D. K. Nichols, S. W. Norris, D. E. Hruby, and R. Jordan.** 2008. Evaluation of orally delivered ST-246 as postexposure prophylactic and antiviral therapeutic in an aerosolized rabbitpox rabbit model. Antiviral Res **79:**121-7.

168. **Nalca, A., and D. K. Nichols.** 2011. Rabbitpox: a model of airborne transmission of smallpox. J Gen Virol **92:**31-5.

169. **Nalca, A., A. W. Rimoin, S. Bavari, and C. A. Whitehouse.** 2005. Reemergence of monkeypox: prevalence, diagnostics, and countermeasures. Clin Infect Dis **41:**1765-71.

170. **Nisalak, A., T. P. Endy, S. Nimmannitya, S. Kalayanarooj, U. Thisayakorn, R. M. Scott, D. S. Burke, C. H. Hoke, B. L. Innis, and D. W. Vaughn.** 2003. Serotype-specific dengue virus circulation and dengue disease in Bangkok, Thailand from 1973 to 1999. Am J Trop Med Hyg **68:**191-202.

171. **Nishiura, H.** 2006. Mathematical and Statistical Analyses of the Spread of Dengue Dengue Bulletin **30:**51-67.

172. **Nobelprize.org.** Ronal Ross - Biography.

173. **Paran, N., Y. Suezer, S. Lustig, T. Israely, A. Schwantes, S. Melamed, L. Katz, T. Preuss, K. M. Hanschmann, U. Kalinke, N. Erez, R. Levin, B. Velan, J. Lower, A. Shafferman, and G. Sutter.** 2009. Postexposure immunization with modified vaccinia virus Ankara or conventional Lister vaccine provides solid protection in a murine model of human smallpox. J Infect Dis **199:**39-48.

174. **Parker, S., A. Nuara, R. M. Buller, and D. A. Schultz.** 2007. Human monkeypox: an emerging zoonotic disease. Future Microbiol **2:**17-34.

175. **Pastoret, P. P., J. Blancou, B. Brochier, I. Thomas, A. Paquot, J. Debruyn, F. Costy, F. Wolff, M. P. Kieny, B. Languet, and et al.** 1988. [Experience with antirabies vaccination of foxes using the oral route coordinated among several European countries and perspectives on the use of recombinant vaccinia-rabies virus]. Parassitologia **30:**149-54.

176. **Pastoret, P. P., B. Brochier, B. Languet, I. Thomas, A. Paquot, B. Bauduin, M. P. Kieny, J. P. Lecocq, J. De Bruyn, F. Costy, and et al.** 1988. First field trial of fox vaccination against rabies using a vaccinia-rabies recombinant virus. Vet Rec **123:**481-3.

177. **Pearcy, M.** 2006. Identification and characterization of the multiple domains of the vaccinia virus E3L protein. Arizona State University.

178. **Pinho, S. T., C. P. Ferreira, L. Esteva, F. R. Barreto, V. C. Morato e Silva, and M. G. Teixeira.** 2010. Modelling the dynamics of dengue real epidemics. Philos Transact A Math Phys Eng Sci **368:**5679-93.

179. **Placido, D., B. A. Brown, 2nd, K. Lowenhaupt, A. Rich, and A. Athanasiadis.** 2007. A left-handed RNA double helix bound by the Z alpha domain of the RNA-editing enzyme ADAR1. Structure **15:**395-404.

180. **Plakhov, I. V., E. E. Arlund, C. Aoki, and C. S. Reiss.** 1995. The earliest events in vesicular stomatitis virus infection of the murine olfactory neuroepithelium and entry of the central nervous system. Virology **209:**257-62.

181. **Popenda, M., J. Milecki, and R. W. Adamiak.** 2004. High salt solution structure of a left-handed RNA double helix. Nucleic Acids Res **32:**4044-54.

182. **Pozo, E.** 2010. Dengue Cases in the Luciano Castillo Colonna region, Peru 2000-2010.

183. **Provincial Health Directorate of Ile, Zambesia.** 2004. Pilot community surveillance project. Final Evaluation Report.

184. **Puddu, P., L. Fantuzzi, P. Borghi, B. Varano, G. Rainaldi, E. Guillemard, W. Malorni, P. Nicaise, S. F. Wolf, F. Belardelli, and S. Gessani.** 1997. IL-12 induces IFN-gamma expression and secretion in mouse peritoneal macrophages. J Immunol **159:**3490-7.

185. **Quenelle, D. C., R. M. Buller, S. Parker, K. A. Keith, D. E. Hruby, R. Jordan, and E. R. Kern.** 2007. Efficacy of delayed treatment with ST-246 given orally against systemic orthopoxvirus infections in mice. Antimicrob Agents Chemother **51:**689-95.

186. **Quenelle, D. C., M. N. Prichard, K. A. Keith, D. E. Hruby, R. Jordan, G. R. Painter, A. Robertson, and E. R. Kern.** 2007. Synergistic efficacy of the combination of ST-246 with CMX001 against orthopoxviruses. Antimicrob Agents Chemother **51:**4118-24.

187. **Quyen, D. V., S. C. Ha, K. Lowenhaupt, A. Rich, K. K. Kim, and Y. G. Kim.** 2007. Characterization of DNA-binding activity of Z alpha domains from poxviruses and the importance of the beta-wing regions in converting B-DNA to Z-DNA. Nucleic Acids Res **35:**7714-20.

188. **Raggo, C., M. Habermehl, L. A. Babiuk, and P. Griebel.** 2000. The in vivo effects of recombinant bovine herpesvirus-1 expressing bovine interferon-gamma. J Gen Virol **81:**2665-73.

189. **Ramirez, J. C., D. Finke, M. Esteban, J. P. Kraehenbuhl, and H. Acha-Orbea.** 2003. Tissue distribution of the Ankara strain of vaccinia

virus (MVA) after mucosal or systemic administration. Arch Virol **148:**827-39.

190. **Ramshaw, I., J. Ruby, A. Ramsay, G. Ada, and G. Karupiah.** 1992. Expression of cytokines by recombinant vaccinia viruses: a model for studying cytokines in virus infections in vivo. Immunol Rev **127:**157-82.

191. **Ramshaw, I. A., M. E. Andrew, S. M. Phillips, D. B. Boyle, and B. E. Coupar.** 1987. Recovery of immunodeficient mice from a vaccinia virus/IL-2 recombinant infection. Nature **329:**545-6.

192. **Reading, P. C., and G. L. Smith.** 2003. Vaccinia virus interleukin-18-binding protein promotes virulence by reducing gamma interferon production and natural killer and T-cell activity. J Virol **77:**9960-8.

193. **Reiter, P., and D. Gubler.** 1997. Suveillance and control of urban dengue vectors. *In* D. Gubler and G. Kuno (ed.), Dengue and dengue hemorrhagic fever. CABI Publishing.

194. **Rich, A., A. Nordheim, and A. H. Wang.** 1984. The chemistry and biology of left-handed Z-DNA. Annu Rev Biochem **53:**791-846.

195. **Rico-Hesse, R., L. M. Harrison, A. Nisalak, D. W. Vaughn, S. Kalayanarooj, S. Green, A. L. Rothman, and F. A. Ennis.** 1998. Molecular evolution of dengue type 2 virus in Thailand. Am J Trop Med Hyg **58:**96-101.

196. **Rico-Hesse, R., L. M. Harrison, R. A. Salas, D. Tovar, A. Nisalak, C. Ramos, J. Boshell, M. T. de Mesa, R. M. Nogueira, and A. T. da Rosa.** 1997. Origins of dengue type 2 viruses associated with increased pathogenicity in the Americas. Virology **230:**244-51.

197. **Riedel, S.** 2005. Edward Jenner and the history of smallpox and vaccination. Proc (Bayl Univ Med Cent) **18:**21-5.

198. **Rizki Akbar, M., R. Agoes, T. Djatie, and S. Kodyat.** 2008. PCR detection of dengue transovarial transmissibility in *Aedes aegypti* in Bandung, Indonesia. Proc ASEAN Congr Trop Med and Parasitol. **3:**84-89.

199. **Rodhain, F., and L. Rosen.** 1997. Mosquito vectors and dengue virus-vector relationships, p. 45-60. *In* D. Gubler and G. Kuno (ed.), Dengue and Dengue Hemorrhagic Fever. UK: CAB International, Wallingford.

200. **Rolph, M. S., W. B. Cowden, C. J. Medveczky, and I. A. Ramshaw.** 1996. A recombinant vaccinia virus encoding inducible nitric oxide synthase is attenuated in vivo. J Virol **70:**7678-85.

201. **Rolph, M. S., I. A. Ramshaw, K. A. Rockett, J. Ruby, and W. B. Cowden.** 1996. Nitric oxide production is increased during murine vaccinia virus infection, but may not be essential for virus clearance. Virology **217:**470-7.

202. **Rosen, L.** 1977. The Emperor's New Clothes revisited, or reflections on the pathogenesis of dengue hemorrhagic fever. Am J Trop Med Hyg **26:**337-43.

203. **Rosen, L., D. A. Shroyer, R. B. Tesh, J. E. Freier, and J. C. Lien.** 1983. Transovarial transmission of dengue viruses by mosquitoes: *Aedes albopictus* and *Aedes aegypti*. Am J Trop Med Hyg **32:**1108-19.

204. **Ross, R.** 1911. The prevention of malaria, 2nd ed. Murray, London.

205. **Rothenburg, S., N. Deigendesch, K. Dittmar, F. Koch-Nolte, F. Haag, K. Lowenhaupt, and A. Rich.** 2005. A PKR-like eukaryotic initiation factor 2alpha kinase from zebrafish contains Z-DNA binding domains instead of dsRNA binding domains. Proc Natl Acad Sci U S A **102:**1602-7.

206. **Rotz, L. D., D. A. Dotson, I. K. Damon, and J. A. Becher.** 2001. Vaccinia (smallpox) vaccine: recommendations of the Advisory Committee on Immunization Practices (ACIP), 2001. MMWR Recomm Rep **50:**1-25; quiz CE1-7.

207. **Sakala, I. G., G. Chaudhri, R. M. Buller, A. A. Nuara, H. Bai, N. Chen, and G. Karupiah.** 2007. Poxvirus-encoded gamma interferon binding protein dampens the host immune response to infection. J Virol **81:**3346-53.

208. **Sanchez, F., M. Engman, L. Harrington, and C. Castillo-Chavez.** 2006. Models for dengue transmission and control, p. 311-326. *In* A. Gumel, C. Castillo-Chavez, R. E. Mickens, D. P. Clemence (ed.), Mathematical Studies on Human Disease Dynamics: Emerging Paradigms and Challenges, vol. 410.

209. **Sbrana, E., R. Jordan, D. E. Hruby, R. I. Mateo, S. Y. Xiao, M. Siirin, P. C. Newman, D. A. R. AP, and R. B. Tesh.** 2007. Efficacy of the antipoxvirus compound ST-246 for treatment of severe orthopoxvirus infection. Am J Trop Med Hyg **76:**768-73.

210. **Schroder, K., P. J. Hertzog, T. Ravasi, and D. A. Hume.** 2004.Interferon-gamma: an overview of signals, mechanisms and functions. J Leukoc Biol **75:**163-89.

211. **Schrum, S., P. Probst, B. Fleischer, and P. F. Zipfel.** 1996. Synthesis of the CC-chemokines MIP-1alpha, MIP-1beta, and RANTES is associated with a type 1 immune response. J Immunol **157:**3598-604.

212. **Sharma, D. P., A. J. Ramsay, D. J. Maguire, M. S. Rolph, and I. A. Ramshaw.** 1996. Interleukin-4 mediates down regulation of antiviral cytokine expression and cytotoxic T-lymphocyte responses and exacerbates vaccinia virus infection in vivo. J Virol **70:**7103-7.

213. **Shors, T., K. V. Kibler, K. B. Perkins, R. Seidler-Wulff, M. P. Banaszak, and B. L. Jacobs.** 1997. Complementation of vaccinia virus deleted of the E3L gene by mutants of E3L. Virology **239:**269-76.

214. **Shtrichman, R., and C. E. Samuel.** 2001. The role of gamma interferon in antimicrobial immunity. Curr Opin Microbiol **4:**251-9.

215. **Singapore, G.** 2009. Singapore uses Cyberspace In fight against dengue, GovMonitor.

216. **Sittisombut, N., A. Sistayanarain, M. J. Cardosa, M. Salminen, S. Damrongdachakul, S. Kalayanarooj, S. Rojanasuphot, J. Supawadee, and N. Maneekarn.** 1997. Possible occurrence of a genetic bottleneck in dengue serotype 2 viruses between the 1980 and 1987 epidemic seasons in Bangkok, Thailand. Am J Trop Med Hyg **57:**100-8.

217. **Smith, E. J., I. Marie, A. Prakash, A. Garcia-Sastre, and D. E. Levy.** 2001. IRF3 and IRF7 phosphorylation in virus-infected cells does not require double-stranded RNA-dependent protein kinase R or Ikappa B kinase but is blocked by Vaccinia virus E3L protein. J Biol Chem **276:**8951-7.

218. **Smith, S. A., and G. J. Kotwal.** 2002. Immune response to poxvirus infections in various animals. Crit Rev Microbiol **28:**149-85.

219. **Smith, S. K., V. A. Olson, K. L. Karem, R. Jordan, D. E. Hruby, and I. K. Damon.** 2009. In vitro efficacy of ST246 against smallpox and monkeypox. Antimicrob Agents Chemother **53:**1007-12.

220. **Smith, V. P., and A. Alcami.** 2002. Inhibition of interferons by ectromelia virus. J Virol **76:**1124-34.

221. **Staib, C., Y. Suezer, S. Kisling, U. Kalinke, and G. Sutter.** 2006. Short-term, but not post-exposure, protection against lethal orthopoxvirus challenge after immunization with modified vaccinia virus Ankara. J Gen Virol **87:**2917-21.

222. **Stittelaar, K. J., J. Neyts, L. Naesens, G. van Amerongen, R. F. van Lavieren, A. Holy, E. De Clercq, H. G. Niesters, E. Fries, C. Maas, P. G. Mulder, B. A. van der Zeijst, and A. D. Osterhaus.** 2006. Antiviral treatment is more effective than smallpox vaccination upon lethal monkeypox virus infection. Nature **439:**745-8.

223. **Swaminathan, S., G. Batra, and N. Khanna.** 2010. Dengue vaccines: state of the art. Expert Opin Ther Pat **20:**819-35.

224. **Symons, J. A., E. Adams, D. C. Tscharke, P. C. Reading, H. Waldmann, and G. L. Smith.** 2002. The vaccinia virus C12L protein inhibits mouse IL-18 and promotes virus virulence in the murine intranasal model. J Gen Virol **83:**2833-44.

225. **Tewari, S. C., V. Thenmozhi, C. R. Katholi, R. Manavalan, A. Munirathinam, and A. Gajanana.** 2004. Dengue vector prevalence and virus infection in a rural area in south India. Trop Med Int Health **9:**499-507.

226. **Thomas, S. J., A. Nisalak, K. B. Anderson, D. H. Libraty, S. Kalayanarooj, D. W. Vaughn, R. Putnak, R. V. Gibbons, R. Jarman, and T. P. Endy.** 2009. Dengue plaque reduction neutralization test (PRNT) in primary and secondary dengue virus infections: How alterations in assay conditions impact performance. Am J Trop Med Hyg **81:**825-33.

227. **Thorne, C. D., J. M. Hirshon, C. D. Himes, and M. A. McDiarmid.** 2003. Emergency medicine tools to manage smallpox (vaccinia) vaccination complications: clinical practice guideline and policies and procedures. Ann Emerg Med **42:**665-80.

228. **Trainor, K. L.** 2008. The use of vaccinia virus E3L amino-terminal mutants in viral oncolysis and characterization in the murine JC cell line. Arizona State University, Tempe.

229. **Verardi, P. H., F. H. Aziz, S. Ahmad, L. A. Jones, B. Beyene, R. N. Ngotho, H. M. Wamwayi, M. G. Yesus, B. G. Egziabher, and T. D. Yilma.** 2002. Long-term sterilizing immunity to rinderpest in cattle vaccinated with a recombinant vaccinia virus expressing high levels of the fusion and hemagglutinin glycoproteins. J Virol **76:**484-91.

230. **Voisin, M. B., D. Buzoni-Gatel, D. Bout, and F. Velge-Roussel.** 2004. Both expansion of regulatory $GR1^{+}CD11b^{+}$ myeloid cells and anergy of T lymphocytes participate in hyporesponsiveness of the lung-associated immune system during acute toxoplasmosis. Infect Immun **72:**5487-92.

231. **Vora, S., I. Damon, V. Fulginiti, S. G. Weber, M. Kahana, S. L. Stein, S. I. Gerber, S. Garcia-Houchins, E. Lederman, D. Hruby, L. Collins, D. Scott, K. Thompson, J. V. Barson, R. Regnery, C. Hughes, R. S. Daum, Y. Li, H. Zhao, S. Smith, Z. Braden, K. Karem, V. Olson, W. Davidson, G. Trindade, T. Bolken, R. Jordan, D. Tien, and J. Marcinak.** 2008. Severe eczema vaccinatum in a household contact of a smallpox vaccinee. Clin Infect Dis **46:**1555-61.

232. **Vynnycky, E., and R. G. White.** 2010. An introduction to infectious disease modelling. Oxford University Press.

233. **Walker, B. A., and P. A. Ward.** 1992. Priming and signal transduction in neutrophils. Biol Signals **1:**237-49.

234. **Wearing, H. J., and P. Rohani.** 2006. Ecological and immunological determinants of dengue epidemics. Proc Natl Acad Sci U S A **103:**11802-7.

235. **White, S.** 2008. The role of the amino terminus of vaccinia virus protein E3L in subcellular localization and pathogenesis. Arizona State University, Tempe.

236. **WHO.** 2009, posting date. Dengue and dengue hemorrhagic fever. Fact sheet N°117. [Online].

237. **WHO.** 1980. The global eradication of smallpox: final report of the Global Commission for the Certification of Smallpox Eradication.

238. **WHO.** 2011. Report of the meeting of the WHO/VMI workshop on dengue modeling.

239. **Williams, C. R., P. H. Johnson, S. A. Long, L. P. Rapley, and S. A. Ritchie.** 2008. Rapid estimation of *Aedes aegypti* population size using simulation modeling, with a novel approach to calibration and field validation. J Med Entomol **45:**1173-9.

240. **Wittek, R.** 2006. Vaccinia immune globulin: current policies, preparedness, and product safety and efficacy. Int J Infect Dis **10:**193-201.

241. **Xiang, Y., R. C. Condit, S. Vijaysri, B. Jacobs, B. R. Williams, and R. H. Silverman.** 2002. Blockade of interferon induction and action by the E3L double-stranded RNA binding proteins of vaccinia virus. J Virol **76:**5251-9.

242. **Xiang, Y., and B. Moss.** 1999. IL-18 binding and inhibition of interferon gamma induction by human poxvirus-encoded proteins. Proc Natl Acad Sci U S A **96:**11537-42.

243. **Xiao, Z., J. M. Curtsinger, M. Prlic, S. C. Jameson, and M. F. Mescher.** 2007. The CD8 T cell response to vaccinia virus exhibits site-dependent heterogeneity of functional responses. Int Immunol **19:**733-43.

244. **Xu, R., A. J. Johnson, D. Liggitt, and M. J. Bevan.** 2004. Cellular and humoral immunity against vaccinia virus infection of mice. J Immunol **172:**6265-71.

245. **Yamashita, T., T. Uchida, A. Araki, and F. Sendo.** 1997. Nitric oxide is an effector molecule in inhibition of tumor cell growth by rIFN-gamma-activated rat neutrophils. Int J Cancer **71:**223-30.

246. **Yang, G., D. C. Pevear, M. H. Davies, M. S. Collett, T. Bailey, S. Rippen, L. Barone, C. Burns, G. Rhodes, S. Tohan, J. W. Huggins, R. O. Baker, R. L. Buller, E. Touchette, K. Waller, J. Schriewer, J. Neyts, E. DeClercq, K. Jones, D. Hruby, and R. Jordan.** 2005. An orally bioavailable antipoxvirus compound (ST-246) inhibits extracellular virus formation and protects mice from lethal orthopoxvirus Challenge. J Virol **79:**13139-49.

247. **Yang, H. M., M. L. Macoris, K. C. Galvani, M. T. Andrighetti, and D. M. Wanderley.** 2009. Assessing the effects of temperature on dengue transmission. Epidemiol Infect **137:**1179-87.

248. **Yilma, T., D. Hsu, L. Jones, S. Owens, M. Grubman, C. Mebus, M. Yamanaka, and B. Dale.** 1988. Protection of cattle against rinderpest with vaccinia virus recombinants expressing the HA or F gene. Science **242:**1058-61.

249. **Zhang, C., M. P. Mammen, Jr., P. Chinnawirotpisan, C. Klungthong, P. Rodpradit, A. Nisalak, D. W. Vaughn, S. Nimmannitya, S. Kalayanarooj, and E. C. Holmes.** 2006. Structure and age of genetic diversity of dengue virus type 2 in Thailand. J Gen Virol **87:**873-83.

250. **Zhang, F., P. R. Romano, T. Nagamura-Inoue, B. Tian, T. E. Dever, M. B. Mathews, K. Ozato, and A. G. Hinnebusch.** 2001. Binding of

double-stranded RNA to protein kinase PKR is required for dimerization and promotes critical autophosphorylation events in the activation loop. J Biol Chem **276:**24946-58.

251. **Zhu, B., Y. Bando, S. Xiao, K. Yang, A. C. Anderson, V. K. Kuchroo, and S. J. Khoury.** 2007. CD11b^{+}Ly-6C(hi) suppressive monocytes in experimental autoimmune encephalomyelitis. J Immunol **179:**5228-37.